Dear Editor, referees, and the readers,

We would like to thank you for your valuable comments and suggestions. In this version, we have undertaken several major changes.

First, we clarified the research objectives and expanded the literature review about the aerosol's impacts on temperature based on referee #1's suggestions.

Second, ERA5 and additional surface albedo products have been included in the study according to the suggestion of referee #1.

Third, more discussions were provided about the aerosol depressing effects.

We also replaced GEBA observations by measurements at the CMA sites in the supplementary material, and more explanations were given to address referee #2's concerns about the observation uncertainty, aerosol effects. CERES assessment for capturing the temporal variation has been included in the supplementary suggested from referee #2.

We provided the significance test and p-values for all regression analyses. The assessment analysis and discussion about satellite climatology have been added based on the reader's suggestions. Besides, the methodology and data description have been revised.

Minor revisions about the grammar and expressions have been done. Please find the attached PDF file (manuscript_tpRAD_Aolin_ACP_**v5**.pdf, upload date: **Nov. 11, 2019**) as the corresponding manuscript.

Thank you very much for your time and efforts in reviewing the manuscript.

Best,

Aolin Jia and co-authors

**Referee #1:**

This is a good job. I recommend this article to be published in ACP after addressing the following issues.

We appreciate your encouragement and we've given a point-by-point response to the comments as follows.

Major comments:

1, The Tibetan Plateau (TP) area in your analysis should be defined clearly when you present Fig. 1.

Thank you for reminding us. We added the definition of the Tibetan Plateau used in this study at **Line 213-214 (new version)**.

> "The Tibetan Plateau region is defined as the Chinese Qinghai-Tibet Plateau in this paper, covering most of the Tibet Autonomous Region and Qinghai in western China (Wang et al., 2016)."

2, The objectives of this paper need to be more clearly stated in the introduction part. Maybe the author needs more references reading.

Thanks for your suggestions. We clarified our research objectives at **Line 69-71**.

> "In this study, we aim to analyze the long-term spatiotemporal variation of surface radiation over the TP by generating a long-term surface radiation datasets from satellite products and model simulations. Solar dimming is to be attributed by analyzing multiple data sources. The depressing effect of aerosols on climate warming needs to be quantified in the end."

Besides, more literature reviews about the impacts of aerosols on temperatures at different spatial scales were summarized in the introduction (**Line 54-59**) and we point out that currently there is no conclusive answer and is still under discussion.

> "Aerosols have a net cooling effect on the global temperature with higher uncertainty from Intergovernmental Panel on Climate Change (IPCC) report (Stocker et al., 2013), whereas Andreae et al. (2005) has suggested that current aerosol loading may cause a hot future. Even Gettelman et al. (2015) contended that the net effect of aerosols on surface temperature can be neglected, Samset et al. (2018) pointed out that aerosol depressed surface temperature by 0.5-1.1 K globally. By contrast, one recent study (Feng and Zou, 2019) argued that aerosols contributed $+0.005 \pm 0.237$ K on global surface temperature change after 2000. Therefore, the aerosol effect on climate warming is still under discussion."

3, To perform more solid results, some data sets need to be analyzed:

3.1, Please add ERA5 reanalysis data into your analysis. ERA5 can be found at https://cds.climate.copernicus.eu/#!/search?text=ERA5&type=dataset

Thanks for your comment. To take advantage of reanalysis datasets for characterizing atmospheric profiles, we've employed ERA5 into our analysis. First, we replaced the ERA-Interim by ERA5 (the newest version) for detecting the temporal variation of column water vapor over the TP since 1979. The results showed that the variation of ERA5 can match with MODIS atmospheric products very well (SFig. 4, note: we added

new results as SFig 1, so this figure number is changed from 3 to 4. SFig figures in the response file are directly used from Supplementary materials).

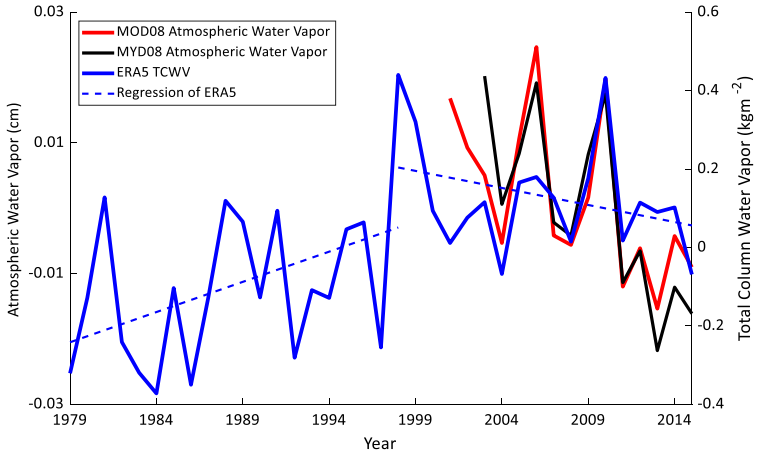


SFig. 4. Temporal annual variation of the atmospheric water vapor from MODIS atmospheric products and ERA5. ERA5 shows a considerable turning point in 1998 and the decreasing trend matches with satellite products very well.

The results demonstrated that the column water vapor trend undergoes considerable changes around 1998 and before this year, it had slightly increased and then it decreased significantly. However, solar radiation didn't respond to this variation based on former studies and our results. The overall variation of the column water vapor was not significant in recent 37 years. Therefore, the influence of the column water vapor can be ignored.

We also included the ERA5 in the cloud fraction analysis to prove that cloud coverage over the TP is decreasing (Figure 5c).

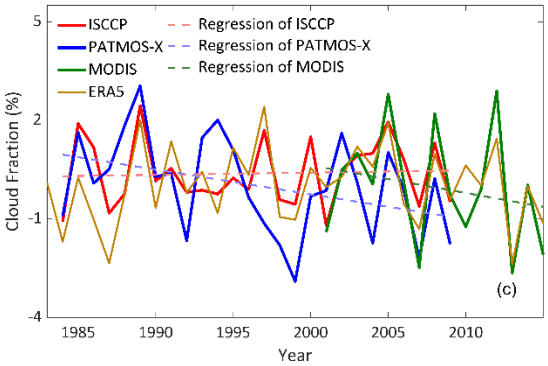


Figure 5(c). Temporal variation in detected factors from remote sensing products over the Tibetan Plateau (TP): (c) cloud fraction.

3.2, Please use more albedo data such as GlobAlbedo, CLARA-SAL, MODIS… (see He et al., 2014). He, T., S. Liang, and D.-X. Song (2014), Analysis of global land surface albedo climatology and spatial-

temporal variation during 1981– 2010 from multiple satellite products, J. Geophys. Res. atmos.,119,10,281–10,298, doi:10.1002/2014JD021667.

Thanks! We included four surface albedo products (GLASS, CLARA, CERES, GlobAlbedo) to calculate the albedo climatology of the TP. These albedo products cover different satellite observation sources.

First, we generated the monthly climatological albedo of each satellite product, and we computed all standard deviations of any possible three climatological albedo combinations at each pixel. Then for each pixel, we chose the product combination that has the lowest standard deviation and calculated the mean value to represent the ground truth. The final result changed little in the graph especially when it shows the regional averaged depressing impact (Figure 8) because the albedo products have close climatology estimation at mid-latitude as the former study suggested (He et al., 2014). We've added more data description and methodology explanation in the manuscript (**Line 168-186**).

> "According to He et al. (2014), the fine-resolution (0.05°) climatological surface albedo products retrieved from satellite observations agree well with each other for all the land cover types in middle to low latitudes. Therefore, we selected four commonly used satellite surface albedo products for calculating the surface albedo climatology over the TP, including the CERES EBAF, the Global LAnd Surface Satellite (GLASS), the Clouds, Albedo, and Radiation-Surface Albedo (CLARA-SAL), and the GlobAlbedo. First, we generated the monthly climatological albedo of each satellite product, and we computed all standard deviations of any possible three product climatology combinations at each pixel. Then for each pixel, we chose the product combination that has the lowest standard deviation and calculated the mean value to represent the ground truth climatology.
>
> …
>
> The CLARA-SAL product is inversed from advanced very high resolution radiometer (AVHRR) observations (Riihelä et al., 2013). Atmospheric correction was done by assuming AOD and ozone is constant. Sensor calibration and orbital drift have been dealt with and the uncertainty of monthly albedo estimation is about 11%. The GlobAlbedo product uses an optimal estimation approach European satellites, including Advanced Along-Track Scanning Radiometer (AATSR), SPOT4-VEGETATION, SPOT5-VEGETATION2, and Medium-Resolution Imaging Spectrometer (MERIS) (Lewis et al., 2013). MODIS surface anisotropy information was used for gap-filling. More detailed algorithm introductions and comparison can be found in (He et al., 2014)."

4, the conclusions need to be deepened. Whether other effects also can slow down surface warming over the TP? Could you conclude that aerosols increase is the major contribution to surface warming mitigation over the TP? Maybe the author needs to add more evidence.

Thanks for your suggestion. We've added more discussions about the depressing effect of aerosols and other factors in terms of water vapor (**Line 456-465**).

> "The attribution of solar dimming over the TP and corresponding aerosol effect quantification revealed that anthropogenic aerosols dominate the solar radiation decrease and depress the climate warming in recent decades. Aerosols are cloud condensation nuclei (CCN) and more CCN may depress the cloud formation and precipitation. Thus future studies need to analyze the indirect effect of aerosol loading (Qian et al., 2015) over there. However, it should be noticed that we don't conclude that TP undergoes warming mitigation. In fact, TP has a rapid warming rate than global warming (Yao et al., 2018) and other varying factors also affect the warming

> rate, in terms of the water vapor variation around 1998 (Supplementary Fig. S3). Water vapor is a weak DSR-absorbing factor but a major greenhouse gas emitting downward longwave radiation, so its decrease might slow down the local warming rate. However, the impact of water vapor variation after 1998 is at an annual scale that cannot match the analysis in this study, thus more further researches may focus on it."

We would like to point out that the TP didn't undergo temperature mitigation. For water vapors, we tried to conduct depressing analysis but there are some limitations. Reanalysis datasets start from 1980 while our depressing analysis focused on decade scales (Figure 8). Besides, CMIP5 didn't release any column water vapor variables or provide some HistoricalMisc experiments designed for water vapors' influences, which means it's hard to conduct related attribution analysis and depressing quantification based on CMIP5 experiments at decadal scales. Therefore, in this study, we only focus on aerosol impacts on climate warming.

We mentioned in the discussion that varying column water vapor trends in 1998 (SFig. 4) could cause some impacts on local warming because it is a weak shortwave absorber but an important greenhouse gas emitting longwave radiation. The decreasing water vapor may depress the local warming and the follow-up researches can work on it at annual scale. In this study, we mainly focus on the impact of aerosols on the long-term temporal scale.

Minor comments:

1, Why the first author is not the corresponding author?

Prof. Liang is the advisor of the first author Aolin Jia who is currently a Ph.D student.

2, In the abstract, the time range needs to be specified for the contribution of 48.6%.

Corrected. Thanks!

3, Please use the orange to replace the yellow color in Fig. 7.

Corrected. Thanks!

4, Please add more words in the caption of Fig. S3.

Corrected. Thanks!

5, There is a good review paper including discussions of aerosol effects over the TP (Qian et al., 2015). Qian, Y., et al.: Light-absorbing particles in snow and ice: Measurement and modeling of climatic and hydrological impact, Adv. Atmos. Sci., 32, 64-91, 2015.

We included it, thanks for your help!

**Referee #2:**

1. I have pointed out that "No long-term observations of DSR and aerosol data support the long-term variations of DSR and anthropogenic aerosol developed in this study", and the authors chose 5 sites from GEBA to support their main conclusion. But it should be noted that the 5 sites from GEBA is also from the observations of Chinese Meteorological Administration. This contradicts with your statement that "We didn't include ground observations from Chinese Meteorological Administration stations due to data discontinuity and large uncertainty". The obvious low values between 1980 and 1990 is the questionable observations, and this sites cannot be used to validate the long-term variations of your fused dataset (see Shi et al., 2008).

Thanks for the valuable comment. We've corrected this mistake. In the revised version, we employed CMA rather than GEBA data. Only observations before 1980 are used in order to avoid the data discontinuity issue after 1980. The revised results show that surface DSR observations can reflect TP dimming since 1958 with large uncertainty [SFig. 2(a), SFig mark means the figure is shown in the supplementary material and directly used here.]

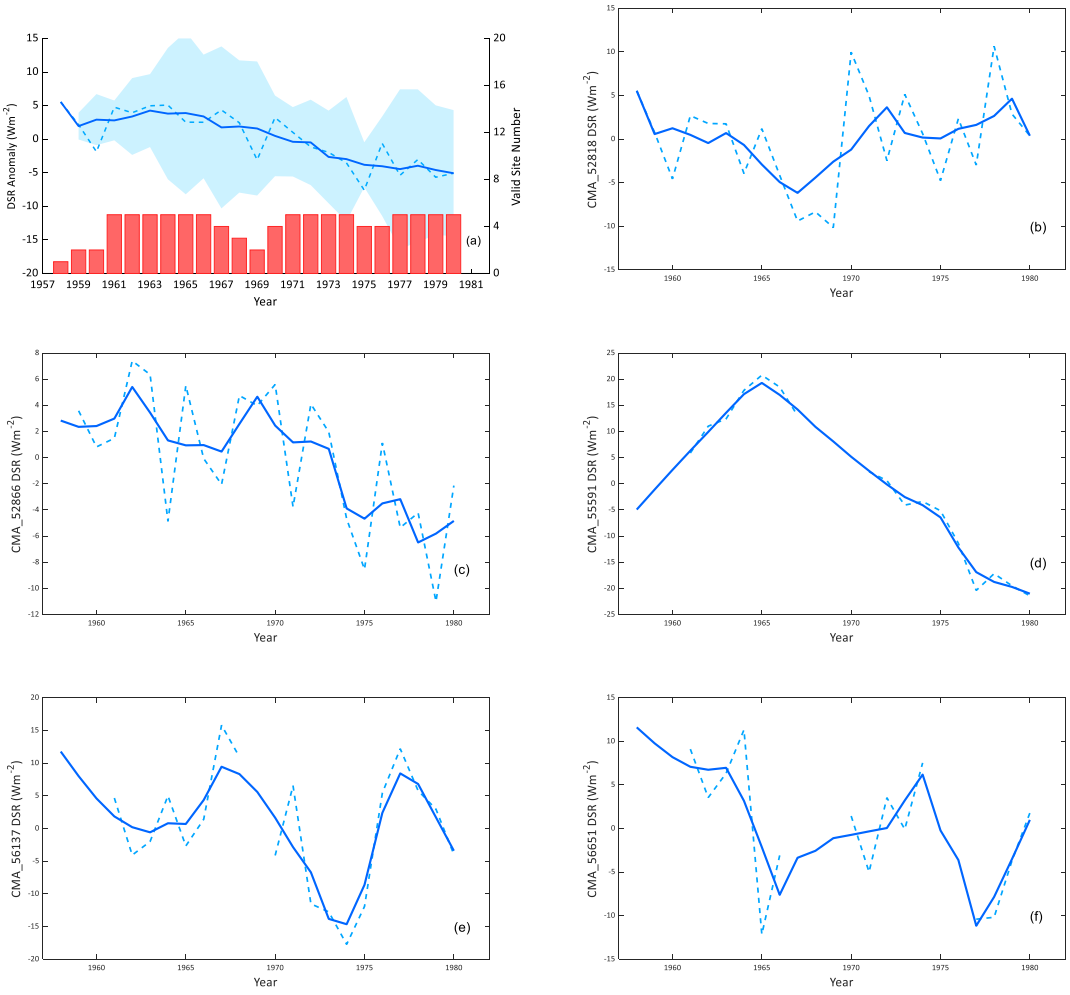


SFig. 2(a). Surface DSR temporal variation of (a) 5 CMA sites mean, (b-f) individual sites. Temporal variations were averaged by the 5-year moving window in order to remove the impact of annual variability.

We still use surface radiation measurement as a reference. 130 CMA radiation sites over China were collected and 12 sites are located in the TP. For detecting the long-term DSR variation, the sites starting to operate after 1970 were not used, so 7 sites left (Figure r1, following figures marked by 'r' are only shown in the response file).

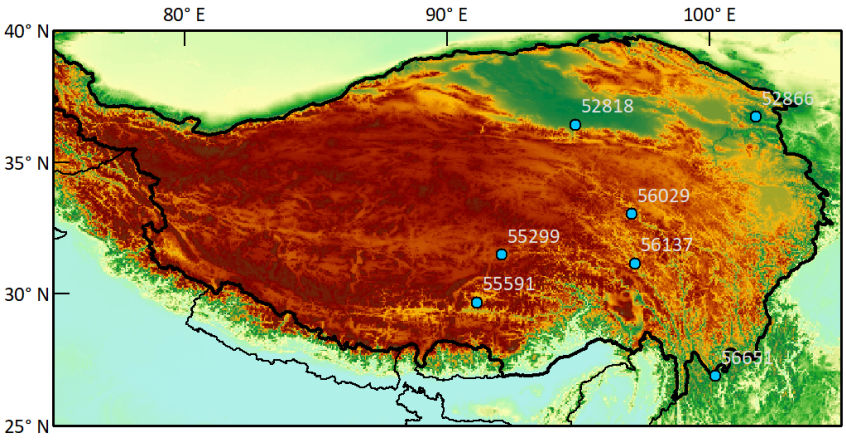


Figure r1. 7 CMA sites distribution.

We drew the averaged DSR temporal variation at 7 sites, and corresponding site numbers at each year is shown by red bars.

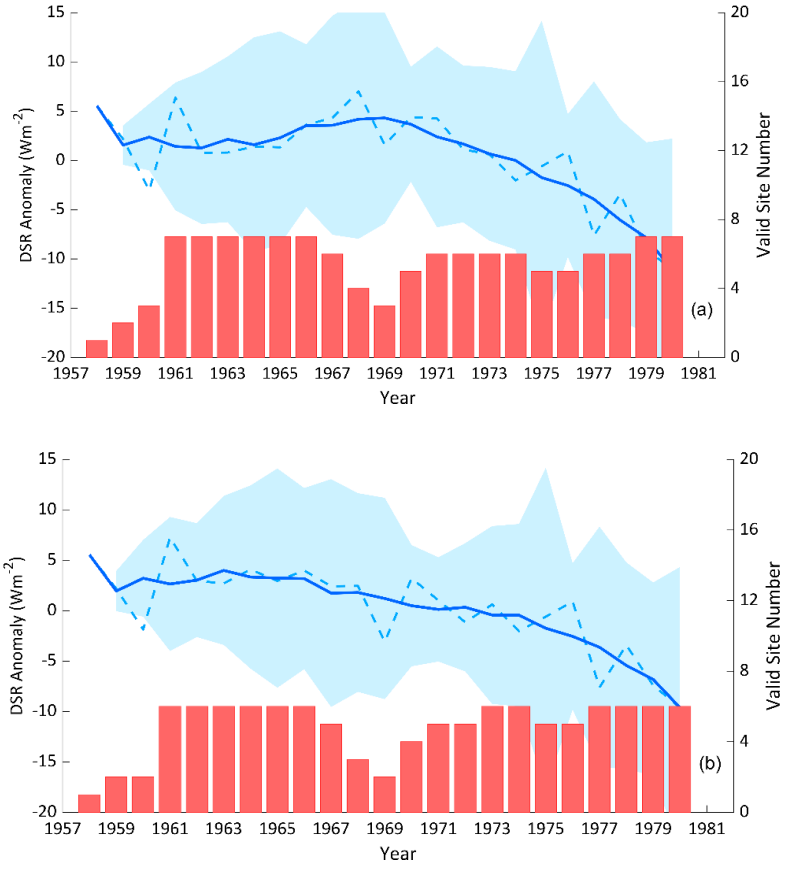


Figure r2. DSR temporal variation at (a) 7 sites, (b) 6 sites without site 56029.

In Figure r2, the dimming time of 7 sites started in 1967, which is different from our study, and the unstable annual anomalies in 1958-1960 and 1968-1970 are mainly caused by missing measurements in some sites in these years. However, sites 56029 and 55299 had continuously missing measurements for more than 5 years. Therefore, considering the data continuity and location sampling (site 56029 is near site 56137, and site 55299 is near site 55591 compared with other sites), we abandoned these two sites in SFig. 2, and the left 5 sites are scattered in TP.

In the SFig. 2, the dimming time started in 1958, and only site 55591 has a different starting time. Sites [56651 and 52866, SFig. 2(c, f)] located in eastern region show clear DSR decreases from 1958, and the other 2 sites have an overall slight decrease with oscillation from 1958. It is consistent with our result (Figure 4a) that TP dimming is more significant in the southeastern region.

We also checked the dimming time change in site averaged results. We found that once site 56029 was removed in the analysis, the starting time would be changed to 1958 [Figure r2 (b)]. It illustrated that the site number and location did considerably affect the starting time. Our data covered the whole TP and caught the solar decrease especially at southeast TP.

In all, both site observations and our results can prove that the TP has undergone dimming since the 1950s. The large uncertainty of site observations and larger dimming trend may be caused by measurement drifts explained by He et al. (2018) who used sunshine duration derived DSR showing a smaller dimming magnitude compared with observed DSR at global scale.

2. how did you reach that "estimated DSR driven by sunshine duration was not calculated either because the method accuracy may be not high enough to capture the influence of aerosols at low-level magnitude."? In my opinion, the accuracy of DSR driven by sunshine duration is generally higher than those of satellite-based DSR and CMIP5. At least, the accuracy of DSR driven by sunshine duration is also higher than that fused by yours.

We speculated that Sunshine Duration (SunDu) derived DSR in TP cannot capture the trend at the decadal scale and SunDu may not represent DSR to show TP dimming especially for the early period at the TP based on the results in He et al. (2018). In their study, He et al. estimated DSR from SunDu from globally distributed site observation pairs based on a widely used method (Yang et al., 2006), and observed DSR is considered as reference and the estimation accuracy is satisfactory at the global scale.

However, we found that the SunDu derived DSR has an opposite trend with observed DSR in TP [Figure r3, also Figure 3 in (He et al., 2018)].

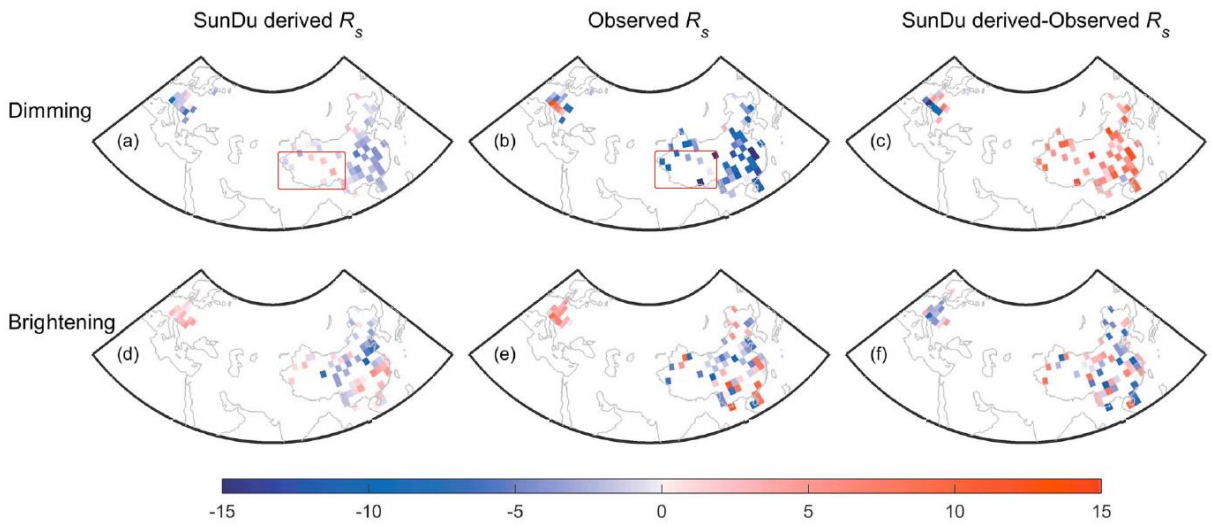


Figure r3. Maps of the decadal trends (units: W/m2 per decade) in 2.5° × 2.5° grids of sunshine duration (SunDu)-derived Rs (a and d), the observed Rs (b and e), and differences between the two data sets (c and f) over China and Europe during two periods of dimming and brightening. "Dimming" denotes the periods of 1959–1989 in China and 1961–1980 in Europe. "Brightening" denotes the periods of 1994–2010 in China and 1980–2009 in Europe.

In Figure r3, the dimming trend from SunDu-derived DSR matched with observed DSR except over the TP region. The paper didn't provide more explanations about the mismatch. However, when they applied this method in more than 2000 sites over china, we found that their SunDu-derived DSR over the TP has no dimming at all time periods (Figure r4, also Figure 4 in (He et al., 2018)).

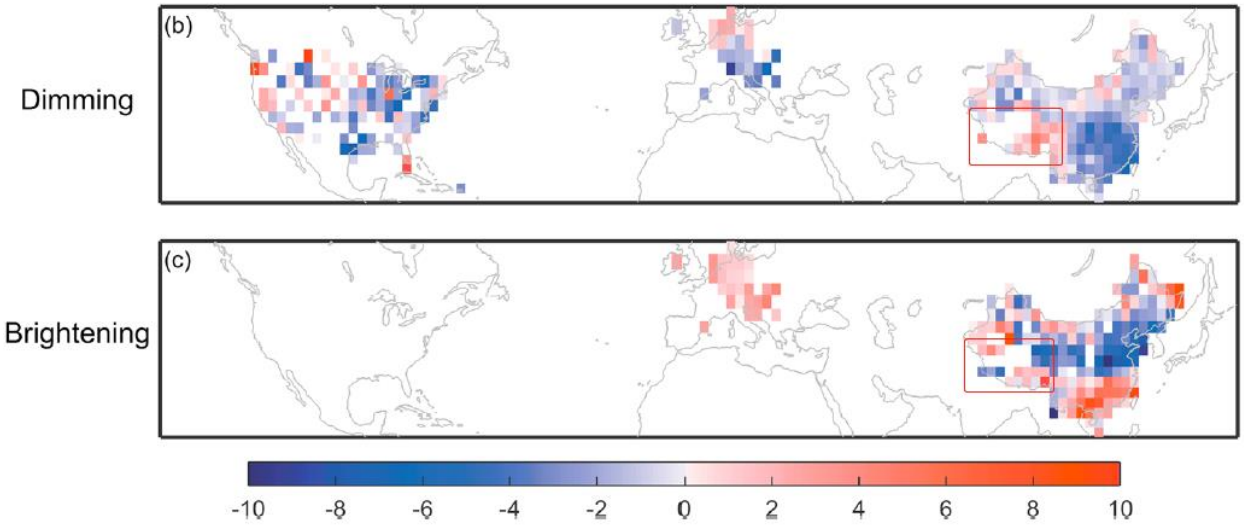


Figure r4. Maps of the decadal trends (units: W/m2 per decade) of all reliable SunDu-derived Rs stations over China, Europe, and the United States in 2.5° × 2.5° grids during three periods. "dimming" denotes the periods of 1959–1989, 1950–1980, and 1952–1980 in China, Europe, and the United States, respectively. "Brightening" denotes the periods of 1994–2010 in China and 1980–2009 in Europe.

They didn't focus on TP so there is no specific explanation of it, but the result is contradictory with our result and all former studies based on direct observations, model simulations, reanalysis, and satellite

observations (Kuang and Jiao, 2016;You et al., 2010;Shi and Liang, 2013;Yang et al., 2012;Yang et al., 2014).

We also contacted with the co-author Martin Wild who is in charge of GEBA network and he also expects that the sign of DSR derived from SunDu is same as the DSR observations.

Dear Aolin Jia,

Thanks for you mail. The Chinese data in GEBA have not been changed with respect to the CMA original data.
There are problems in the Chinese radiation data quality as you are sure aware, and as documented in many papers.
I had a visitor from CMA (Yang Su) visiting me for a year and working with me on the improvement of the quality of the dataset. I attach 2 related papers recently published in J. Climate.
Unfortunely those data are not public due to the Chinese data policy.
As for the Sunshine duration trends, I also expect them to be of the same sign as the radiation data. You may contact the Beijing group for more details on their analysis.

Kind regards
Martin

---

Prof. Martin Wild
Institute for Atmospheric and Climate Science
ETH Zurich
Universitaetsstr. 16
CH-8092 Zurich (Switzerland)

Figure r5. Email from Martin Wild

Besides, we discussed this issue with the first author of the paper, who provided some valuable details about the estimated DSR over the TP. They explained that studying different time periods may result in different trends, it's true but unfortunately it cannot explain that why the overall trend at two time period is brightening especially at southeastern TP [Figure r6 (b), site 56651 is at the southeastern TP while the trend is overall negative]. The sites [Figure r6 (a)] they provided showed that these sites have dimming trend that matched former results, while the whole trend shown in Figure r4 is still brightening at dimming period (1952 - 1989), which is different from the DSR observations [SFig. 2 (a)]. We infer that even for the SunDu sites, the dimming time varied at different locations that matched what we found using DSR observations.

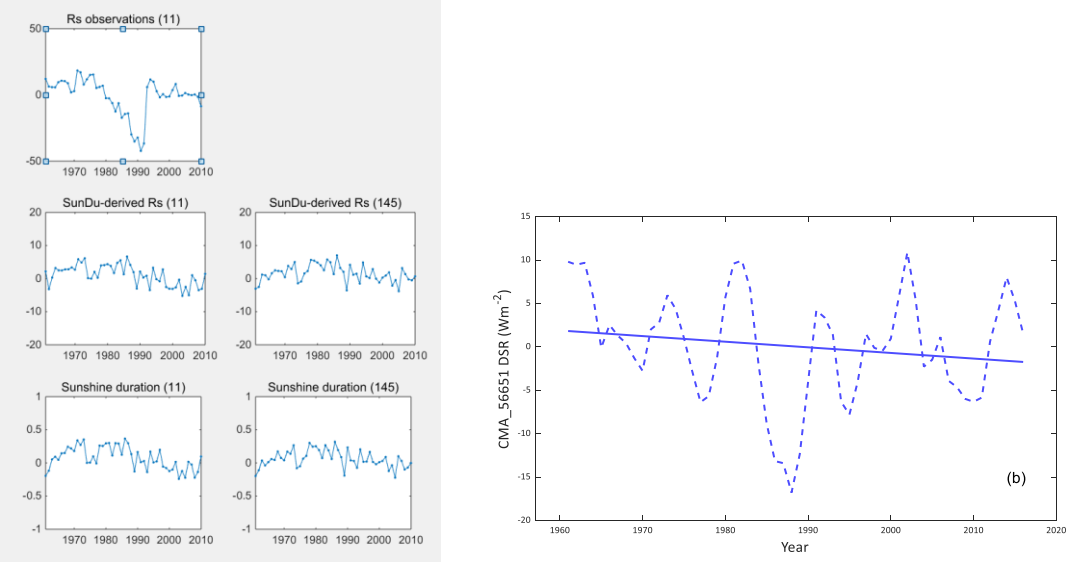


Figure r6. (a) Site samples the author provided for us; (b) DSR temporal variation of CMA 56651. Temporal variations were averaged by the 5-year moving window in order to remove the impact of annual variability.

Therefore, we speculated that SunDu-derived DSR couldn't be able to capture the observed DSR temporal variation in TP and SunDu may not represent DSR to show the dimming at the TP. According to Manara et al. (2017), SunDu has a different sensitivity to atmospheric turbidity changes that is estimated by aerosol optical depth (AOD). SunDu may lose its representability at low AOD level. We infer that this is the reason why this method didn't capture the dimming trend in the TP and SunDu may not represent DSR in the TP at low AOD level.

Additionally, the accuracy (standard deviation of bias, STD) of SunDu-derived DSR over China is about 19.32 $Wm^{-2}$ (He et al., 2018), and our validation showed that the standard deviation of the calibrated data bias is 20.64 $Wm^{-2}$. Considering that the validation of gridded data has scale mismatch effect while their validation results are observation pairs, we think our result is comparable to theirs. Besides, their validation sampling is over China while our validation samples are only limited in TP, where DSR is large and the bias and STD could be larger, let alone the measurement environment in TP is not as good as other regions and might introduce large uncertainty.

More discussions of physical relationship between DSR and SunDu and the estimation algorithm suitability are beyond the scope of this study, therefore, we didn't include more experiments assessing the estimation algorithm and directly used DSR observations as the references.

3. As you also known that TP is one of the cleanest areas in the world, and compared to other factors, such as cloud and water vapor, it's effect on the DSR over the TP may be ignorable. Thus, it can not cause the phenomenon of solar dimming over the TP.

Thanks! When we estimate instantaneous DSR at all-sky conditions, it's reasonable to ignore the influence of AOD because its influence is small compared to the DSR absolute value. However, when we analyze the impact at the decadal scale, any contributing factor that has a directional decrease or increase trend will affect the DSR trend accordingly. We also calculated the radiative effect of aerosols in Figure 6 (a), ~5 $Wm^{-2}$ difference of decadal variation between the clean and aerosol case simulations cannot be ignored.

Besides, we also calculated the increased aerosol radiative forcing caused by AOD increase since 1998 based on Yang et al. (2012). The increased radiative forcing is about 1.97 $Wm^{-2}$, which can also prove that it is not ignorable.

As we explained in the last reply, it's true that TP is one of the cleanest areas in the world and the corresponding aerosol climatology is low. However, when we talk about solar dimming over the TP, we mainly focus on the DSR decreasing phenomenon over there, which is characterized by the variation of DSR decadal anomalies rather than the absolute magnitude. Besides, it's necessary to point out that when aerosol loadings in the atmosphere are at a low magnitude, direct radiative effects (scattering and absorption effect) play a dominant role in the interaction between aerosols and the atmosphere (Li et al., 2017). Therefore, even TP has a clean condition, it is easily affected by aerosols increase.

4. You did not answer my question fully: "Why did you use the CERES EBAF DSR to calibrate the CMIP5 DSR data since the satellite radiation products generally can not capture the long-term DSR variations. Or you can demonstrate that the CERES EBAF DSR can reflect the long-term variations of DSR?". Even if the CERES EBAF DSR can capture long-term variations of DSR over the other regions, it not necessarily can capture long-term variations of DSR over the TP.

Thanks for your comment. We understand your concern.

First we've proved in the previous reply (Figure r7) that CERSE EBAF 4.0 can capture the absolute value variation over the CAMP network in the TP even there is a systematic bias at some sites.

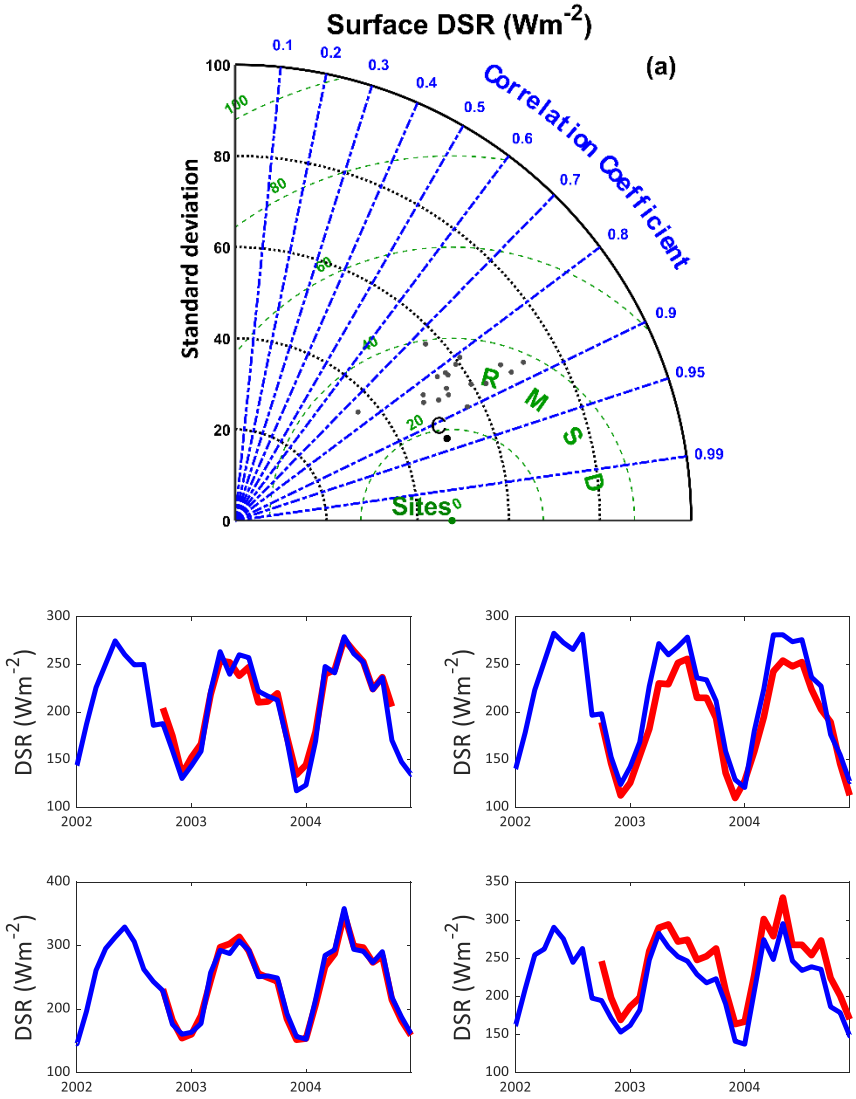


Figure r7. (a) Taylor diagram of solar validation of CERES EBAF (**black dot C**) and 18 CMIP5 models (**grey dots**). (b) Monthly variation of CERES EBAF (**blue line**) and site observations (**red line**). Only sites that were run more than 2 years long were shown here.

Then we used 11 CMA sites located in TP (deleted one that missed continuous measurement for 3 years) to prove that CERES EBAF 4.0 DSR can capture the overall temporal annual anomaly variation observed by CMA since 2001 over the TP (SFig. 1). Therefore, we can choose CERES as the reference at each pixel to calibrate the model simulation results. We added the CERES analysis into the supplementary as SFig. 1. Thanks for reminding us.

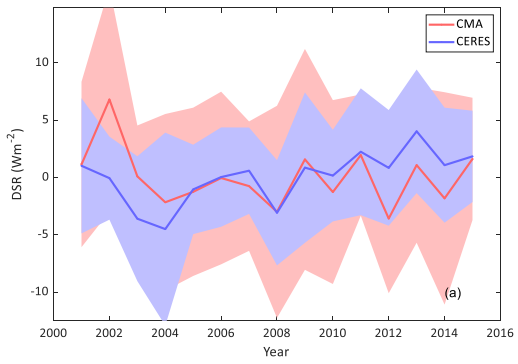
CMA
CERES
DSR (Wm-2)
Year
(a)

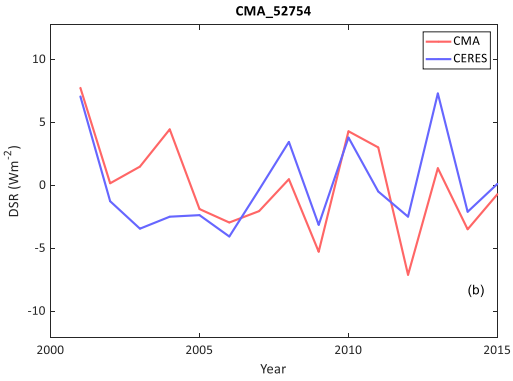
CMA_52754
CMA
CERES
DSR (Wm-2)
Year
(b)

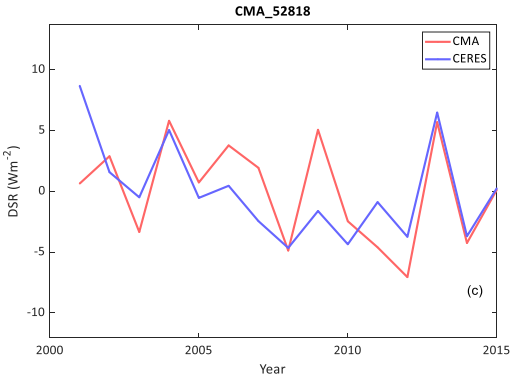
CMA_52818
CMA
CERES
DSR (Wm-2)
Year
(c)

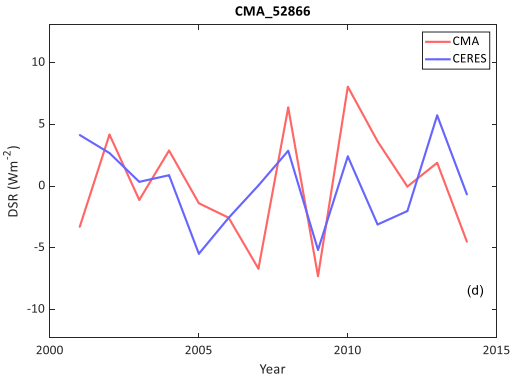
CMA_52866
CMA
CERES
DSR (Wm-2)
Year
(d)

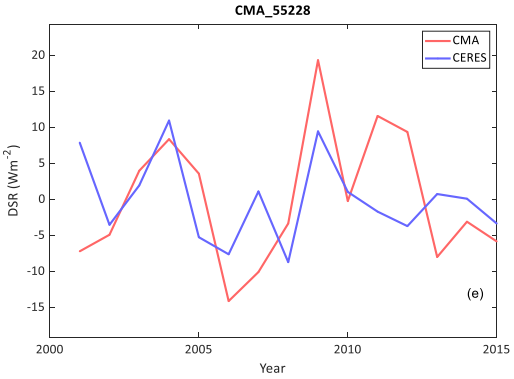
CMA_55228
CMA
CERES
DSR (Wm-2)
Year
(e)

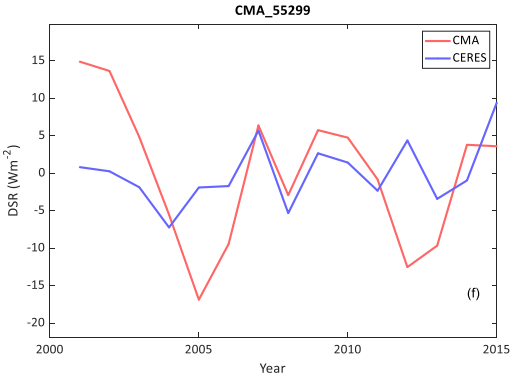
CMA_55299
CMA
CERES
DSR (Wm-2)
Year
(f)

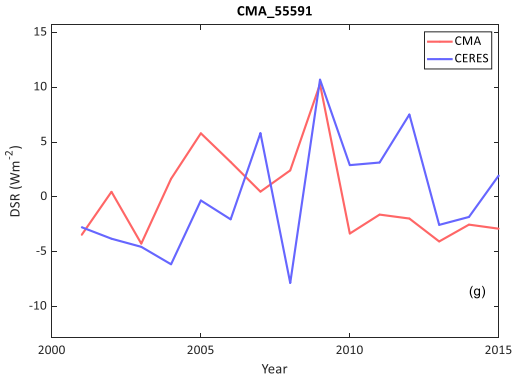
CMA_55591
CMA
CERES
DSR (Wm-2)
Year
(g)

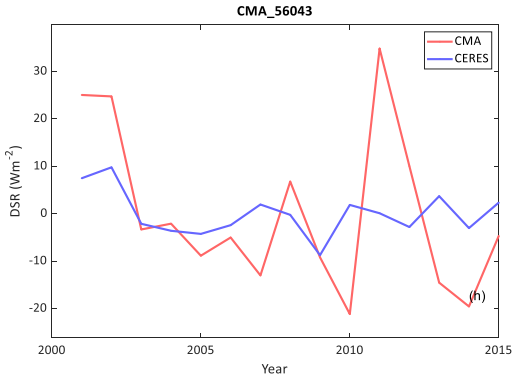
CMA_56043
CMA
CERES
DSR (Wm-2)
Year
(h)

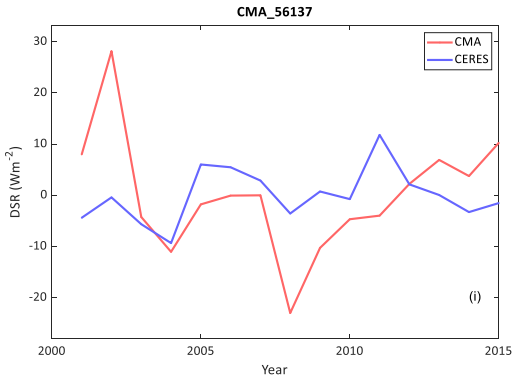
CMA_56137
CMA
CERES
DSR (Wm-2)
Year
(i)

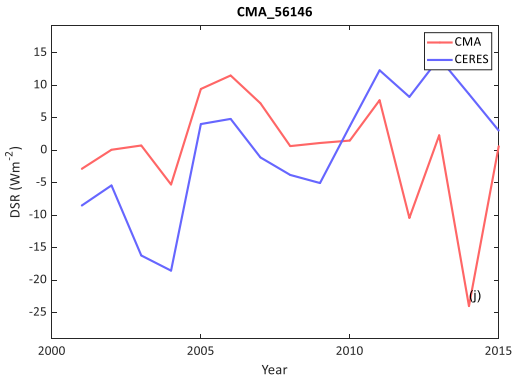
CMA_56146
CMA
CERES
DSR (Wm-2)
Year
(j)

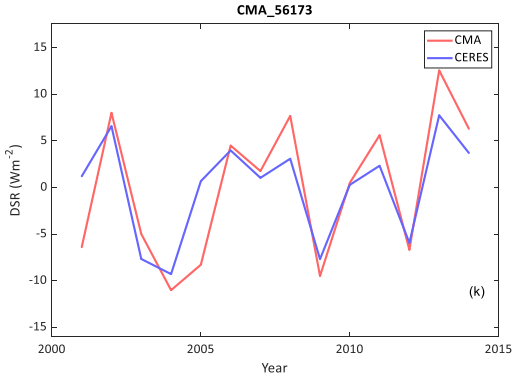
CMA_56173
CMA
CERES
DSR (Wm-2)
Year
(k)

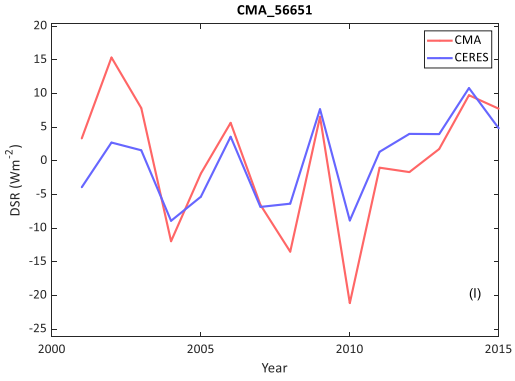
CMA_56651
CMA
CERES
DSR (Wm-2)
Year
(l)

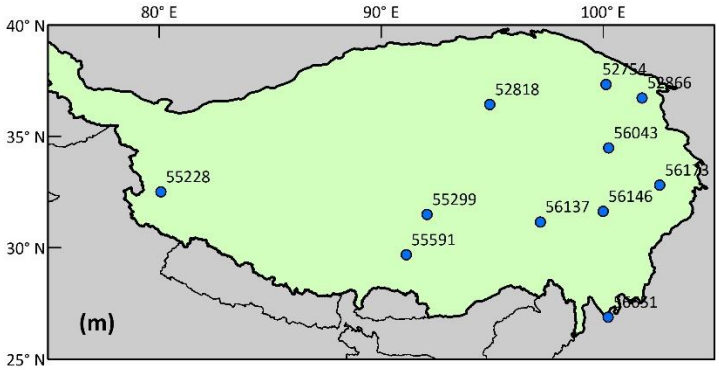
80° E
90° E
100° E
40° N
35° N
30° N
25° N
52754
52866
52818
56043
56173
55228
55299
56137
56146
55591
56651
(m)

Fig. S1: Surface DSR temporal variation of CERES and all CMA radiation sites at TP (a) 11 CMA sites mean, (b-l) individual sites, and (m) 11 sites distribution

5. Because the 5 sites from the GEBA is measured by the Chinese Meteorological Administration and is the same as the observations of CMA. Thus, the question "The DSR over the Tibetan Plateau is decreased since 1950, which was different with the points derived based on the observations or based on the sunshine based DSR" should be re-answered.

Thanks very much for providing this valuable suggestion.

Base on the analysis in Q2, we suggested that the different start time of TP dimming from the previous study based on SunDu and our result is caused limited representability of SunDu to DSR at the TP. Therefore, we still selected DSR measurement as ground reference data. By analyzing DSR measurements, we concluded that sites at different locations show various dimming start time. Our data can cover the whole TP area especially the southeastern TP. Thus they may have a different start time.

**Reader #1:**

The Tibetan Plateau is a region which undergoes significant climate change. Air temperatures have increased with 1.39 K since 1850 while the amount of incident solar radiation decreased. The consequences of this solar dimming phenomenon on surface warming are still unclear. Previous research shows contradictory conclusions regarding the proper attribution of solar dimming. Therefore, the roles of clouds and aerosols will be investigated in this study to provide more clarity regarding the causes and impacts of solar dimming.

The paper is well written and the different sub-sections improve the readability and enable the reader to search for specific sections. I feel confident about the data analysis and interpretation done by the authors. However, there are some important remarks regarding certain assumptions, significance of results and data visualisation. I would strongly recommend considering and including these remarks in the manuscript before publication. I will come back to these remarks in more depth in the remainder of this review. Firstly, I want to emphasise what I thought to be very good and interesting about this research. To start with the introduction which describes in a clear and convincing way why this research is relevant. The current controversy regarding the proper attribution of solar dimming is a driving force for this research to introduce new knowledge and provide a conclusive answer. In order to generate this new knowledge, multiple high-quality data sources have been used: model simulations, remote sensing products and ground measurements. The methods applied seem quite advanced and are well-documented in previous literature which makes the methods trustworthy because it can be checked and compared with other research. Especially the improved accuracy of the generated downward surface radiation datasets by applying the NNLS method is a very strong aspect of this research. The solar dimming phenomenon has a large effect on local but also on global climate change. It turns out that humans are largely responsible for the increase of air pollution which turns out to be the main driving factor of solar dimming. The role of human activities in remote areas is discussed and emphasises the societal relevance of the topic.

We greatly appreciate your positive comments.

**Major argument 1:**

The method which is used for the attribution analysis of solar dimming is the optimal fingerprinting method. It's is based on a linear relationship between driving variables and a responding variable, in this case downward shortwave radiation (DSR). When the scaling factor is larger than zero at a certain significance level, the variable has a positive contribution towards the responding variable. My concern regarding this method is that no value of the significance level is given in the manuscript. The results of the attribution analysis indicate that anthropogenic aerosols (AA) are the main cause of solar dimming. However, it's not clearly described or listed if other variables were tested with optimal fingerprinting method besides the noAA simulation and if there were variables which didn't reach the required significance level and are consequently left out of the analysis. The CMIP5 simulations with and without AAs have uncertainties which are indicated by the shaded area in figure 6a. Zhou et al. (2018) calculated the 5%-95% confidence intervals using Monte Carlo simulations. Do these shaded areas and errors bars represent the same confidence intervals and are they calculated in a similar manner? It is stated that the overall variation is of significance tested but the outcomes of these statistical tests or thresholds (p-values, r-values, etc.) are not included. The time over which the method is applied is divided in two periods: 1950-2005 and 1970-2005. Is the selection of these periods linked with the respective increase and decrease of downward longwave and shortwave radiation? Do you believe that two periods are enough to describe the trend in the data? Yao et al. (2018) described for example that the heating of the Tibetan Plateau began in the 1960s but reached

the highest levels in the last 30 years which indicates that significant changes in the climate have occurred within the selected periods.

The results show that the scaling factor is positive for the AA simulation and negative for the noAA simulation, which supports the conclusion that AAs are the main driver of solar dimming. Especially the scaling factor for the AA simulation for 1970-2005 seems convincing with small error bars and a mean value close to 1. If other variables would have been included in the analysis, the scaling factors could be compared with the scaling factor of the AA simulation. This would show the relative contribution of other factors and possibly strengthen the assumption that AAs are indeed the main driving factor. It can be observed that the scaling factors become more positive and more negative for the shorter time period. The error for noAA (1970-2005) is quite substantial in my opinion because the total length of the error bars covers approximately 1/3 of the length of the y-axis of the graph. The negative scaling factor for noAA is attributed to the decrease in cloud cover. The evidence for this statement is obtained from figure 5c where the temporal variation in cloud cover from three satellite data sources is shown. However, the satellite data only covers the period 1980-2005/2015. Thus, from the period 1950-1980 there is no data available to support this conclusion. In addition, the trend of the ISCCP data shows a slight increase of cloud cover which doesn't support the statement that the cloud fraction decreased over time.

I would recommend providing the value(s) of the significance level in the methodology section and indicate if certain variables were left out of the analysis. Could these variables be included when the significance level would change and would this make a difference for the outcomes of the analysis in your opinion? The results of the analysis would be more robust if the values of statistical tests and thresholds are included with the results and figures in the manuscript. Currently I have to believe that the variation is of significance tested without this statement being supported by numbers. Could you elaborate a bit more the selection of the two different time periods in the methodology section, why did you choose for these periods? Am I correctly assuming that it's related to the turning-point of the increase of longwave radiation and the decrease of shortwave radiation? The negative scaling factor of the noAA simulation, with the largest uncertainty, is completely attributed to the decrease in cloud cover which is supported by 2 out of 3 data sources whereas the third data source indicates a slight increase in cloud cover. What is your opinion on the controversy regarding these results and do you have possible suggestions for other factors besides cloud cover which could play a role? Perhaps it would be nice to add a paragraph of discussion concerning the remarks related to this argument in the manuscript.

Thank you for suggesting to include the significance level and we've added the explanation into the methodology (2.2.2). The shaded area in all figures is the standard deviation of model average at each year and we added the explanation in Figure 6 caption. For the (b), we also used Monte Carlo simulations to quantify the uncertainty at 5% - 95% significance level. The p-value of the impact factor in 1950 – 2005 (1970 - 2005) is 0.216 (0.042). The impact factor in 1970 - 2005 passed the significance test. We also added significance statistics (p-value) in other figures.

The introduction of the optimal fingerprinting method has been revised (2.2.2). $X_i$ in the formula are the DSR simulation results from averages of aerosol-driven experiment ensembles and non-aerosol-driven experiment ensembles in this study. It's not reasonable by directly including natural factors into the formula because a simple coefficient cannot represent the relationship between driving factors and DSR. Therefore, the historical DSR is the weighted average of DSR simulation at different forcing cases. The HistoricalMsic experiments didn't release DSR simulation results for all atmospheric factors (e.g. water vapor, cloud cover) and mainly focused on anthropogenic forcings (e.g. AA, Ozone, and $CO_2$, …). Therefore, for the solar dimming attribution, we only used AA and noAA HistoricalMisc experiment in the study and assumed that noAA experiment can represent cloud/water vapor impacts on surface downward shortwave radiation.

We applied the optimal fingerprint analysis for two time periods because we found that the impact of AA after 1950s is not large enough or significant (Figure 6b): the impact factor is small and p-value is larger than 0.05. We think it is because of the time period between 1950-1970 when AA, noAA, and historical simulations all have a similar slowly decreasing trend (Figure 6a). Then we ignored this time period (1950 - 1970) and focused on the time span after 1970 to check the corresponding impact and significance because after this year when noAA is pretty much stable while AA and historical records are decreasing considerably (Figure 6a). We didn't include the time period since 1980 and afterward because 1) the speed wasn't accelerated and 2) the time span is half of the former ones that the statistical amount is not comparable. When the statistical number is small, we found the statistics became unstable and easily affected by annual anomalies. Therefore, after 1980, we prefer to use satellite products and reanalysis datasets to demonstrate our analysis.

Additionally, we inferred that the negative impact of noAA is mainly affected by decreasing cloud coverage with a larger uncertainty bar since 1970. As a matter of fact, DSR was driven by more forcings in noAA than AA experiments, introducing more uncertainties among model simulations after 1970. Therefore, it is possible that noAA impact factor shows a larger uncertainty bar. We inferred that cloud coverage dominated the negative natural impact because water vapor has been quite stable since 1980s (Supplementary Fig. 4) that had little impact on the dimming. More explanations about this concern were provided in the corresponding content (**Line 409 - 414**). Your concern is valuable to this study.

As for the cloud cover variation, we followed referee#1's suggestion and included ERA5 as a long-term dataset. It matches our results:

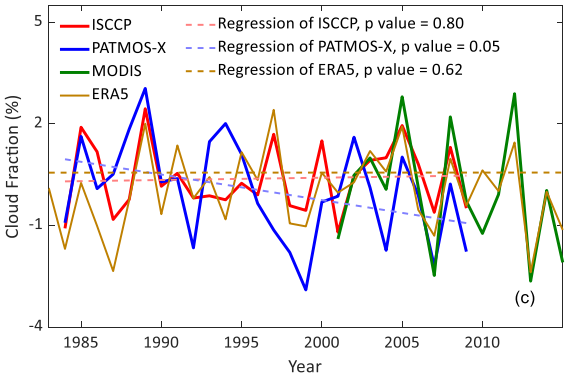


Figure 5(c). Temporal variation in detected factors from remote sensing products over the Tibetan Plateau (TP): (c) cloud fraction.

The trend (1984 - 2015) of ISCCP is 0.068% per decade but the p-value is 0.80; PATMOS-X is -0.754% per decade; ERA5 is -0.024% per decade but the p-value is 0.62; and CERES is -0.843% per decade (2001-2015) as a reference. 3 of 4 products meet our assumption (except ISCCP) while ISCCP can match with CERES well and the overall trend of ISCCP and CERES is negative. Besides, the trend value is affected by the annual anomaly and the beginning year. They all have a negative slope if we choose the time span since 1985 and all significantly decreased while starting since 1989. At least all the long-term cloud products were included for proving that the cloud coverage is not the dimming driver.

In fact, the cloud cover decrease over the TP is not a new argument and former studies also found cloud coverage decrease at site scale, which is consistent with the satellite observations (Kuang and Jiao,

2016;Yang et al., 2012). Therefore, there are some site observations supporting the cloud coverage decrease before 1980.

We didn't aim to duplicate the site analysis, thus we calculated the temporal variation of the regional averaged cloud average by using revised long term satellite products. It's the first time people use revised cloud products to analyze the cloud change over the TP. ISCCP wasn't excluded from the analysis because we need to demonstrate the uncertainties among long-term datasets and we don't want to only keep the evidence that strongly supports our results. We added more discussions in the manuscript. Thanks for your suggestions.

Major argument 2:

Shortwave and longwave radiative effects are separated in order to quantify the depressing effect of aerosols on surface warming. It is assumed that the change in air temperature is dominated by the change in surface skin temperature interacting with the air temperature through radiative and thermal processes and the change in atmospheric circulation. Consequently, the variable f is calculated which represents the sensitivity of air temperature to 1 W/m2 radiative forcing. For this analysis I'm wondering whether it's valid to employ values of α, εy and S which are calculated by taking the mean values of satellite products for several years. Is there a substantial variation between different products and how large or small is the error estimate of this mean value? From the introduction and other studies, it becomes clear that this region undergoes significant climate change which is supported for example by the analysis done by Yao et al. (2018) regarding oxygen isotopes in ice cores collected at glaciers at various locations. The Tibetan Plateau contains large amounts of snow and ice and is called the Third Pole for a reason. Warming and consequent melting of snow and ice could substantially change the albedo. The positive snow-albedo feedback could accelerate the change in albedo and warming over the Tibetan Plateau (Zhang et al. 2003). In addition, other studies indicate that black carbon (BC) and dust are responsible for about a 20% reduction of the albedo (Schmale et al. 2017). However, the results in this study show that the amount of dust decreased over time. Is the amount of BC somehow related to the amount of PM2.5 and could this be responsible for the decrease in albedo besides the decrease due to snowmelt? My main concern regarding this method is whether it's valid to assume that a mean value can represent the rapid changes caused by a positive feedback mechanism in combination with other factors like dust and BC. Additionally, it's not clearly stated over how many years this average is taken, if multiple averages were used for different time periods and which satellite products were used.

The results show that the aerosol radiative forcing has been increasing by 8.08 W/m2 between the first and last 30 years of climatology. However, the supplementary figure S5 shows a negative forcing anomaly which implies a decrease of the radiative forcing. The depressing effect of aerosols on air temperature is calculated using two methods: first-order approximations of the direct near-surface air temperature response to each radiative and thermodynamic component (α, εy and S are included using this method) and multiple noAA simulations. It can be observed that the methods show similar depressing magnitudes in the supplementary figure S6. If the albedo is overestimated because the effects of the snow-albedo feedback can't be captured by taking the mean value, the temperature anomaly could start to deviate and will likely result in a larger value. Consequently, this will have an effect on the mean of the two methods which is represented in figure 8.

Could you elaborate a bit more on the thought of reasoning behind the assumption of employing the mean values of satellite products for these variables (especially concerning the albedo). What are the exact values and sources of these variables which were used for the analysis and do they correspond with previous

studies or observations? Perhaps an analysis of the albedo from the downward shortwave radiation products could be included to visualise the temporal variation of the albedo. It's stated in other research that dust and BC can be responsible for a reduction in the albedo besides the snow-albedo feedback. In this research it's shown that dust shows a decreasing trend since 2000 whereas PM2.5, which is related to air pollution, shows an increasing trend. Could there be a possible relationship between PM2.5 and BC which could also contribute to the change in albedo and would you perhaps consider this in the manuscript or future research? Related to the suggestion of the previous major argument, could you include the statistical information regarding the shaded areas in figure 8, S5 and S6.

Thanks. We assumed that the extraterrestrial condition and surface cover type didn't change much especially at 1 lat/lon degree spatial scale and use surface albedo ($\alpha$), surface emissivity ($\varepsilon_s$), and extraterrestrial incoming solar radiation (S) climatology to calculate the depressing effect. The corresponding satellite products and time span are listed in Table 2 marked as a depressing effect in usage column.

We use the mean value of satellite products from 2001 – 2015 to calculate the $\alpha$, $\varepsilon_s$ and S for time span consistency. We calculate the temporal variation of each variable in summer and calculate the standard deviation to prove the reasonability of our assumptions. Based on figure r1, S and $\varepsilon_s$ don't have significant temporal trend (p-value >0.05) and the standard deviation is small. As the comment mentioned above, in recent years the TP undergoes significant climate change while surface cover types and TOA at 1-degree spatial scale didn't change much, so it's reasonable to use variable climatology in the equation.

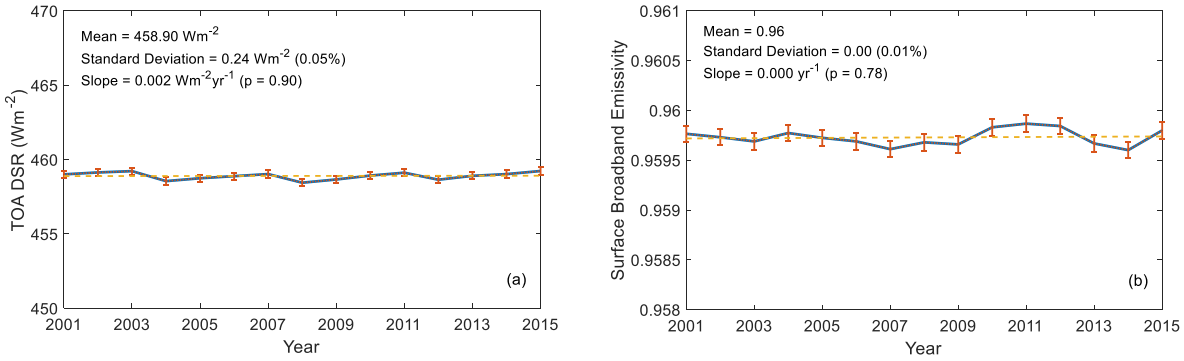


**Figure r1 (Supplementary Fig. 8).** Temporal variation of (a) TOA DSR and (b) surface broadband emissivity over the TP since 2001.

For the surface albedo, we followed referee #1's suggestion that replaced the single one satellite product by multiple albedo satellite products (GLASS, CLARA, CERES, GlobAlbedo) to calculate the albedo climatology of the TP. These albedo products cover different satellite observation sources and they have close climatology estimation at mid-latitude as the former study suggested (He et al., 2014). First, we generated the monthly climatological albedo of each satellite product, and we computed all standard deviations of any possible three climatological albedo combinations at each pixel. Then for each pixel, we chose the product combination that has the lowest standard deviation and calculated the mean value to represent the ground truth. We've added more data description and methodology explanation in the manuscript (**Line 168-186**).

Then we did the same temporal analysis for the combined surface albedo data:

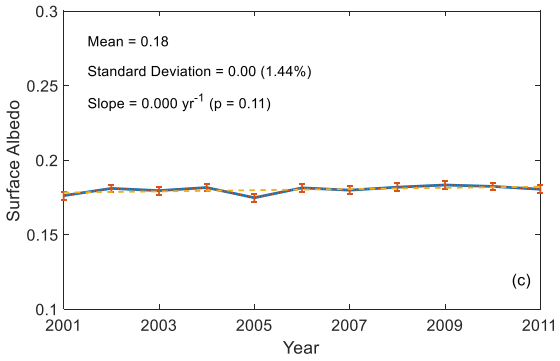


Figure r1 **(Supplementary Fig. 8)**. Temporal variation of (c) surface albedo over the TP since 2001.

The combined albedo data also kept stable in recent years. We didn't use satellite products to calibrate upward shortwave radiation (USR) for getting surface albedo because there are few USR surface observations to validate the calibration result. Considering that surface albedo didn't change significantly at 1-degree spatial scale, we think it is reasonable to use albedo climatology as input. We've added the figure r1 into the supplementary.

As for the contradiction of 8.08 Wm-2 and SFig. 5, it's the issue of explanation. We've concluded that aerosol radiative forcing negatively affects the surface radiation budget, so the aerosol forcing in SFig 6 (the old version is SFig 5) is actually increasing, which means negative forcing. Thanks!

We discussed that we would consider the aerosol impact on the surface albedo and indirect function for cloud formation over the TP in the future study. This point has been added into the manuscript, Thanks for your suggestions!

**Major argument 3:**

The final aerosol depressing effect on the Tibetan Plateau climate warming is calculated by taking the average over two data sources where one included and the other ignored the heat exchange with the surroundings. The first-order approximation which consists mainly of remote sensing products ignored the heat exchange with the surroundings. The CMIP5 noAA simulations are assumed to be less reliable but did compute the influence of the interaction with other regions. Thus, it is stated that the remote sensing products had more reliable input than the model calculations but this is not supported by numbers/ statistical tests/ previous literature. Furthermore, it seems counterintuitive because the accuracy of the CMIP5 datasets is improved by the NNLS method. Is it a sound methodology to lump these two sources of data together for the final depressing effect and assume that the exchange is considered to a certain extent? Personally, I'm not convinced by the assumption that the interaction with the surroundings can largely be ignored. In the introduction it is stated that the Tibetan Plateau is a weak heat sink in winter but a strong heat source in summer which is already indicative for differences between the seasons. Also, it's mentioned that the large-scale orography is crucial for water and heat exchange between the Pacific Ocean and Eurasia

This assumption focusses on the exchange of heat with the surroundings but what about other types of exchanges? Aerosols resulting from air pollution in surrounding areas enter the Asian tropopause aerosol layer by deep convection. From here they are consequently transported to other locations. This is an important pathway for anthropogenic aerosols to enter the Tibetan Plateau, which is thought to be the main cause for solar dimming in this region (Lau et al. 2018). Furthermore, the depressing effect calculation is

assuming that the change in air temperature is mainly driven by radiative and thermal processes and the change in atmospheric circulation: advection of cold and warm air masses. Again, related to an interaction with the surroundings. Are these interactions included in the results? Could you elaborate a bit more on the points mentioned above in the reply-to-the-reviewer?

I would like to see the supporting material in the manuscript regarding the statement that remote sensing products have a more reliable input than model calculations. A follow-up point of discussion is then related to taking the mean value of these data sources. Figure S5 shows the mean value of the two datasets (with and without interaction). When the two sources of data are separately added to the figure, it enables a visualisation of how they differ/ relate to each other and what their magnitude is in comparison to the mean value. Furthermore, can you justify why the heat exchange is ignored while substantial differences between seasons are found? The final depressing effect propagates in the calculation of the air temperature anomaly which plays a key role in the interpretation and attribution of the solar dimming phenomenon and its effects on surface warming over the Tibetan Plateau.

Thanks for your opinion. TOA DSR is from satellite product that is the only possible observation, thus we consider using it rather than the TOA DSR from CMIP5 into the estimation. CMIP5 didn't release surface emissivity and we used ASTER Surface emissivity product to get broadband emissivity.

As for the surface radiation products, we proved that surface CERES DSR satellite product has significantly high accuracy than individual model simulations and can capture the variation of site observations (See open discussion response to #2, Q4, https://www.atmos-chem-phys-discuss.net/acp-2019-553/acp-2019-553-AC2-supplement.pdf). Besides, based on limited surface albedo observations we proved that the combined surface albedo satellite product has high accuracy than individual model simulations. We've added the figure r2 into the supplementary.

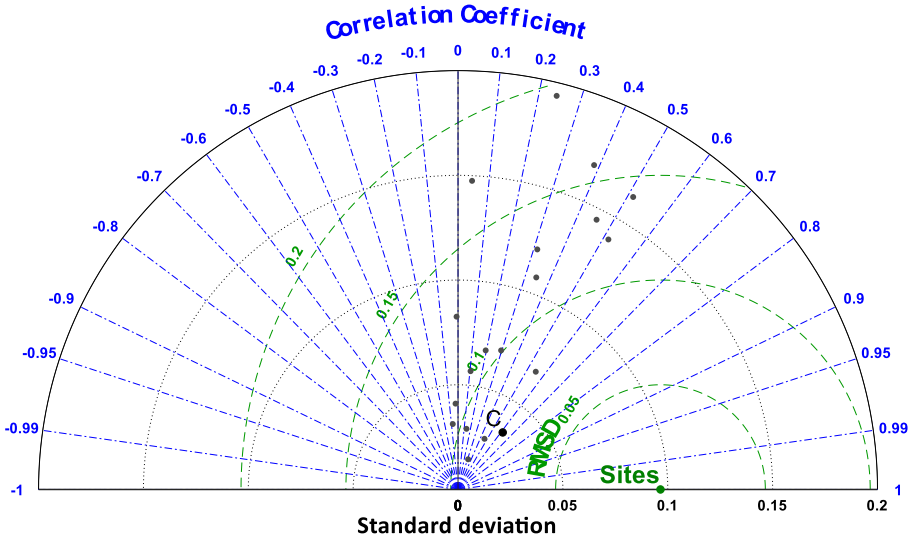


Figure r2 **(Supplementary Fig. 8)**. Taylor diagram of solar validation of CERES EBAF (**black dot C**) and 18 CMIP5 models (**grey dots**) based on the CAMP network.

We used calibrated DSR with TOA DSR to estimate the atmospheric shortwave transmissivity and as we mentioned the surface upward radiation is not calibrated due to limited surface validation data, and we also proved the surface albedo didn't change much. Therefore, we use albedo climatology as input and there is

no contradiction between high accuracy of calibrated DSR results and low accuracy of low CMIP5 TOA DSR and albedo data.

$$\Delta T_a = 1/f\ (S(1-\alpha)\Delta\tau - S\tau\Delta\alpha - \lambda E + \varepsilon_s \sigma T_a^4 \Delta\varepsilon_a$$
$$+ \rho C_d((T_s - T_a)/r_a^2)\Delta r_a) + \Delta T_a^{cir},$$

where the *f* is:

$$f = \rho C_d / r_a + 4\varepsilon_s \sigma \varepsilon_a T_a^3,$$

We used the first-order approximation to estimate the depressing effect of aerosol loading and assumed that near the surface, the Ta change is mainly affected by near-surface radiation and thermal process. In the equation, we ignored the influence from surrounding areas because we would like to express that we only focused on aerosol radiative interaction with Ta (the first item, $1/f\ S(1-\alpha)\Delta\tau$) on Ta, $\Delta T_a^{cir}$ and evapotranspiration parts in the equation are ignored. $\Delta T_a^{cir}$ does have a considerable impact on Ta, but for the aerosol radiative process, we consider that the convective transportations of heat and energy have little impacts on aerosol radiative process. Advective transportation can load more aerosols but it was already demonstrated by the variation of atmospheric transmissivity.

For the aerosol radiative effect, aerosols mainly scatter or absorb the direct and diffuse (mainly direct) downward shortwave radiation. It is possible that the surrounding diffuse light can affect the target pixel by scattering more diffuse light, but we considered it ignorable at 1 lat/lon degree. Besides, these two methods didn't have a significant magnitude difference, therefore, we think the assumption is acceptable. We revised the manuscript to clarify that this method mainly focuses on aerosol radiative effect and the statement "it ignored the heat exchange with surrounding areas" was deleted because heat exchange has little correlation with aerosol radiative process part and will mislead readers.

## MINOR ARGUMENTS

**Minor issue 1:** There is a difference in the validation of shortwave and longwave radiation due to a system bias at the GAME and CAMP networks caused by disparate instruments. The manuscript states that it's a "minor validation difference" but could you please provide a quantification of the difference?

Thanks! We added the quantification in the manuscript. The minor validation RMSE difference (4.68 Wm-2 in DSR and 9.18 Wm-2 in DLR) between the two networks is the system bias mainly caused by disparate instruments and different site numbers.

**Minor issue 2:** Can the spatial mismatch between radiation datasets and site observations be ignored, even though this is in line with former studies? Especially because the results of this study focus on spatiotemporal variation over the Tibetan Plateau it seems a bit counterintuitive to accept a spatial mismatch in data validation.

Yes, for the downward radiation, we consider the spatial mismatch can be ignored. This is because the downward radiation is hardly affected by the surface heterogeneity. The former study also did the analysis for the downward radiation about spatial mismatch issue (Schwarz et al., 2017), it turns out the sites can represent large spatial areas. In fact, the RMSE results in the study include the uncertainty from the spatial mismatch issue, but comparing with other products that have similar spatial scale, our calibrated datasets have better validation results.

**Minor issue 3:** Firstly, it is stated that deep convective clouds have little influence over the Tibetan Plateau whereas further in the text it is described that aerosols enter the Asian tropopause aerosol layer by deep convection. I assume that deep convection occurs in the regions surrounding the Tibetan Plateau and the aerosols are consequently transported. Thus, deep convective clouds are important but in an indirect pathway.

Thanks. We found that the locations of deep convective clouds are very limited (scattering at some pixels) and it's hard to affect the whole TP. It's a reasonable inference that deep convective clouds have an indirect influence on the dimming over the TP and the advective transportation process has been demonstrated in the former study (Lau et al., 2018). Currently, we focus on the direct effect and don't aim to link all the vertical convective interactions with deep convective clouds. This issue can be discussed in future study.

**Minor issue 4:** The overall variation of multiple models (AA and noAA simulations) is of significance tested in temporal analysis and optimal fingerprinting method. However, no values of a statistical test are given.

Thanks! We added the significance level. The p-value of the impact factor in 1950 – 2005 (1970 - 2005) is 0.216 (0.042).

MINOR ISSUES

**Page 1, line 12**: missing "a" before "higher accuracy"

Thanks! We've revised it.

**Page 1, line 15**: "the fastest decrease in DSR is in the southeastern TP". Maybe it looks nicer to write that the fastest decreases occurs/ can be found in the southeastern TP.

Thanks! We've revised it.

**Page 2, lines 31 and 33**: Firstly, increased surface air temperature is mentioned in line 31. Afterwards in line 33 this suddenly becomes surface temperatures. Is the same variable meant here or are we talking about two different things?

Thanks! We've revised all the related issues.

**Page 2, line 41**: Please be careful with the word "significantly" when it's not supported by a value or reference.

Thanks! We've revised it.

**Page 2, lines 42 and 43**: I would recommend being consistent with terminology. In the abstract and in line 36 the term is introduced as solar dimming whereas in these lines it's mentioned as TP dimming.

Thanks! We've revised them.

**Page 2, line 47**: missing "the" before "TP"

Thanks! We've revised all the related issues.

**Page 2, line 48**: “spatial temporal variation” is used whereas elsewhere in the paper the word spatiotemporal variation is used. Or say: “spatial and temporal variation”.

Thanks! We’ve revised it.

**Page 3, line 72**: It’s stated that datasets are chosen which have a spatial resolution less than 2º. However, in Table 1 there are two datasets which have a resolution of 2.50º x 1.88º and one with 2.50º x 1.26º. Are these datasets not used in the analysis? If they are not used it might be better to remove them from the table.

Thanks! They are used in the analysis because we selected the models that at least one dimension is less than 2 degrees. We’ve revised the statement.

**Page 3, line 84**: Perhaps it’s better to move the link to the reference section of the manuscript. It seems out of place here.

Thanks! We’ve replaced all URLs to references.

**Page 4, line 103**: Is spatiotemporal resolution meant, or spatial and temporal resolution?

Thanks! We’ve revised it.

**Page 5, line 130**: I think that “lack” should become lacking. Or “because the sensor calibaration lacks long-term stability”.

Thanks! We’ve revised it.

**Page 5, line 150**: missing “a” before “comparable accuracy”

Thanks! We’ve revised it.

**Page 6, line 166**: Perhaps it’s better to move the link to the reference section of the manuscript. It seems out of place here.

Thanks! We’ve revised it.

**Page 6, line 168**: Perhaps it’s better to move the link to the reference section of the manuscript. It seems out of place here.

Thanks! We’ve revised it.

**Page 6, line 171**: I would phrase the beginning of this sentence slightly different. Perhaps “collected data from 5 GEBA sites” or “included 5 sites from the GEBA network”.

Thanks! We’ve revised it.

**Page 6, line 173**: I would phrase this sentence slightly different. Perhaps “even though the number of sites is not large enough...”.

Thanks! We’ve revised it.

**Page 7, line 194**: “Given that radiative fluxes are always positive, ....”. What kind of sign convention is used here? Usually downward directed fluxes are positive whereas upward direction fluxes are negative (a loss for the surface).

Thanks! We’ve revised it.

**Page 10, line 278**: compressing does not seem like the right word in this context. Perhaps counteracting or diminishing the greenhouse effect?
Thanks! We’ve revised it.

**Page 10, line 279**: missing “the” before “TP”
Thanks! We’ve revised it.

**Page 11, line 319**: missing ”a” before **“**different conclusion”
Thanks! We’ve revised it.

**Page 12, line 339**: missing “the” before “TP” **Page 12, line 340**: missing “the” before “TP”
Thanks! We’ve revised it.

**Page 12, line 343**: missing “the” before “TP”
Thanks! We’ve revised it.

**Page 12, line 357**: “causing **a lower** elevation in the model than **in** reality”
Thanks! We’ve revised it.

**Page 26, Figure 1**: The elevation map which is plotted as background has a scale ranging between 0 and 9000 m. It’s difficult to figure out at which location the individual ground networks are located. Could you please add a scale which is better to read?
We redrew the Figure 1, thanks!

**Page 26, Figure 1**: In the central Tibetan Plateau, the network is quite dense and the symbols overlap each other. Could it be possible to provide a zoom-in on this specific area?
We redrew the Figure 1, thanks!

**Page 26, Figure 1**: The caption became very long because all the projects are mentioned by their full name instead of the abbreviation.
We could but the abbr. needs to be explained when the figures are separated from the main text. Therefore, we didn’t use the abbreviation.

**Page 28, Figure 3**: The Shi and Liang data covers a relatively small amount of time in comparison with the CMIP5 data. Therefore, I think that adding the regression (for the short period only) is not adding a lot of extra surprising information because the trend is already quite obvious from the time-series. In addition, no statistics regarding the regression are mentioned.
Thanks. We’ve deleted the regression.

**Page 28, Figure 4**: The caption doesn't mention which data is used for Surface DSR, DLR and Mean Air Temperature. This is mentioned for the air temperature data obtained from ground measurements.
Thanks. We added the information.

**Page 28, Figure 4**: In the caption of the figure suddenly a p-value of <0.01 shows up which is not clearly mentioned in the manuscript.

We've added the significance level in the manuscript. Thanks!

**Page 29, Figure 5**: In all four panels are linear regression lines added, again without any extra statistical information.
We've added the significance test statement in the caption. Thanks!

**Page 29, Figure 6**: The shaded area is not explained in the caption. Are these confidence intervals? For the second panel, the link with the methodology can be a bit stronger so it becomes clear that this figure belongs to the optimal fingerprinting method.
We added more explanations in the caption. Thanks!

**Page 30, Figure 7**: There is a regression line plotted but there are only four points in the figure, and again no statistical significance mentioned.
We deleted the regression lines because we would like to show the clear difference between summer and other seasons in this figure and the regression lines are useless.

**Page 30, Figure 7**: I would have phrased the first line in the caption different because now it seems that the changes are variable instead of variables which are changing.
We revised it.

**Page 7, Figure 7**: In the manuscript, only an explanation is given for the summer season while the other three seasons are plotted as well. Why is it useful to leave them in the figure when nothing is mentioned about them?
Thanks! We would like to show the difference between summer and other seasons. They are left to be compared with summer points. We don't aim to explain all the points and would like to figure out the fastest dimming season and demonstrate the possible reasons.

**Page 7, Figure 8**: The data source is not completely clear to me from the figure caption. Additionally, extra lines which are not represented in the legend are present in the figure (yellow, light-blue and orange). What do these lines represent? The caption and legend should have provided this information. Finally, the shaded area is not explained in the caption. Are these confidence intervals?
The shaded areas in the study are the standard deviation of model average. We've revised the captions and the figure. Data source in Figure 7 is added (CMIP5 model average) and data source in Figure 8 is explained in the corresponding methodology (satellite products used in the first-order approximation method are listed in table 2 and auxiliary meteorological variables like wind, and relative humidity are from CMIP5 historical experiments. NoAA derived air temperature (Ta) data in another method are from CMIP5 HistoricalMisc experiments; and Historical Ta is from the average of four air temperature datasets). Thanks for providing your concern.

**Supplementary material:**

**Page 4, Figure S2 and S3**: The statistical quantification is lacking for the regression (e.g. R2-values).

Thanks. We've revised it.

**Page 5, Figure S5 and S6**: The shaded areas represent uncertainties but it's not mentioned how large these uncertainties are. Is it the 5%-95% confidence interval? The light-red colour in Figure S6 is difficult to see.

We've revised the caption and figure. Thanks.

## References


Andreae, M. O., Jones, C. D., and Cox, P. M.: Strong present-day aerosol cooling implies a hot future, Nature, 435, 1187, 2005.

Feng, H., and Zou, B.: Satellite-based estimation of the aerosol forcing contribution to the global land surface temperature in the recent decade, Remote Sensing of Environment, 232, 111299, 2019.

Gettelman, A., Shindell, D., and Lamarque, J.-F.: Impact of aerosol radiative effects on 2000–2010 surface temperatures, Climate dynamics, 45, 2165-2179, 2015.

He, T., Liang, S., and Song, D. X.: Analysis of global land surface albedo climatology and spatial‐temporal variation during 1981–2010 from multiple satellite products, Journal of Geophysical Research: Atmospheres, 119, 10,281-210,298, 2014.

He, Y., Wang, K., Zhou, C., and Wild, M.: A revisit of global dimming and brightening based on the sunshine duration, Geophysical Research Letters, 45, 4281-4289, 2018.

Kuang, X. X., and Jiao, J. J.: Review on climate change on the Tibetan Plateau during the last half century, J Geophys Res-Atmos, 121, 3979-4007, 10.1002/2015jd024728, 2016.

Lau, W. K. M., Yuan, C., and Li, Z.: Origin, Maintenance and Variability of the Asian Tropopause Aerosol Layer (ATAL): The Roles of Monsoon Dynamics, Sci Rep, 8, 3960, 10.1038/s41598-018-22267-z, 2018.

Lewis, P., Brockmann, C., and Muller, J.: GlobAlbedo: Algorithm theoretical basis document V4-12, in: Technical Report, 2013.

Li, Z., Rosenfeld, D., and Fan, J.: Aerosols and their impact on radiation, clouds, precipitation, and severe weather events, in: Oxford Research Encyclopedia of Environmental Science, 2017.

Manara, V., Brunetti, M., Maugeri, M., Sanchez‐Lorenzo, A., and Wild, M.: Sunshine duration and global radiation trends in Italy (1959–2013): To what extent do they agree?, Journal of Geophysical Research: Atmospheres, 122, 4312-4331, 2017.

Qian, Y., Yasunari, T. J., Doherty, S. J., Flanner, M. G., Lau, W. K., Ming, J., Wang, H., Wang, M., Warren, S. G., and Zhang, R.: Light-absorbing particles in snow and ice: Measurement and modeling of climatic and hydrological impact, Advances in Atmospheric Sciences, 32, 64-91, 2015.

Riihelä, A., Manninen, T., Laine, V., Andersson, K., and Kaspar, F.: CLARA-SAL: a global 28 yr timeseries of Earth's black-sky surface albedo, Atmospheric Chemistry and Physics, 13, 3743-3762, 2013.

Samset, B., Sand, M., Smith, C., Bauer, S., Forster, P., Fuglestvedt, J., Osprey, S., and Schleussner, C. F.: Climate impacts from a removal of anthropogenic aerosol emissions, Geophysical Research Letters, 45, 1020-1029, 2018.

Schwarz, M., Folini, D., Hakuba, M. Z., and Wild, M.: Spatial Representativeness of Surface‐Measured Variations of Downward Solar Radiation, Journal of Geophysical Research: Atmospheres, 122, 13,319-313,337, 2017.

Shi, Q. Q., and Liang, S. L.: Characterizing the surface radiation budget over the Tibetan Plateau with ground-measured, reanalysis, and remote sensing data sets: 2. Spatiotemporal analysis, J Geophys Res-Atmos, 118, 8921-8934, 10.1002/jgrd.50719, 2013.

Wang, Z., Li, Z., Xu, M., and Yu, G.: River morphodynamics and stream ecology of the Qinghai-Tibet Plateau, CRC Press, 2016.

Yang, K., Koike, T., and Ye, B.: Improving estimation of hourly, daily, and monthly solar radiation by importing global data sets, Agricultural and Forest Meteorology, 137, 43-55, 2006.

Yang, K., Ding, B. H., Qin, J., Tang, W. J., Lu, N., and Lin, C. G.: Can aerosol loading explain the solar dimming over the Tibetan Plateau?, Geophysical Research Letters, 39, Artn L2071010.1029/2012gl053733, 2012.

Yang, K., Wu, H., Qin, J., Lin, C. G., Tang, W. J., and Chen, Y. Y.: Recent climate changes over the Tibetan Plateau and their impacts on energy and water cycle: A review, Global Planet Change, 112, 79-91, 10.1016/j.gloplacha.2013.12.001, 2014.

Yao, T., Xue, Y., Chen, D., Chen, F., Thompson, L., Cui, P., Koike, T., Lau, W. K.-M., Lettenmaier, D., and Mosbrugger, V.: Recent Third Pole's rapid warming accompanies cryospheric melt and water cycle intensification and interactions between monsoon and environment: multi-disciplinary approach with observation, modeling and analysis, Bulletin of the American Meteorological Society, 2018.
You, Q. L., Kang, S. C., Flugel, W. A., Sanchez-Lorenzo, A., Yan, Y. P., Huang, J., and Martin-Vide, J.: From brightening to dimming in sunshine duration over the eastern and central Tibetan Plateau (1961-2005), Theoretical and Applied Climatology, 101, 445-457, 10.1007/s00704-009-0231-9, 2010.

# Air pollution slows down surface warming over the Tibetan Plateau

Aolin Jia[1], Shunlin Liang[1], Dongdong Wang[1], Bo Jiang[2], Xiaotong Zhang[2]

[1]Department of Geographical Sciences, University of Maryland, College Park, MD, 20742, USA
[2]State Key Laboratory of Remote Sensing Science, Faculty of Geographical Science, Beijing Normal University, Beijing, 10085, China

*Correspondence to*: Shunlin Liang (sliang@umd.edu)

**Abstract.** The Tibetan Plateau (TP) plays a vital role in regional and global climate change. The TP has been undergoing significant surface warming since 1850, with an air temperature increase of 1.39 K and surface solar dimming resulting from decreased incident solar radiation. The causes and impacts of solar dimming on surface warming are unclear. In this study, long-term (from 1850–2015) surface downward radiation datasets over the TP are developed by integrating 18 Coupled Model Intercomparison Project Phase 5 (CMIP5) models and satellite products. The validation results from two ground measurement networks show that the generated downward surface radiation datasets have a higher accuracy than the mean of multiple CMIP5 and the fused datasets of reanalysis and satellite products. After analyzing the generated radiation data with four air temperature datasets, we found that downward shortwave radiation (DSR) remained stable before 1950 and then declined rapidly at a rate of -0.53 W $m^{-2}$ per decade and that the fastest decrease in DSR ~~is~~ occurs in the southeastern TP. Evidence from site measurements, satellite observations, reanalysis, and model simulations suggested that the TP solar dimming was primarily driven by increased anthropogenic aerosols. The TP solar dimming is stronger in summer, at the same time that the increasing magnitude of the surface air temperature is the smallest. The cooling effect of solar dimming offsets surface warming on the TP by 0.80 ± 0.28 K (48.6 ± 17.3%) in summer since 1850. It helps us understand the role of anthropogenic aerosols in climate warming, and highlights the need for additional studies to be conducted to quantify the influence of air pollution on regional climate change over the TP.

## 1 Introduction

The Tibetan Plateau (TP), the so-called Third Pole, covers an area of approximately 2.65 × $10^2$ $km^2$ and has an average elevation of more than 4000 m. It contains the largest ice mass outside of the polar regions (Yao et al., 2007) which supplies several major rivers that sustain billions of people in China and South Asia, dominating regional social stabilization and development. The TP is a weak heat sink in winter but a strong heat source in summer and dominates the atmospheric circulation (Wu et al., 2015). The mechanical and thermal forcing of the large-scale orography is crucial for the formation of the Asian summer monsoon (Boos and Kuang, 2010) and water and heat exchange between the Pacific Ocean and Eurasia (Wu et al., 2012). The TP anticyclone transports water vapor and chemical gases into the lower stratosphere (Fu et al., 2006).

Therefore, the local climate pattern over the TP plays a vital role in the climate in southern China (Xu et al., 2013), the boreal climate (Sampe and Xie, 2010), and global climate change (Cai et al., 2017).

The TP is currently undergoing significant climate change (Yao et al., 2018), such as increased surface air temperature (Kuang and Jiao, 2016) and downward longwave radiation (DLR), as well as decreased downward solar radiation (DSR) (You et al., 2010) which is a solar dimming phenomenon that can impact surface air temperatures (Wild et al., 2007) and precipitation (Wild, 2009). However, the causes of solar dimming over the TP are not yet conclusive (Kuang and Jiao, 2016;Xie and Zhu, 2013;Xie et al., 2015). Changes in DSR are mainly controlled by atmospheric clouds and aerosols (Liang et al., 2010) at century-level scales. You et al. (2013) suggested that aerosols have played an important role in solar dimming over the TP in recent decades, while Tang et al. (2011) speculated that solar dimming over the TP might be caused by cloud cover changes that have a comparable influence on solar dimming to that of aerosol loading changes. Although some studies have suggested that brown clouds that are formed due to aerosols over the Indian Ocean and Asia (Ramanathan et al., 2007) might be transported to the TP by the summer monsoon, Yang et al. (2012) and (2014) contended that the main drivers are deep convective clouds and atmospheric water vapor, and that aerosol radiative forcing is too small to result in the ~~significantly~~ decreased DSR over the TP. These studies clearly show contradictory conclusions regarding the proper attribution of the ~~TP~~ solar dimming; therefore, the roles of aerosols and clouds in ~~TP~~ solar dimming still need to be determined. Moreover, some of these studies were mainly based on ground measurements at a limited number of sites that cannot represent the entire TP. Furthermore, the surface observed sunshine duration data that were used for estimating DSR (Wang, 2014;Yang et al., 2006) were not available over the TP until the 1960s. Regardless, the statistical model can hardly capture the low aerosols' influences on surface solar radiation by sunshine duration ~~especially at complex terrains in TP~~because sunshine duration has a lower sensitivity than DSR to atmospheric turbidity changes that is estimated by aerosol optical depth (AOD) (Manara et al., 2017). Thus, considering that remote sensing has been developed for several decades, it provides a valuable opportunity to employ satellite observations to monitor spatiotemporal~~spatial temporal~~ variations at regional scales.

The radiative effect of anthropogenic aerosols has not yet been well quantified ~~by observations~~ over the TP, ~~and this~~ which ~~information~~ is necessary for understanding the role of anthropogenic aerosols in climate warming, and revealing impacts of human activities in remote areas. Aerosols have a net cooling effect on the global temperature with higher uncertainty from Intergovernmental Panel on Climate Change (IPCC) report (Stocker et al., 2013), whereas Andreae et al. (2005) have suggested that current aerosol loading may cause a hot future. Even Gettelman et al. (2015) contended that the net effect of aerosols on surface temperature can be neglected, Samset et al. (2018) pointed out that aerosol depressed surface temperature by 0.5-1.1 K globally. By contrast, one recent study (Feng and Zou, 2019) argued that aerosols contributed + 0.005 ± 0.237 K on global surface temperature change after 2000. Therefore, the aerosol effect on climate warming is still under discussion. Model simulations (Ji et al., 2015) have shown that carbonaceous aerosols have positive radiative forcing effects on climate warming over the TP, leading to a 0.1–0.5 °C warming in the monsoon season, while some studies have demonstrated that anthropogenic aerosols (AAs) have a cooling effect on local climate warming (Smith et al., 2016;Sundström et al., 2015). Gao et al. (2015)

contended that aerosols cool the surface 0.8 – 2.8 K in North China Plain, and Li et al. (2015) calculated the aerosol impact on climate warming in different seasons over arid-semiarid and humid-semiarid areas, and across China, and showed that China undergoes a cooling rate of −0.86 to −0.76 °C per century due to increased aerosols. However, ~~these~~ former conclusions were mainly based on model simulations (Liao et al., 2015) and have not yet been combined with observations. Therefore, there is no consistent result of quantifying the impact of anthropogenic aerosols on climate warming especially at the TP and the observations from multiple data sources are urgently needed in the quantification.

In this study, we aim to analyze the long-term spatiotemporal variation of surface radiation over the TP by generating long-term surface radiation datasets from satellite products and model simulations. Solar dimming is to be attributed by analyzing multiple data sources. The depressing effect of aerosols on climate warming needs to be quantified in the end. Calibrated by the Clouds and the Earth's Radiant Energy System Energy Balanced and Filled (CERES EBAF) Edition 4.0 surface downward radiation products (Kato et al., 2018), long-term (from 1850–2015) surface DSR and DLR datasets over the TP were developed by merging 18 Coupled Model Intercomparison Project Phase 5 (CMIP5) models (Taylor et al., 2012). Site validation and comparison were processed to the calibrated data, the CMIP5 model outputs, and other long-term radiation products. The spatiotemporal variations in the generated surface radiation datasets and four long-term air temperature datasets were initially analyzed, and the TP solar dimming was attributed by using multiple types of satellite and reanalysis data, which were confirmed by climate model simulations. We characterized the seasonal difference of the TP solar dimming and further quantified the depressing effect on local climate warming since 1850 using two methods driven by satellite observations and model simulations.

## 2 Data and Methodology

### 2.1 Data

#### 2.1.1 Coupled Model Intercomparison Project Phase 5 (CMIP5) data

The CMIP5 (Taylor et al., 2012) datasets with at least one dimension of spatial resolutions less than 2° were chosen in the paper, and 18 monthly modeled datasets (summarized in Table 1) from the Historical experiment were included, which cover 1850 to 2005; the following years (2006–2015) of records are from the Representative Concentration Pathway (RCP) 8.5 experiment. We used the first ensemble (r1i1p1) only of each experiment to reduce the calibration complexity of surface downward radiation. Aerosol optical depth (AOD), precipitation, and wind speed from the Historical (1850 - 2005) and RCP8.5 (2006 - 2015) experiments of the models were used to analyze differences in dimming magnitudes at seasonal scales (Figure 7). Surface temperature, wind speed, and relative humidity were employed for calculating the aerosol depressing effect due to the long-term coverage. The corresponding HistoricalMisc experiment (i.e., an experiment that combined different specific forcings) data were also utilized in the attribution analysis, including downward shortwave radiation driven by AA and noAA (all forcings except AA). NoAA derived near-surface air temperature from multiple model ensembles is used in the depressing

effect analysis. The PiControl experiment provided the natural internal variation utilized in the optimal fingerprinting method (Methodology 2.2.2). The attribution and depressing effect calculation included all the available variable ensembles of each model, including wind speed, precipitation, surface temperature, air temperature, and relative humidity. All datasets were resampled into 1 Lat/Lon degree using a bilinear interpolation method. CMIP5 datasets are available from the Intergovernmental Panel on Climate Change (IPCC) data distribution center at the website (PCMDI, 2013).

### 2.1.2 Remote sensing and assimilation products

#### 2.1.2.1 Clouds and the Earth's Radiant Energy System Energy Balanced and Filled (CERES EBAF) radiation products

The CERES EBAF-surface Edition 4.0 monthly downward shortwave and longwave radiation products (Kato et al., 2018) were employed as a benchmark for calibrating simulated CMIP5 surface radiation by a non-negative least square (NNLS) regression approach (Bro and De Jong, 1997) (Methodology 2.2.1). Comparing with former solar radiation products, CERES EBAF has been comprehensively assessed and considered as the most advanced surface radiation satellite product. It is usually used as a reference for model and reanalysis validation (Zhang et al., 2015;Zhang et al., 2016). It can capture the temporal variation of surface radiation by comparing it with surface measurements (Supplementary Fig. S1). Besides, former studies have already used the CERES EBAF DSR product for applications and analysis (Feng and Wang, 2018;Ma et al., 2015). This new version contains surface fluxes consistent with the top-of-atmosphere (TOA) fluxes provided from the CERES Energy Balanced and Filled Top of Atmosphere (EBAF-TOA) data product. They also used improved cloud properties that are corrected by cloud profiling radar, and consistent input sources are employed, such as temperature, humidity, and aerosol data, in order to solve the spurious anomaly problem (Jia et al., 2018;Jia et al., 2016). All the advantages help to quantify the absolute magnitude and temporal trend of surface DSR (Feng and Wang, 2019). The CERES EBAF-TOA Edition 4.0 monthly TOA albedo product (Loeb et al., 2018) was used for computing the temporal variation in the TOA albedo over the Tibetan Plateau (TP) in the dimming attribution analysis. The CERES EBAF TOA solar radiation and surface albedo products ~~was~~ were used as a monthly climatology. ~~and~~TOA solar radiation was combined with the calibrated surface DSR data to compute the atmospheric shortwave transmissivity in the aerosol depressing effect quantification. Meta information on the included products is summarized in Table 2. All products were pre-processed into 1 degree at a monthly scale for further analysis to unify the spatial and temporal resolutions.

#### 2.1.2.2 Aerosol, cloud, and dust products

Multiple aerosol, cloud, and dust products were employed for the attribution of solar dimming. The averages of the Moderate Resolution Imaging Spectroradiometer (MODIS) MOD/MYD08 Collection 6.1 aerosol optical depth (AOD) 550 products that combine the Dark Target and Deep Blue algorithms were used for detecting aerosol variations over the TP. The MOD/MYD08 C6.1 cloud fraction was also included in the attribution analysis. In MODIS C6.1, the brightness temperature biases and trending were substantially reduced compared to C6, which affected the cloud retrieval and also caused large uncertainty with respect to the AOD over elevated areas (Sogacheva et al., 2018). Additionally, the MODIS AOD coverage increased in C6.1.

The Sea-Viewing Wide Field-of-View Sensor (SeaWiFS) AOD550 product (Sayer et al., 2012) utilized 12 candidate aerosol models for generating the aerosol lookup tables (Hsu et al., 2012), and AODs at different wavelengths have been retrieved over land with the use of the Deep Blue algorithm (Pozzer et al., 2015). The SeaWiFS AOD550 product was used for calculating the aerosol temporal variation over the TP.

The aerosol index data were inversed from Total Ozone Mapping Spectrometer (TOMS)-Nimbus 7, TOMS-Probe, and Ozone Monitoring Instrument (OMI) at different time periods (Ahmad et al., 2006). We employed TOMS N7 records from 1980 to 1992, TOMS Probe from 1997 to 2004, and OMI from 2005 to 2015. By using the 340- and 380-nm wavelength channels (which have negligible dependence on ozone absorption), the aerosol index was defined based on backscattered radiance measured by TOMS and OMI and the radiance calculated from a radiative transfer model for a pure Rayleigh condition (Hsu et al., 1999). This approach measures the relative amount of aerosols and has a comparable relationship with AOD (McPeters et al., 1998).

Particulate matter (PM) 2.5, characterizing very small particles that have a diameter of < 2.5 μm and are produced by human activities, is a common index of air pollution (Wang et al., 2015). We employed the PM2.5 satellite products to link the aerosol loading with air pollution. The PM2.5 satellite product is calculated from MODIS, Multi-angle Imaging SpectroRadiometer (MISR), and SeaWiFS AOD products based on a relationship generated from a chemical transport model (Van Donkelaar et al., 2016), and its uncertainty is determined by ground measurements.

MERRA2 aerosol products are the new generation reanalysis data that have assimilated MODIS and MISR land aerosol products since 2000 (Randles et al., 2017). Dust column mass density from MERRA2 was included for comparison of the temporal variation with PM2.5 data to determine whether the AOD increase was due to air pollution.

International Satellite Cloud Climatology Project (ISCCP) and Pathfinder Atmospheres–Extended (PATMOS-X) provide long-term cloud fraction products, however, the trend is spurious (Evan et al., 2007). This is because of the satellite zenith angle, equatorial crossing time, and because ~~of~~ the sensor calibration lacks long-term stability. Corrected cloud fraction datasets (Norris and Evan, 2015), which were used for solar dimming attribution in this paper, employed an empirical method for removing artifacts from the ISCCP and PATMOS-X, and the corrected cloud products have been used for providing evidence for climate change in satellite cloud records in other studies (Norris et al., 2016).

The European Centre for Medium-Range Weather Forecasts reanalysis 5 (ERA5) (Hersbach and Dee, 2016), as the newest reanalysis dataset, is also employed for attributing the solar dimming. ERA5 is the fifth generation of ECMWF atmospheric reanalyses and follows the widely used ERA-Interim. By comparing with ERA-Interim, it has higher spatial and temporal resolutions and finer atmospheric levels. In addition, it includes various newly reprocessed datasets and recent instruments that could not be ingested in ERA-Interim. ERA5 provides atmospheric profiles with high accuracy by assimilating conventional observations (e.g., balloon samples, buoy measurements) and satellite retrievals. Therefore, total column water vapor and cloud fraction from ERA5 are used in the study. ~~(Service, 2017)~~

Diagnosing Earth's Energy Pathways in the Climate system (DEEP-C) TOA albedo was calculated by the DEEP-C monthly TOA absorbed solar radiation (ASR) (Allan et al., 2014) and monthly TOA incoming solar radiation climatology from the CERES EBAF-TOA Ed4.0 product. The DEEP-C TOA albedo was used for detecting the radiative influence of increasing aerosols in the dimming attribution. Central to the DEEP-C TOA radiation reconstruction are monthly observations of the TOA radiation from the CERES scanning instruments after 2000 and Earth Radiation Budget Satellite (ERBS) wide field of view (WFOV) nonscanning instrument from 1985 to 1999. A strategy was required to homogenize the satellite datasets (Allan et al., 2014), and the ~~European Centre for Medium-Range Weather Forecasts interim reanalysis (~~ERA-Interim~~)~~ has provided atmospheric information since 1979, also using a subset of nine climate models to represent direct and indirect aerosol radiative forcings.

#### 2.1.2.3 ~~Global LAnd Surface Satellite (GLASS) s~~Surface albedo products

According to He et al. (2014), the fine-resolution (0.05°) climatological surface albedo products retrieved from satellite observations agree well with each other for all the land cover types in middle to low latitudes. Therefore, we selected four commonly used satellite surface albedo products for calculating the surface albedo climatology over the TP, including the CERES EBAF, the Global LAnd Surface Satellite (GLASS), the Clouds, Albedo, and Radiation-Surface Albedo (CLARA-SAL), and the GlobAlbedo from 2001 to 2011 (covered by the four products). First, we generated the monthly climatological albedo of each satellite product, and we computed all standard deviations of any possible three product climatology combinations at each pixel. Then for each pixel, we chose the product combination that has the lowest standard deviation and calculated the mean value to represent the ground truth climatology.

~~The GLASS surface albedo product provides ancillary data for calculating the aerosol depressing effect.~~ The GLASS albedo product from MODIS observations is based on two direct albedo estimation algorithms (He et al., 2014); one designed for surface reflectance and one for TOA reflectance (Qu et al., 2014). The statistics-based temporal filtering fusion algorithm is used to integrate these two albedo products (Liu et al., 2013a). The GLASS albedo product has been assessed by ground measurements and the MODIS albedo product and has a comparable accuracy (Liu et al., 2013b). The CLARA-SAL product is inversed from advanced very high resolution radiometer (AVHRR) observations (Riihelä et al., 2013). Atmospheric correction was done by assuming AOD and ozone is constant. Sensor calibration and orbital drift have been dealt with and the uncertainty of monthly albedo estimation is about 11%. The GlobAlbedo product uses an optimal estimation approach European satellites, including Advanced Along-Track Scanning Radiometer (AATSR), SPOT4-VEGETATION, SPOT5-VEGETATION2, and Medium-Resolution Imaging Spectrometer (MERIS) (Lewis et al., 2013). MODIS surface anisotropy information was used for gap-filling. More detailed algorithm introductions and comparison can be found in He et al. (2014).

#### 2.1.2.4 Advanced Spaceborne Thermal Emission and Reflection Radiometer Global Monthly Emissivity Dataset (ASTER_GED)

The ASTER surface emissivity data were also used for calculating the aerosol depressing effect. The ASTER_GED data products are generated using the ASTER Temperature Emissivity Separation algorithm (Gillespie et al., 1998) atmospheric correction method. This algorithm uses MODIS Atmospheric Profiles product MOD07 and the MODTRAN 5.2 radiative transfer model, snow cover data from the standard monthly MODIS/Terra snow cover monthly global 0.05° product MOD10CM, and vegetation information from the MODIS monthly gridded NDVI product MOD13C2 (NASA JPL. ASTER Global Emissivity Dataset, 2016). Surface broadband emissivity is calculated according to Cheng et al. (2014).

### 2.1.3 Ground measurements

Utilized for surface radiation validation, ground radiation measurement sites over the TP are mainly from two ground networks (Global Energy and Water Exchanges [GEWEX] Asian Monsoon Experiment [GAME] (Yasunari, 1994) and Coordinated Energy and Water Cycle Observation Project (CEOP) Asia-Australia Monsoon Project [CAMP] (Leese, 2001)) that cover 1995–2005. The GAME was proposed as an international project under the Global Energy and Water Exchanges (GEWEX) program to understand the processes associated with the energy and hydrological cycle of the Asian monsoon system, and its variability. The data are available at GAME-ANN (2005). The CAMP, which followed the GAME, focused on water and energy fluxes and reservoirs over specific land areas and monsoonal circulations. These data are available at CAMPTibet (2006) ~~http://metadata.diasjp.net/dmm/doc/CEOP_CAMP_Tibet-DIAS-en.html~~. We ignored the spatial representative difference between site observations and downward radiation datasets in line with former studies (Wang and Dickinson, 2013;Zhang et al., 2015).

We also collected ~~5 sites~~ground observations from 5 China Meteorological Administration ~~Global Energy Balance Archive (GEBA)~~(CMA) sites over the TP to detect long-term temporal variation of surface DSR from ~~1960~~ 1958 to ~~2000~~1980. ~~The China Meteorology Administration (CMA) network~~The observations after 1980s ~~is~~are not included due to ~~a systematic error in the 1990s~~the data discontinuity issue (Zhang et al., 2015). ~~This ground measurement network is developed and maintained at ETH Zurich and the random error of DSR is 2% for annual means (Zhang et al., 2015).~~ Even the site amount is not large enough to represent the whole TP, the sampled surface measurements can reflect the ground truth and ~~support~~ prove the ~~our conclusion~~dimming over the TP (Supplementary Fig. S2). 22 sites that observed downward radiation in the TP were included in this study, and their distribution is shown in Figure 1. The Tibetan Plateau region is defined as the Chinese Qinghai-Tibet Plateau in this paper, covering most of the Tibet Autonomous Region and Qinghai in western China (Wang et al., 2016).

### 2.1.4 Surface air temperature datasets

Four long-term surface air temperature datasets were used for characterizing the temporal variation over the TP and corresponding aerosol depressing effect; the Berkley Earth Surface Temperature land surface air temperature dataset (BEST-LAND) (Rohde et al., 2013), Climate Research Unit Temperature Data Set version 4 (CRU-TEM4v) (Jones et al., 2012), National Aeronautics and Space Administration Goddard Institute for Space Studies (NASA-GISS) (Hansen et al., 2010), and National Oceanic and Atmospheric Administration National Center for Environmental Information (NOAA-NCEI) (Smith et

al., 2008). These data were interpolated and homogenized from ground observation networks. Rao et al. (2018) provided data assessment of the four air temperature datasets, and a brief summary of the datasets is provided in Supplementary Table S1.

### 2.2 Methodology

#### 2.2.1 Calibration method

Long-term series surface downward radiation data are urgently needed for characterizing the spatial-temporal variation of surface radiation budget over the TP, and they are also essential for the solar dimming attribution and calculating the aerosol radiative forcing and depressing effect on the increasing air temperature. To generate a long-term series surface downward radiation data record with high accuracy, a non-negative least squares (NNLS) regression (Bro and De Jong, 1997) approach was employed for merging multiple CMIP5 model records. The non-negative multiple linear models are utilized because the non-negativity constraint of NNLS only applies a non-subtractive combination of all components (Eq. [1]).

$$y = \sum a_i x_i \,, (a_i \geq 0), \tag{1}$$

where $y$ is the calibrated radiation data, $a_i$ is the coefficient of each CMIP5 model simulation $x_i$.

The calibration was done pixel by pixel to avoid the influence of geolocation and elevation. Given that downward radiative fluxes are always positive, a key assumption here is that the CERES radiative flux can be expressed as a non-negative linear combination of each model output at each grid. One CMIP5 model may hardly present the variations in the actual radiative fluxes but should not have any negative contributions. To avoid the influence from the seasonal cycle on the expression of the inter-annual variation of the radiative flux, the fusion models were generated monthly. The CERES satellite products aid NNLS to provide the best-weighted combination for each CMIP5 model, producing improved validation results compared to those produced by only using the mean of all model outputs. Mean Bias Error (MBE), Root-Mean-Square-Error (RMSE), and $R^2$ were utilized for quantifying site validation and comparing with the mean CMIP5 data and multiple satellite and reanalysis product fused radiation data from Shi and Liang (2013). The temporal variation and comparison among products are calculated by using latitude-weighted average over the TP. ~~Detailed~~ A detailed description of assessment methods ~~are~~ is introduced in Jia et al. (2018).

#### 2.2.2 Attribution analysis

Optimal fingerprinting is a common method in the attribution analysis of model data. It is based on a linear relationship, and, if the scaling factor is > 0 at a certain significance level, the variable has a positive contribution toward the responding variable. The optimal fingerprinting method has been widely applied for climate change detection and attribution (Sun et al., 2014;Zhou et al., 2018). It is assumed that the response variable has a linear relationship with different driving variables (Eq. [2]):

$$y = \sum \beta_i x_i + \varepsilon, \tag{2}$$

where $\varepsilon$ is the modeled natural internal variation obtained from the CMIP5 piControl Experiment, and $\beta_i$ is the scaling factor of each driving variable. $x_i$ are the DSR simulation results from averages of aerosol-driven experiment ensembles and non-aerosol-driven experiment ensembles in this study. If the scaling factor is > 0 at a certain significance level (in this study, 5% – 95% uncertainties are estimated based on Monte Carlo simulations), the variable has a positive contribution toward the responding variable. In CMIP5 HistoricalMisc experiment, anthropogenic forcings are focused, thus in this study only experiment with anthropogenic aerosols (AA) and without AA (noAA) were employed for the attribution. Impact simulations of cloud/water vapor are not covered in the experiment and we assumed that noAA experiment can represent the model simulation about the cloud/water vapor impacts on surface downward shortwave radiation.

### 2.2.3 Depressing effect

For quantitating the depressing effect of aerosols on surface warming over the TP, the shortwave and longwave radiative effects must be separated. To calculate the relationship between the surface air temperature increase and surface radiation components, it is necessary to decompose the energy sources into separate mechanisms. The land surface energy balance is given by Eq. (3):

$$S_n + L_n = \lambda E + H + G, \tag{3}$$

where $S_n$ is the net shortwave radiation, $L_n$ is the net longwave radiation, $\lambda$ is the latent heat of vaporization, $E$ is evapotranspiration, $H$ is the sensible heat flux, and $G$ is the ground heat flux that was neglected for the long time period. They can be decomposed in Eq. (4) as:

$$S\tau(1-\alpha) + \varepsilon_s\sigma(\varepsilon_a T_a^4 - T_s^4) = \lambda E + \rho C_d\,(T_s - T_a)/r_a, \tag{4}$$

where $S$ is the TOA solar radiation, $\tau$ is the atmospheric shortwave transmissivity (ratio between the calibrated surface DSR and S), $\alpha$ is the surface albedo, $\varepsilon_s$ is the surface broadband emissivity, $T_a$ is the air temperature, $T_s$ is the surface skin temperature, and $r_a$ is the aerodynamic resistance at 2 m height. $\sigma$ is equal to $5.67 \times 10^{-8}$ W m$^{-2}$ K$^{-4}$, $\rho$ is 1.21 kg m$^{-3}$, and $C_d$ is 1013 J kg$^{-1}$ K$^{-1}$. $\varepsilon_a$ is the air emissivity parameterized based on Carmona et al. (2014) that has the highest accuracy by comparing with other parameterization methods (Guo et al., 2019). Considering that the $\Delta T_a$ is mainly dominated by the change in $T_s$ interacting with $T_a$ through radiative and thermal processes and the change in atmospheric circulation ($\Delta T_a^{cir}$, for example, advection of cold and warm air masses), a first-order approximation of the direct near-surface temperature response to each component (Zeng et al., 2017) is derived from Eq. (5) and Eq. (6):

$$\Delta T_a = 1/f\,(S(1-\alpha)\Delta\tau - S\tau\Delta\alpha - \lambda E + \varepsilon_s\sigma T_a^4\Delta\varepsilon_a + \rho C_d((T_s - T_a)/r_a^2)\Delta r_a) + \Delta T_a^{cir}, \tag{5}$$

where the $f$ is:

$$f = \rho C_d/r_a + 4\varepsilon_s\sigma\varepsilon_a T_a^3, \tag{6}$$

and $f^{-1}$ represents the land surface air temperature sensitivity to 1 W m$^{-2}$ radiative forcing at the land surface. We assumed that $S$, $\lambda$, $\rho$, $C_d$, $\sigma$, and $\varepsilon_s$ are independent of $T_s$. We employed the $\alpha$, $\varepsilon_s$, and $S$ climatologies and the mean values of the satellite products for several years (details in Table 2). Therefore, the $T_a$ response to the surface DSR change is calculated by the first term (related to $\Delta\tau$) in the formula. $\Delta T_a^{cir}$ are not computed in the analysis because they have limited impact on aerosol radiative effect. Based on Eq. (7):

$$\mathrm{DLR} = \sigma \varepsilon_a T_a^4, \tag{7}$$

from Eq. (8) we can also obtain the relationship between $\Delta T_a$ and $\Delta$DLR:

$$\Delta T_a^{DLR} = \Delta\mathrm{DLR}/(4\sigma\varepsilon_a T_a^3). \tag{8}$$

We then added the depressing effect from $\Delta$DSR and $\Delta$DLR to get the aerosol depressing effect on the TP climate warming. ~~Although t~~The first-order approximation method included many reliable remote sensing products and ~~had more reliable input than the model calculation~~it's reasonable to use climatology of the TOA and surface variables in the equation (Supplementary Fig. S8)~~, it ignored the heat exchange with surrounding areas~~. ~~Hence, w~~We also calculated the depressing effect of AAs by employing the CMIP5 air temperature data from multiple noAA simulations, which used physical parametrization methods~~computed the influence of the interaction with other regions~~. The two methods can validate each other. We then compared the two results (Supplementary Fig. ~~S5~~S7) and calculated the mean value as the final depressing effect result.

## 3 Results and discussion

### 3.1 Validation and comparison of the calibrated downward radiation data

From January 1995 to December 2005, in situ observations were collected at 17 sites for monthly validation of DSR and DLR. The scatter diagrams and validation results of the CERES calibrated data, mean CMIP5, and reanalysis and satellite fused product from Shi and Liang (2013) at two networks are shown in Figure 2.

Figure 2 indicates that the CERES calibrated datasets have the lowest bias and RMSE for DSR and DLR validation at GAME and CAMP network, and the $R^2$ at CAMP network has the highest. The bias of the calibrated DSR at CAMP (GAME) is -0.27 (-3.68) Wm$^{-2}$ and the RMSE is 20.59 (25.27) Wm$^{-2}$, whereas the bias of calibrated DLR at CAMP (GAME) is 0.63 (-4.31) Wm$^{-2}$ and the RMSE is 11.90 (21.08) Wm$^{-2}$. We can conclude that by using the NNLS method, the CERES calibration decreased the data bias and RMSE and improved the $R^2$, providing the best-weighted combination for each CMIP5 model and producing better validation results than those produced by only using the mean of all model outputs and data from former studies. The minor validation RMSE difference (4.68 Wm$^{-2}$ in DSR and 9.18 Wm$^{-2}$ in DLR) between the two networks is ~~the system bias~~ mainly caused by disparate instruments and different site numbers. We ignored the spatial mismatch between site observations and downward radiation datasets in line with former studies (Wang and Dickinson, 2013;Zhang et al., 2015).

Moreover, the annual anomaly temporal variation was compared with the data from Shi and Liang (2013) and is shown in Figure 3.

The annual temporal variation illustrates that two products have a similar temporal trend of DSR and DLR at a decadal scale over the TP, and that the CERES calibrated data have longer time spans. The DSR output shown by Shi and Liang (2013) has a slightly larger decreasing trend, which may be because GEWEX and ISCCP surface radiation products have high weights in the model, and the related spurious cloud trend causes an overestimated dimming trend (Evan et al., 2007). Feng and Wang (2018) utilized a cumulative probability density function-based method to fuse CERES and longer time reanalysis surface DSR data, however in this study they only calibrated individual reanalysis whereas in the present study we merged multiple CMIP5 data that cover longer time span and include more climate general model simulations. Besides, most reanalysis did not include aerosol variation information, which is important to determine the DSR decadal variation and characterize the aerosol radiative forcing.

### 3.2 Characterizing long-term variations in air temperature and surface downward radiation over the Tibetan Plateau

Air temperatures slowly increased from 1850 to 2015. The DLR increased gradually prior to 1970 but rapidly during the following period. The DSR remained stable and decreased rapidly afterward, revealing an opposite trend to the DLR and air temperature (Figure 4a). In total, DSR decreased by 4.1 W $m^{-2}$ from 1850 to 2015 with a gradient of -0.53 W $m^{-2}$ per decade after 1950, and DLR increased from 0.21 W $m^{-2}$ per decade to 1.52 W $m^{-2}$ per decade after 1970. Air temperature has increased by 1.39 K since 1850. Prior to 1950, increased air temperature was mainly triggered by increased DLR. Air temperature slightly decreased from 1950 to 1970, because both DSR and DLR decreased during that period. Although DLR increased rapidly after 1970, the air temperature gradient has not considerably changed, mainly due to solar dimming diminishing~~compressing~~ the greenhouse effect. The solar dimming over the TP is also detected by long-term ground DSR observations from 5 ~~GEBA~~ CMA sites since ~~1960~~ 1958 (Supplementary Fig. ~~S1~~S2) when the measurements were set up. Because heat exchange with other regions in the summer and winter are mostly counteracted, we ignored the interaction at decadal scales and suggested that air temperature is mainly driven by local radiation components. All four surface air temperature datasets show similar temporal trends, especially on the decadal scale.

The long-term spatiotemporal variations in downward surface radiation over the TP and surrounding regions are illustrated in Figure 4b and 4c. Figure 4b demonstrates that the DSR decrease rate in the central region is about -0.08 W $m^{-2}$ per decade, much lower than in surrounding areas. The fastest decrease in DSR appears in the southeastern TP at a gradient of about -0.37 W $m^{-2}$ per decade since 1850. Northern India, South Asia, and southern China show a substantially dimming trend with a gradient of about -0.65 W $m^{-2}$ per decade. The DLR has increased, especially in the central and northern TP (Figure 4c). However, the rate of increase is much slower in the southern and southeastern TP, with a gradient of approximately 0.21 W $m^{-2}$ per decade.

### 3.3 Attribution to the Tibetan Plateau solar dimming

#### 3.3.1 Analysis of satellite products and reanalysis

Both observed satellite products and reanalysis datasets provide evidence that AAs are the major driver of the significant decrease in the DSR over the TP. The aerosol optical depth (AOD) products from the SeaWiFS (Sayer et al., 2012) and MODIS 08 C6.1 (Levy et al., 2007) satellite products demonstrated similar annual anomalies and slightly increasing trends after 1998 (Figure 5a). The aerosol index, which measures the relative amount of aerosols and has a comparable relationship with AOD (McPeters et al., 1998), shows that the number of aerosols has been escalating over the past 30 years (Figure 5a). The AOD has increased 0.0098 over the TP based on the trend, causing approximately 1.97 $Wm^{-2}$ of dimming since 1998, according to multiple CMIP5 AA simulations over the TP and near linear relationship between AOD and radiative forcing at this magnitude level (Yang et al., 2012). This is larger than the calibrated DSR dimming result of 1.10 $Wm^{-2}$, and we inferred that some of the dimming caused by the aerosol increase is offset by decreased cloud cover (Figure 5c).

The PM2.5 satellite product (Van Donkelaar et al., 2015) also showed an increasing trend after 2000 (Figure 5b), while MERRA2 dust loading (Randles et al., 2017), which has been assimilated from MODIS and MISR land aerosol products since 2000, has been decreasing. Particulate matter (PM) 2.5, characterizing very small particles that have a diameter of less than 2.5 micrometers and are produced by human activities, is a common index for measuring air pollution (Wang et al., 2015). The variation in PM2.5 and dust indicates that increased aerosols are mainly from air pollution rather than from natural causes.

Based on the corrected cloud fraction datasets (Norris and Evan, 2015) from ERA5, the ~~ISCCP and~~ Pathfinder Atmospheres–Extended (PATMOS-X) and the average cloud fraction from MOD/MYD08 C6.1, the results demonstrate that the cloud fraction over the TP has been decreasing since 1980 (Figure 5c), indicating a trend opposite to the TP solar dimming. The temporal variation of ISCCP and ERA5 is stable with a larger *p* value than 0.05. Even different long-term products have uncertainties especially before 1990, the overall variation is decreasing after 1990. Therefore, we inferred that the overall trend demonstrated that cloud coverage is not a dimming driver. Moreover, former studies also found the decreasing cloud coverage trend based on site observations since 1960s (Kuang and Jiao, 2016;Yang et al., 2012). The overall temporal variation of TOA albedo from DEEP-C (Allan et al., 2014) and CERES presents an increasing trend with a magnitude of ~0.01 over the TP from 1985 to 2015 (Figure 5d). The TOA albedo is an important component of Earth's energy budget and is mainly influenced by clouds and aerosols. It can be inferred that aerosols over the TP were recently increasing, reflecting more solar radiation into space and causing the TOA albedo increase and solar dimming at the surface.

Yang et al. (2012) argued that aerosols had limited radiative forcing compared with the DSR decrease over the TP, however, ground observations used in these studies were only from one AErosol RObotic NETwork (AERONET) site at the center of the TP (30.773 °N, 90.962 °E). Furthermore, the site was less impacted by surrounding regions and so cannot represent the entire TP, especially the edge regions that are more easily contaminated by air pollution from surrounding areas (Cao et al., 2010).

Yang et al. (2012) and (2014) also suggested that the increasing trend in the deep convective clouds were attributed to the ~~TP~~ solar dimming, however, our analysis has a different conclusion. We used the cloud top pressure and cloud optical depth released by MODIS at different atmospheric levels to detect which pixels are deep convective clouds. The threshold is based on the definition of ISCCP (Rossow and Schiffer, 1999). Then, we calculated the ratio of deep convective clouds in all pixels over the TP and obtained the temporal variation and spatial distribution. Moreover, regardless of cloud type, the cloud mainly affects the DSR by cloud optical depth, so we reviewed the temporal variation of the total cloud optical depth. The analysis illustrates that even though the ratio of deep convective clouds is increasing (Supplementary Fig. ~~S2a~~S3a), deep convective clouds only appeared in the south and west of the TP (Supplementary Fig. ~~S2b~~S3b). Additionally, the overall cloud optical depth has been slightly decreasing over the past 15 years (Supplementary Fig. ~~S2a~~S3a). Therefore, deep convective clouds have little influence over the entire TP.

By analyzing MODIS satellite products and ERA5 reanalysis, w~~W~~e also assessed the temporal variation of the atmospheric water vapor and total column water vapor (Supplementary Fig. ~~S3~~S4), suggested as an important driving factor of ~~TP~~ the solar dimming by Yang et al. (2012), and the temporal variation illustrated that water vapor has been considerably decreasing since 1998 over the TP. However, solar dimming did not show a similar turning point around 1998 in their site observations and our results, and rather the overall increasing trend of water vapor since 1980 was limited. Therefore, the influence of water vapor variations can be ignored. The Yang et al. (2012) study also identified this phenomenon by using ECMWF Re-Analysis (ERA)-40, however, ~~this research~~the analysis result ceased in 2005 and did not show an overall turning trend.

Although satellite products analysis only began in 1980, observational records have existed for more than 30 years, and the spatial extent of the satellite data over the entire TP supports our conclusions. Figure 4b shows that the regions of China, India, and South Asia surrounding the TP have large populations and serious air pollution. Balloon-borne observations (Tobo et al., 2007) and remote sensing products (Vernier et al., 2015) have shown that fine aerosols can be transported over the TP region and enter the Asian tropopause aerosol layer by deep convection via two key pathways over heavily polluted regions (Lau et al., 2018). Moreover, other studies also reported that black carbon deposition altered surface snow albedo and accelerated melting in the TP mountain ranges (Qian et al., 2015). Because of the decreasing dust amount trend the TP, we infer that the increased aerosols are mainly due to air pollution around the TP. Although the TP is still one of the cleanest areas in the world and the aerosol climatology is low, the dimming can be demonstrated by the variation of DSR decadal anomalies. It is necessary to point out that direct radiative effects (scattering and absorption effect) play a dominant role in the interactions between aerosols and the atmosphere (Li et al., 2017) when the aerosol loading is low. Thus the TP is easily affected by the aerosols increase under a clean atmosphere condition.

### 3.3.2 Analysis of model simulations

The long-term model simulation results also show that AAs are the main driving factor of solar dimming. Based on the multiple CMIP5 HistoricalMisc (an experiment combining different specific forcings) model ensembles, we found that the calibrated

DSR and the DSR driven by AAs and noAA had stable variations before 1950. The calibrated DSR obviously decreased after 1950 (Figure 6a). Only the AA-driven DSR can capture the dimming trend since 1950, therefore we can conclude that AAs are the main signal at the decadal scale, while the factors in the noAA-driven model process (such as cloud cover and water vapor) can be ignored. We also detected the AA and noAA driving factors using the optimal fingerprint method, and observed that AAs had a positive contribution, especially after 1970 (Figure 6b) when AA and historical data showed considerable decrease while noAA kept stable. The impact factor of noAA is negative, and the satellite cloud products reveal the same conclusion after 1980 (Figure 5c), i.e., that the cloud fraction has been decreasing and has had a negative contribution to the TP solar dimming. DSR was driven by more forcings in noAA than AA experiments, introducing more uncertainties among models simulations after 1970. Therefore, it is possible that noAA impact factor shows a larger uncertainty bar. We inferred that cloud coverage dominated the negative natural impact because water vapor is quite stable since 1980s (Supplementary Fig. 4) that had little impact on the dimming.~~Therefore, the attribution results from model simulations match the evidence from the satellite data very well.~~

General climate models have coarser spatial resolution, causing ~~the~~ a lower elevation in the model ~~is lower~~ than ~~the~~ in reality and this may cause higher AOD estimation over highland area. However, when we compared the multiple CMIP5 AOD with site measurements, it demonstrates that the overall magnitude and monthly variation of CMIP5 AOD match the AERONET observations (Supplementary Fig. ~~S4~~S5), even though it is slightly higher than the AOD in the non-monsoon season. Therefore, it is reasonable to include the CMIP5 AA and noAA simulations in the attribution work. Results of multiple models have uncertainties that~~,~~ ~~which~~ are illustrated as colored shadow (standard deviation at each year) and the impact factor of analysis in 1970 – 2005 passed the significance test~~, but the overall variation is of significance tested in temporal analysis and optimal fingerprint method~~.

### 3.4 Depressing effects of aerosols on climate warming in summer

By comparing the first 30 years of climatology (1850–1880) and the last 30 years of climatology (1985–2015), we found that the TP solar dimming is stronger in summer (from June to August), at the same time that the increasing magnitude of the surface air temperature is the smallest (Figure 7a). Multiple CMIP5 model ensembles show that changes in precipitation and wind speed over the TP during different seasons were related to the AOD increase. Precipitation in summer had the greatest decrease relative to other seasons, while AOD increased more in the summer (Figure 7b). Furthermore, the wind speed clearly decreased in summer compared to other seasons (Figure 7c). The TP is a strong heat source in summer, forming a sensible heat–derived air-pump that dominates the atmospheric circulation (Wu et al., 2015) and conveys aerosols into the lower stratosphere (Lau et al., 2018). However, increased precipitation will reduce the aerosol duration lifetime considerably (Liao et al., 2015), and wind speed also controls aerosol diffusion. Hence it is evident that less precipitation and lower wind speeds in summer resulted in greater aerosol stability.

Although aerosols have considerably influenced summer downward radiation over the TP, their radiative effect on climate warming has not been quantitatively calculated. By employing the multiple noAA model simulations, the temporal variation of aerosol radiative forcing over the TP are illustrated in the Supplementary Fig. ~~S5~~S6. It demonstrates that the aerosol radiative forcing has been increasing about 8.08 $Wm^{-2}$ by calculating the difference between the first 30 years of climatology (1850–1880) and the last 30 years of climatology (1985–2015).

Quantification of the depressing effect from AAs is essential for evaluating the impact of air pollution on local and continental climate warming and is also vital for improving our understanding of the role of human activities in remote areas. The depressing effects of aerosols on air temperature in summer (Figure 8) were calculated using two methods: one is using first-order approximations of the direct near-surface air temperature response to each radiative and thermodynamic component and is based on remote sensing and modeling data; the other is calculated by using multiple noAA simulations. The two methods had similar depressing magnitudes (Supplementary Fig. ~~S6~~S7), and the mean is shown in Figure 8. Surface air temperature increased almost 0.86 K (Figure 7a) over the TP in summer when comparing the first 30 years and the last 30 years, whereas the increasing magnitude of the surface air temperature that has no aerosol impact (the red line in Figure 8) is approximately 1.64 ± 0.28 K, which indicates that approximately 0.80 ± 0.28 K (48.6 ± 17.3%) of the local climate warming over the TP has been depressed by aerosols since 1850 in summer.

The first-order approximation method utilized many remote sensing products as climatology and forcing input, which are more reliable than the model simulation~~s~~ input (Supplementary Fig. 8), ~~but it ignored the heat exchange with surrounding areas. Hence,~~ while we also calculated the depressing effect of AAs by employing the CMIP5 air temperature data from multiple noAA simulations that used physical parameterization methods~~, which computed the influence of the interaction with other regions~~. Two methods can validate with each other. Then we calculated the mean value as the final depressing effect result for including the advantages of these two methods.

The attribution of solar dimming over the TP and corresponding aerosol effect quantification revealed that anthropogenic aerosols dominate the solar radiation decrease and depress the climate warming in recent decades. Aerosols are cloud condensation nuclei (CCN) and more CCN may depress the cloud formation and precipitation. Moreover, the black carbon aerosol deposition may affect snow albedo feedback (Qian et al., 2015). Thus future studies need to analyze the indirect effect of aerosol loading (Qian et al., 2015) over there. However, it should be noticed that we don't conclude that the TP undergoes warming mitigation. In fact, the TP has a rapid warming rate than global warming (Yao et al., 2018) and other varying factors also affect the warming rate, in terms of the water vapor variation around 1998 (Supplementary Fig. S4). Water vapor is a weak DSR-absorbing factor but major greenhouse gas emitting downward longwave radiation, so its decrease might slow down the local warming rate. However, the impact of water vapor variation after 1998 is at an annual scale that cannot match the analysis in this study, thus follow-up researches may focus on it.

## 4 Conclusions

The TP plays a vital role in regional and global climate change due to its location and orography. Former studies have proven that this region undergoes significant climate change, however, the causes and impacts of solar dimming are still under debate. Calibrated by the CERES EBAF surface downward radiation products and using NNLS method, long-term (from 1850–2015) surface DSR and DLR datasets over the TP were developed by merging 18 CMIP5 models. Compared with the mean of multiple CMIP5 data and fusion data from former studies, the CERES calibrated data had the lowest bias and RMSE for DSR and DLR validation at GAME and CAMP network, and the highest $R^2$ at CAMP network. The calibrated DSR and DLR have similar temporal trends over the TP at a decadal scale compared to the fusion of multiple reanalysis and satellite products.

Based on calibrated surface downward radiation data and four sets of air temperature data, we characterized the spatiotemporal variation in surface radiation along with air temperature. The TP is currently experiencing substantial climate warming and solar dimming at the surface. In total, DSR decreased by 4.1 W $m^{-2}$ from 1850 to 2015 with a gradient of -0.53 W $m^{-2}$ per decade after 1950, and DLR increased from 0.21 W $m^{-2}$ per decade to 1.52 W $m^{-2}$ per decade after 1970. Air temperature has increased by 1.39 K since 1850. The dimming is also detected from long-term observing ~~GEBA~~ CMA sites. Spatial and temporal analyses illustrated that the DSR decrease rate in the central region was approximately -0.08 W $m^{-2}$ per decade, much lower than in surrounding areas. The fastest decrease in DSR appeared in the southeastern TP at a gradient of about -0.37 W $m^{-2}$ per decade since 1850, and DLR has increased, especially in the central and northern TP. However, the rate of increase is much slower in the southern and southeastern TP, with gradients of approximately 0.21 W $m^{-2}$ per decade.

By employing satellite and reanalysis products of aerosols, PM2.5, dust, cloud fractions, and TOA albedo, we determined that anthropogenic aerosols were the main cause of the solar dimming over the TP. The aerosol optical depth and the aerosol index has increased since the 1980s over the TP and increasing PM2.5 and decreasing dust linked the increasing aerosol to air pollution. We also proved from satellite products and reanalysis data that deep convective cloud and atmospheric water vapor are not the main drivers, due to limited distribution and magnitude since the 1980s. Furthermore, the overall cloud optical depth is decreasing. Additional evidence from multiple CMIP5 HistoricalMisc experiment ensembles also supports this conclusion that anthropogenic aerosols were the main cause of solar dimming over the TP.

Solar dimming over the TP is stronger in summer when the increasing magnitude of the surface air temperature is the smallest. Decreased precipitation and wind speeds triggered increased aerosol stability. Comparing the averages of the first 30 years (1850–1880) and last 30 years (1985–2015), the surface air temperature increased by approximately 0.86 K over the TP in the summer. ~~Relying on calculated aerosol radiative forcings, t~~The depressing effect of aerosol was calculated using two methods and both of which showed similar depressing magnitude. The increasing magnitude of the surface air temperature (with no aerosol impact) was approximately 1.58 K, which means approximately 0.80 ± 0.28 K (48.6 ± 17.3%) of the local climate warming over the TP has been depressed by aerosols ~~since~~ from 1850 to 2015 in summer. The study reveals the impacts of human activities on regional warming, even in remote areas, and highlights the need for additional studies to be conducted to

quantify the influence of air pollution on regional climate change over the TP. ~~Therefore, w~~We will focus on the influences of air pollution on local precipitation over the TP and surrounding areas in the next work.

## Author contributions

S. Liang conceived and scoped the research. A. Jia, B. Jiang, and X. Zhang downloaded and pre-processed the data. A. Jia and D. Wang performed data statistics and the interpretation of the results. A. Jia and S. Liang wrote the manuscript. All authors contributed to revising the article.


## Acknowledgments

This study was supported by NASA under grant 80NSSC18K0620 and the Chinese Grand Research Program on Climate Change and Response (projects 2016YFA0600101 and 2016YFA0600103). We gratefully acknowledge the Intergovernmental Panel on Climate Change (IPCC) data distribution center for providing the model simulation outputs. We also thank the CERES science team, MODIS science team, Goddard Earth Sciences Data and Information Services Center (GES DISC), Earth Observing System Data and Information System (EOSDIS), Atmospheric Composition Analysis Group at Dalhousie University, Research Data Archive at the National Center for Atmospheric Research (NCAR), GLASS science team, and Land Processes Distributed Active Archive Center (LP DAAC) for providing satellite and reanalysis products. We acknowledge the Berkeley Earth, Goddard Institute for Space Studies, National Centers for Environmental Information, and Climate Research Unit for providing near-surface air temperature datasets. We also thank the GEWEX Asian Monsoon Experiment (GAME), CEOP Asia-Australia Monsoon Project, and Aerosol Robotic Network for providing ground measurements.


## Data and code availability

The authors declare that the data we generated will be available after acceptance. All datasets supporting the findings of this study were identified by referring citations in the references section. Analysis scripts are available by request to S. Liang.

## Competing financial interests

The authors declare no competing financial interests.

## References


Ahmad, S. P., Torres, O., Bhartia, P., Leptoukh, G., and Kempler, S.: Aerosol index from TOMS and OMI measurements, Proc. of the 86th AMS annual meeting, 2006,

Allan, R. P., Liu, C., Loeb, N. G., Palmer, M. D., Roberts, M., Smith, D., and Vidale, P. L.: Changes in global net radiative imbalance 1985–2012, Geophysical research letters, 41, 5588-5597, 2014.

Andreae, M. O., Jones, C. D., and Cox, P. M.: Strong present-day aerosol cooling implies a hot future, Nature, 435, 1187, 2005.

Boos, W. R., and Kuang, Z. M.: Dominant control of the South Asian monsoon by orographic insulation versus plateau heating, Nature, 463, 218-U102, 10.1038/nature08707, 2010.

Bro, R., and De Jong, S.: A fast non-negativity-constrained least squares algorithm, Journal of Chemometrics: A Journal of the Chemometrics Society, 11, 393-401, 1997.

Cai, D. L., You, Q. L., Fraedrich, K., and Guan, Y. N.: Spatiotemporal Temperature Variability over the Tibetan Plateau: Altitudinal Dependence Associated with the Global Warming Hiatus, Journal of Climate, 30, 969-984, 10.1175/Jcli-D-16-0343.1, 2017.

http://metadata.diasjp.net/dmm/doc/CEOP_CAMP_Tibet-DIAS-en.html, access: Dec. 15, 2006.

Cao, J., Tie, X., Xu, B., Zhao, Z., Zhu, C., Li, G., and Liu, S.: Measuring and modeling black carbon (BC) contamination in the SE Tibetan Plateau, Journal of Atmospheric Chemistry, 67, 45, 2010.

Carmona, F., Rivas, R., and Caselles, V.: Estimation of daytime downward longwave radiation under clear and cloudy skies conditions over a sub-humid region, Theoretical and applied climatology, 115, 281-295, 2014.

Cheng, J., Liang, S., Yao, Y., Ren, B., Shi, L., and Liu, H.: A comparative study of three land surface broadband emissivity datasets from satellite data, Remote Sensing, 6, 111-134, 2014.

Dufresne, J.-L., Foujols, M.-A., Denvil, S., Caubel, A., Marti, O., Aumont, O., Balkanski, Y., Bekki, S., Bellenger, H., and Benshila, R.: Climate change projections using the IPSL-CM5 Earth System Model: from CMIP3 to CMIP5, Climate Dynamics, 40, 2123-2165, 2013.

Evan, A. T., Heidinger, A. K., and Vimont, D. J.: Arguments against a physical long-term trend in global ISCCP cloud amounts, Geophysical Research Letters, 34, 2007.

Feng, F., and Wang, K.: Merging satellite retrievals and reanalyses to produce global long-term and consistent surface incident solar radiation datasets, Remote Sensing, 10, 115, 2018.

Feng, F., and Wang, K.: Determining factors of monthly to decadal variability in surface solar radiation in China: evidences from current reanalyses, Journal of Geophysical Research: Atmospheres, 2019.

Feng, H., and Zou, B.: Satellite-based estimation of the aerosol forcing contribution to the global land surface temperature in the recent decade, Remote Sensing of Environment, 232, 111299, 2019.

Franklin, C. N., Sun, Z., Bi, D. H., Dix, M., Yan, H. L., and Bodas-Salcedo, A.: Evaluation of clouds in ACCESS using the satellite simulator package COSP: Regime-sorted tropical cloud properties, J Geophys Res-Atmos, 118, 6663-6679, 10.1002/jgrd.50496, 2013.

Fu, R., Hu, Y., Wright, J. S., Jiang, J. H., Dickinson, R. E., Chen, M., Filipiak, M., Read, W. G., Waters, J. W., and Wu, D. L.: Short circuit of water vapor and polluted air to the global stratosphere by convective transport over the Tibetan Plateau, Proc Natl Acad Sci U S A, 103, 5664-5669, 10.1073/pnas.0601584103, 2006.

http://www.hyarc.nagoya-u.ac.jp/game/phase-1/game-aan.html, access: Dec. 15, 2005.

Gao, Y., Zhang, M., Liu, Z., Wang, L., Wang, P., Xia, X., Tao, M., and Zhu, L.: Modeling the feedback between aerosol and meteorological variables in the atmospheric boundary layer during a severe fog–haze event over the North China Plain, Atmospheric Chemistry and Physics, 15, 4279-4295, 2015.

Gent, P. R., Danabasoglu, G., Donner, L. J., Holland, M. M., Hunke, E. C., Jayne, S. R., Lawrence, D. M., Neale, R. B., Rasch, P. J., Vertenstein, M., Worley, P. H., Yang, Z. L., and Zhang, M. H.: The Community Climate System Model Version 4, Journal of Climate, 24, 4973-4991, 10.1175/2011jcli4083.1, 2011.

Gettelman, A., Shindell, D., and Lamarque, J.-F.: Impact of aerosol radiative effects on 2000–2010 surface temperatures, Climate dynamics, 45, 2165-2179, 2015.

Gillespie, A., Rokugawa, S., Matsunaga, T., Cothern, J. S., Hook, S., and Kahle, A. B.: A temperature and emissivity separation algorithm for Advanced Spaceborne Thermal Emission and Reflection Radiometer (ASTER) images, IEEE transactions on geoscience and remote sensing, 36, 1113-1126, 1998.

GLOBE, T.: Team and others (Hastings, David A., Paula K. Dunbar, Gerald M. Elphingstone, Mark Bootz, Hiroshi Murakami, Hiroshi Maruyama, Hiroshi Masaharu, Peter Holland, John Payne, Nevin A. Bryant, Thomas L. Logan, J.-P. Muller, Gunter Schreier, and John S. MacDonald), eds., 1999, The Global Land One-kilometer Base Elevation (GLOBE) Digital Elevation Model, Version, 1, 80305-83328,

Gordon, H. B., O'Farrell, S., Collier, M., Dix, M., Rotstayn, L., Kowalczyk, E., Hirst, T., and Watterson, I.: The CSIRO Mk3.5 climate model, CSIRO and Bureau of Meteorology, 2010.

Guo, Y., Cheng, J., and Liang, S.: Comprehensive assessment of parameterization methods for estimating clear-sky surface downward longwave radiation, Theoretical and applied climatology, 135, 1045-1058, 2019.

Hansen, J., Ruedy, R., Sato, M., and Lo, K.: Global surface temperature change, Reviews of Geophysics, 48, 2010.

He, T., Liang, S., and Song, D. X.: Analysis of global land surface albedo climatology and spatial-temporal variation during 1981–2010 from multiple satellite products, Journal of Geophysical Research: Atmospheres, 119, 10,281-210,298, 2014.

Hersbach, H., and Dee, D.: ERA5 reanalysis is in production, ECMWF newsletter, 147, 5-6, 2016.

Hsu, N., Gautam, R., Sayer, A., Bettenhausen, C., Li, C., Jeong, M., Tsay, S., and Holben, B.: Global and regional trends of aerosol optical depth over land and ocean using SeaWiFS measurements from 1997 to 2010, 2012.

Hsu, N. C., Herman, J., Torres, O., Holben, B., Tanre, D., Eck, T., Smirnov, A., Chatenet, B., and Lavenu, F.: Comparisons of the TOMS aerosol index with Sun-photometer aerosol optical thickness: Results and applications, Journal of Geophysical Research: Atmospheres, 104, 6269-6279, 1999.

Ji, Z. M., Kang, S. C., Cong, Z. Y., Zhang, Q. G., and Yao, T. D.: Simulation of carbonaceous aerosols over the Third Pole and adjacent regions: distribution, transportation, deposition, and climatic effects, Climate Dynamics, 45, 2831-2846, 10.1007/s00382-015-2509-1, 2015.

Jia, A., Jiang, B., Liang, S., Zhang, X., and Ma, H.: Validation and Spatiotemporal Analysis of CERES Surface Net Radiation Product, Remote Sensing, 8, 90, 2016.

Jia, A., Liang, S., Jiang, B., Zhang, X., and Wang, G.: Comprehensive Assessment of Global Surface Net Radiation Products and Uncertainty Analysis, Journal of Geophysical Research Atmospheres, 2018.

Jones, P., Lister, D., Osborn, T., Harpham, C., Salmon, M., and Morice, C.: Hemispheric and large-scale land-surface air temperature variations: An extensive revision and an update to 2010, Journal of Geophysical Research: Atmospheres, 117, 2012.

Jungclaus, J. H., Lorenz, S. J., Timmreck, C., Reick, C. H., Brovkin, V., Six, K., Segschneider, J., Giorgetta, M. A., Crowley, T. J., Pongratz, J., Krivova, N. A., Vieira, L. E., Solanki, S. K., Klocke, D., Botzet, M., Esch, M., Gayler, V., Haak, H., Raddatz, T. J., Roeckner, E., Schnur, R., Widmann, H., Claussen, M., Stevens, B., and Marotzke, J.: Climate and carbon-cycle variability over the last millennium, Clim Past, 6, 723-737, 10.5194/cp-6-723-2010, 2010.

Kato, S., Rose, F. G., Rutan, D. A., Thorsen, T. J., Loeb, N. G., Doelling, D. R., Huang, X., Smith, W. L., Su, W., and Ham, S.-H.: Surface irradiances of edition 4.0 Clouds and the Earth's Radiant Energy System (CERES) Energy Balanced and Filled (EBAF) data product, Journal of Climate, 31, 4501-4527, 2018.

Kuang, X. X., and Jiao, J. J.: Review on climate change on the Tibetan Plateau during the last half century, J Geophys Res-Atmos, 121, 3979-4007, 10.1002/2015jd024728, 2016.

Lau, W. K. M., Yuan, C., and Li, Z.: Origin, Maintenance and Variability of the Asian Tropopause Aerosol Layer (ATAL): The Roles of Monsoon Dynamics, Sci Rep, 8, 3960, 10.1038/s41598-018-22267-z, 2018.

Leese, J. A.: Coordinated Enhanced Observing Period (CEOP) Implementation Plan, International GEWEX Project Office, 2001.

Levy, R. C., Remer, L., Mattoo, S., Vermote, E., and Kaufman, Y.: Second-generation algorithm for retrieving aerosol properties over land from MODIS spectral reflectance, J. Geophys. Res, 112, D13, 2007.

Lewis, P., Brockmann, C., and Muller, J.: GlobAlbedo: Algorithm theoretical basis document V4-12, in: Technical Report, 2013.

Li, C., Zhao, T., and Ying, K.: Effects of anthropogenic aerosols on temperature changes in China during the twentieth century based on CMIP5 models, Theoretical and Applied Climatology, 125, 529-540, 10.1007/s00704-015-1527-6, 2015.

Li, Z., Rosenfeld, D., and Fan, J.: Aerosols and their impact on radiation, clouds, precipitation, and severe weather events, in: Oxford Research Encyclopedia of Environmental Science, 2017.

Liang, S., Wang, K., Zhang, X., and Wild, M.: Review on estimation of land surface radiation and energy budgets from ground measurement, remote sensing and model simulations, Selected Topics in Applied Earth Observations and Remote Sensing, IEEE Journal of, 3, 225-240, 2010.

Liao, H., Chang, W., and Yang, Y.: Climatic effects of air pollutants over China: A review, Advances in Atmospheric Sciences, 32, 115-139, 2015.

Liu, N., Liu, Q., Wang, L., Liang, S., Wen, J., Qu, Y., and Liu, S.: A statistics-based temporal filter algorithm to map spatiotemporally continuous shortwave albedo from MODIS data, Hydrology and Earth System Sciences, 17, 2121-2129, 2013a.

Liu, Q., Wang, L., Qu, Y., Liu, N., Liu, S., Tang, H., and Liang, S.: Preliminary evaluation of the long-term GLASS albedo product, International Journal of Digital Earth, 6, 69-95, 2013b.

Loeb, N. G., Doelling, D. R., Wang, H. L., Su, W. Y., Nguyen, C., Corbett, J. G., Liang, L. S., Mitrescu, C., Rose, F. G., and Kato, S.: Clouds and the Earth's Radiant Energy System (CERES) Energy Balanced and Filled (EBAF) Top-of-Atmosphere (TOA) Edition-4.0 Data Product, Journal of Climate, 31, 895-918, 10.1175/Jcli-D-17-0208.1, 2018.

Long, M. C., Lindsay, K., Peacock, S., Moore, J. K., and Doney, S. C.: Twentieth-century oceanic carbon uptake and storage in CESM1 (BGC), Journal of Climate, 26, 6775-6800, 2013.

Ma, Q., Wang, K., and Wild, M.: Impact of geolocations of validation data on the evaluation of surface incident shortwave radiation from Earth System Models, Journal of Geophysical Research: Atmospheres, 120, 6825-6844, 2015.

Manara, V., Brunetti, M., Maugeri, M., Sanchez-Lorenzo, A., and Wild, M.: Sunshine duration and global radiation trends in Italy (1959–2013): To what extent do they agree?, Journal of Geophysical Research: Atmospheres, 122, 4312-4331, 2017.

McPeters, R. D., Bhartia, P., Krueger, A. J., Herman, J. R., Wellemeyer, C. G., Seftor, C. J., Jaross, G., Torres, O., Moy, L., and Labow, G.: Earth probe total ozone mapping spectrometer (TOMS): data products user's guide, 1998.

Meehl, G. A., Washington, W. M., Arblaster, J. M., Hu, A. X., Teng, H. Y., Kay, J. E., Gettelman, A., Lawrence, D. M., Sanderson, B. M., and Strand, W. G.: Climate Change Projections in CESM1(CAM5) Compared to CCSM4, Journal of Climate, 26, 6287-6308, 10.1175/Jcli-D-12-00572.1, 2013.

Mochizuki, T., Chikamoto, Y., Kimoto, M., Ishii, M., Tatebe, H., Komuro, Y., Sakamoto, T. T., Watanabe, M., and Mori, M.: Decadal Prediction Using a Recent Series of MIROC Global Climate Models, Journal of the Meteorological Society of Japan, 90a, 373-383, 10.2151/jmsj.2012-A22, 2012.

Norris, J. R., and Evan, A. T.: Empirical Removal of Artifacts from the ISCCP and PATMOS-x Satellite Cloud Records, Journal of Atmospheric and Oceanic Technology, 32, 691-702, 10.1175/jtech-d-14-00058.1, 2015.

Norris, J. R., Allen, R. J., Evan, A. T., Zelinka, M. D., O'dell, C. W., and Klein, S. A.: Evidence for climate change in the satellite cloud record, Nature, 536, 72-75, 2016.

http://www.ipcc-data.org/sim/gcm_monthly/AR5/Reference-Archive.html, access: Dec. 15, 2013.

Pozzer, A., De Meij, A., Yoon, J., Tost, H., Georgoulias, A., and Astitha, M.: AOD trends during 2001–2010 from observations and model simulations, Atmospheric Chemistry and Physics, 15, 5521-5535, 2015.

Qian, Y., Yasunari, T. J., Doherty, S. J., Flanner, M. G., Lau, W. K., Ming, J., Wang, H., Wang, M., Warren, S. G., and Zhang, R.: Light-absorbing particles in snow and ice: Measurement and modeling of climatic and hydrological impact, Advances in Atmospheric Sciences, 32, 64-91, 2015.

Qu, Y., Liu, Q., Liang, S., Wang, L., Liu, N., and Liu, S.: Direct-estimation algorithm for mapping daily land-surface broadband albedo from MODIS data, IEEE Transactions on Geoscience and Remote sensing, 52, 907-919, 2014.

Ramanathan, V., Ramana, M. V., Roberts, G., Kim, D., Corrigan, C., Chung, C., and Winker, D.: Warming trends in Asia amplified by brown cloud solar absorption, Nature, 448, 575, 2007.

Randles, C., Da Silva, A., Buchard, V., Colarco, P., Darmenov, A., Govindaraju, R., Smirnov, A., Holben, B., Ferrare, R., and Hair, J.: The MERRA-2 aerosol reanalysis, 1980 onward. Part I: System description and data assimilation evaluation, Journal of Climate, 30, 6823-6850, 2017.

Rao, Y., Liang, S., and Yu, Y.: Land surface air temperature data are considerably different among BEST-LAND, CRU-TEM4v, NASA-GISS, and NOAA-NCEI, Journal of Geophysical Research: Atmospheres, 2018.

Riihelä, A., Manninen, T., Laine, V., Andersson, K., and Kaspar, F.: CLARA-SAL: a global 28 yr timeseries of Earth's black-sky surface albedo, Atmospheric Chemistry and Physics, 13, 3743-3762, 2013.

Rohde, R., Muller, R., Jacobsen, R., Muller, E., Perlmutter, S., Rosenfeld, A., Wurtele, J., Groom, D., and Wickham, C.: A new estimate of the average Earth surface land temperature spanning 1753 to 2011. Geoinfor Geostat Overview 1: 1, of, 7, 2, 2013.

Rossow, W. B., and Schiffer, R. A.: Advances in understanding clouds from ISCCP, Bulletin of the American Meteorological Society, 80, 2261-2288, 1999.

Sampe, T., and Xie, S. P.: Large-Scale Dynamics of the Meiyu-Baiu Rainband: Environmental Forcing by the Westerly Jet, Journal of Climate, 23, 113-134, 10.1175/2009jcli3128.1, 2010.

Samset, B., Sand, M., Smith, C., Bauer, S., Forster, P., Fuglestvedt, J., Osprey, S., and Schleussner, C. F.: Climate impacts from a removal of anthropogenic aerosol emissions, Geophysical Research Letters, 45, 1020-1029, 2018.

Sayer, A., Hsu, N., Bettenhausen, C., Jeong, M., Holben, B., and Zhang, J.: Global and regional evaluation of over-land spectral aerosol optical depth retrievals from SeaWiFS, 2012.

Scoccimarro, E., Gualdi, S., Bellucci, A., Sanna, A., Giuseppe Fogli, P., Manzini, E., Vichi, M., Oddo, P., and Navarra, A.: Effects of tropical cyclones on ocean heat transport in a high-resolution coupled general circulation model, Journal of Climate, 24, 4368-4384, 2011.

Service, C. C. C.: ERA5: Fifth generation of ECMWF atmospheric reanalyses of the global climate, 2017.

Shi, Q., and Liang, S.: Characterizing the surface radiation budget over the Tibetan Plateau with ground-measured, reanalysis, and remote sensing data sets: 1. Methodology, Journal of Geophysical Research: Atmospheres, 118, 9642-9657, 2013.

Smith, D. M., Booth, B. B., Dunstone, N. J., Eade, R., Hermanson, L., Jones, G. S., Scaife, A. A., Sheen, K. L., and Thompson, V.: Role of volcanic and anthropogenic aerosols in the recent global surface warming slowdown, Nature Climate Change, 6, 936, 2016.

Smith, T. M., Reynolds, R. W., Peterson, T. C., and Lawrimore, J.: Improvements to NOAA's historical merged land–ocean surface temperature analysis (1880–2006), Journal of Climate, 21, 2283-2296, 2008.

Sogacheva, L., Leeuw, G. d., Rodriguez, E., Kolmonen, P., Georgoulias, A. K., Alexandri, G., Kourtidis, K., Proestakis, E., Marinou, E., and Amiridis, V.: Spatial and seasonal variations of aerosols over China from two decades of multi-satellite observations–Part 1: ATSR (1995–2011) and MODIS C6. 1 (2000–2017), Atmospheric Chemistry and Physics, 18, 11389-11407, 2018.

Sun, Y., Zhang, X., Zwiers, F. W., Song, L., Wan, H., Hu, T., Yin, H., and Ren, G.: Rapid increase in the risk of extreme summer heat in Eastern China, Nature Climate Change, 4, 1082, 2014.

Sundström, A. M., Arola, A., Kolmonen, P., Xue, Y., de Leeuw, G., and Kulmala, M.: On the use of a satellite remote-sensing-based approach for determining aerosol direct radiative effect over land: a case study over China, Atmospheric Chemistry and Physics, 15, 505-518, 10.5194/acp-15-505-2015, 2015.

Tang, W.-J., Yang, K., Qin, J., Cheng, C., and He, J.: Solar radiation trend across China in recent decades: a revisit with quality-controlled data, Atmospheric Chemistry and Physics, 11, 393-406, 2011.

Taylor, K. E., Stouffer, R. J., and Meehl, G. A.: An overview of CMIP5 and the experiment design, Bulletin of the American Meteorological Society, 93, 485, 2012.

Tjiputra, J. F., Roelandt, C., Bentsen, M., Lawrence, D. M., Lorentzen, T., Schwinger, J., Seland, O., and Heinze, C.: Evaluation of the carbon cycle components in the Norwegian Earth System Model (NorESM), Geoscientific Model Development, 6, 301-325, 10.5194/gmd-6-301-2013, 2013.

Tobo, Y., Iwasaka, Y., Shi, G.-Y., Kim, Y.-S., Ohashi, T., Tamura, K., and Zhang, D.: Balloon-borne observations of high aerosol concentrations near the summertime tropopause over the Tibetan Plateau, Atmospheric Research, 84, 233-241, 10.1016/j.atmosres.2006.08.003, 2007.

Van Donkelaar, A., Martin, R. V., Brauer, M., and Boys, B. L.: Global Annual PM2. 5 Grids from MODIS, MISR and SeaWiFS Aerosol Optical Depth (AOD), 1998-2012, Palisades, NY: NASA Socioeconomic Data and Applications Center (SEDAC). doi, 10, H4028PFS, 2015.

Van Donkelaar, A., Martin, R. V., Brauer, M., Hsu, N. C., Kahn, R. A., Levy, R. C., Lyapustin, A., Sayer, A. M., and Winker, D. M.: Global estimates of fine particulate matter using a combined geophysical-statistical method with information from satellites, models, and monitors, Environ Sci Technol, 50, 3762-3772, 2016.

Vernier, J. P., Fairlie, T. D., Natarajan, M., Wienhold, F. G., Bian, J., Martinsson, B. G., Crumeyrolle, S., Thomason, L. W., and Bedka, K. M.: Increase in upper tropospheric and lower stratospheric aerosol levels and its potential connection with Asian pollution, J Geophys Res Atmos, 120, 1608-1619, 10.1002/2014JD022372, 2015.

Voldoire, A., Sanchez-Gomez, E., y Mélia, D. S., Decharme, B., Cassou, C., Sénési, S., Valcke, S., Beau, I., Alias, A., and Chevallier, M.: The CNRM-CM5. 1 global climate model: description and basic evaluation, Climate Dynamics, 40, 2091-2121, 2013.

Volodin, E. M., Dianskii, N. A., and Gusev, A. V.: Simulating present-day climate with the INMCM4.0 coupled model of the atmospheric and oceanic general circulations, Izv Atmos Ocean Phy+, 46, 414-431, 10.1134/S000143381004002x, 2010.

Wang, K., and Dickinson, R. E.: Global atmospheric downward longwave radiation at the surface from ground-based observations, satellite retrievals, and reanalyses, Reviews of Geophysics, 51, 150-185, 2013.

Wang, K.: Measurement biases explain discrepancies between the observed and simulated decadal variability of surface incident solar radiation, Sci Rep-Uk, 4, 6144, 2014.

Wang, Y., Zhang, X., Sun, J., Zhang, X., Che, H., and Li, Y.: Spatial and temporal variations of the concentrations of PM 10, PM 2.5 and PM 1 in China, Atmospheric Chemistry and Physics, 15, 13585-13598, 2015.

Wang, Z., Li, Z., Xu, M., and Yu, G.: River morphodynamics and stream ecology of the Qinghai-Tibet Plateau, CRC Press, 2016.

Wild, M., Ohmura, A., and Makowski, K.: Impact of global dimming and brightening on global warming, Geophysical Research Letters, 34, 10.1029/2006gl028031, 2007.

Wild, M.: Global dimming and brightening: A review, Journal of Geophysical Research: Atmospheres, 114, 2009.

Wu, G. X., Liu, Y. M., He, B., Bao, Q., Duan, A. M., and Jin, F. F.: Thermal Controls on the Asian Summer Monsoon, Sci Rep-Uk, 2, ARTN 40410.1038/srep00404, 2012.

Wu, G. X., Duan, A. M., Liu, Y. M., Mao, J. Y., Ren, R. C., Bao, Q., He, B., Liu, B. Q., and Hu, W. T.: Tibetan Plateau climate dynamics: recent research progress and outlook, Natl Sci Rev, 2, 100-116, 10.1093/nsr/nwu045, 2015.

Wu, T., Yu, R., Zhang, F., Wang, Z., Dong, M., Wang, L., Jin, X., Chen, D., and Li, L.: The Beijing Climate Center atmospheric general circulation model: description and its performance for the present-day climate, Climate dynamics, 34, 123, 2010.

Xie, H., and Zhu, X.: Reference evapotranspiration trends and their sensitivity to climatic change on the Tibetan Plateau (1970–2009), Hydrol Process, 27, 3685-3693, 2013.

Xie, H., Zhu, X., and Yuan, D. Y.: Pan evaporation modelling and changing attribution analysis on the Tibetan Plateau (1970-2012), Hydrol Process, 29, 2164-2177, 10.1002/hyp.10356, 2015.

Xu, X. D., Lu, C. G., Ding, Y. H., Shi, X. H., Guo, Y. D., and Zhu, W. H.: What is the relationship between China summer precipitation and the change of apparent heat source over the Tibetan Plateau?, Atmos Sci Lett, 14, 227-234, 10.1002/asl2.444, 2013.

Yang, K., Koike, T., and Ye, B.: Improving estimation of hourly, daily, and monthly solar radiation by importing global data sets, Agricultural and Forest Meteorology, 137, 43-55, 2006.

Yang, K., Ding, B. H., Qin, J., Tang, W. J., Lu, N., and Lin, C. G.: Can aerosol loading explain the solar dimming over the Tibetan Plateau?, Geophysical Research Letters, 39, Artn L2071010.1029/2012gl053733, 2012.

Yang, K., Wu, H., Qin, J., Lin, C. G., Tang, W. J., and Chen, Y. Y.: Recent climate changes over the Tibetan Plateau and their impacts on energy and water cycle: A review, Global Planet Change, 112, 79-91, 10.1016/j.gloplacha.2013.12.001, 2014.

Yao, T., Pu, J., Lu, A., Wang, Y., and Yu, W.: Recent glacial retreat and its impact on hydrological processes on the Tibetan Plateau, China, and surrounding regions, Arctic, Antarctic, and Alpine Research, 39, 642-650, 2007.

Yao, T., Xue, Y., Chen, D., Chen, F., Thompson, L., Cui, P., Koike, T., Lau, W. K.-M., Lettenmaier, D., and Mosbrugger, V.: Recent Third Pole's rapid warming accompanies cryospheric melt and water cycle intensification and interactions between

monsoon and environment: multi-disciplinary approach with observation, modeling and analysis, Bulletin of the American Meteorological Society, 2018.

Yasunari, T.: GEWEX-related Asian monsoon experiment (GAME), Advances in space research, 14, 161-165, 1994.

You, Q., Sanchez-Lorenzo, A., Wild, M., Folini, D., Fraedrich, K., Ren, G., and Kang, S.: Decadal variation of surface solar radiation in the Tibetan Plateau from observations, reanalysis and model simulations, Climate Dynamics, 40, 2073-2086, 2013.

You, Q. L., Kang, S. C., Pepin, N., Flugel, W. A., Sanchez-Lorenzo, A., Yan, Y. P., and Zhang, Y. J.: Climate warming and associated changes in atmospheric circulation in the eastern and central Tibetan Plateau from a homogenized dataset, Global Planet Change, 72, 11-24, 10.1016/j.gloplacha.2010.04.003, 2010.

Yukimoto, S., ADACHI, Y., HOSAKA, M., SAKAMI, T., YOSHIMURA, H., HIRABARA, M., TANAKA, T. Y., SHINDO, E., TSUJINO, H., and DEUSHI, M.: A New Global Climate Model of the Meteorological Research Institute: MRI-CGCM3—Model Description and Basic Performance—, Journal of the Meteorological Society of Japan, 90, 23-64, 2012.

Zeng, Z., Piao, S., Li, L. Z. X., Zhou, L., Ciais, P., Wang, T., Li, Y., Lian, X., Wood, E. F., Friedlingstein, P., Mao, J., Estes, L. D., Myneni, Ranga B., Peng, S., Shi, X., Seneviratne, S. I., and Wang, Y.: Climate mitigation from vegetation biophysical feedbacks during the past three decades, Nature Climate Change, 7, 432-436, 10.1038/nclimate3299, 2017.

Zhang, X., Liang, S., Wild, M., and Jiang, B.: Analysis of surface incident shortwave radiation from four satellite products, Remote Sensing of Environment, 165, 186-202, 2015.

Zhang, X., Liang, S., Wang, G., Yao, Y., Jiang, B., and Cheng, J.: Evaluation of the Reanalysis Surface Incident Shortwave Radiation Products from NCEP, ECMWF, GSFC, and JMA Using Satellite and Surface Observations, Remote Sensing, 8, 225, 2016.

Zhou, C., Wang, K., and Qi, D.: Attribution of the July 2016 Extreme Precipitation Event Over China's Wuhang, Bulletin of the American Meteorological Society, 99, S107-S112, 2018.

**Table 1: Summary of the Coupled Model Intercomparison Project Phase 5 (CMIP5) surface downward radiation simulations used in this study.**

| Name | Spatial Resolution | | Reference |
|---|---|---|---|
| | **Longitude** | **Latitude** | |
| **CMCC-CM** | 0.75° | 0.75° | Scoccimarro et al. (2011) |
| **CESM1-CAM5** | 1.25° | 0.94° | Meehl et al. (2013) |
| **CESM1-BGC** | 1.25° | 0.94° | Long et al. (2013) |
| **CCSM4** | 1.25° | 0.94° | Gent et al. (2011) |
| **MRI-CGCM3** | 1.13° | 1.13° | Yukimoto et al. (2012) |
| **BCC-CSM1.1m** | 1.13° | 1.13° | Wu et al. (2010) |
| **MIROC5** | 1.41° | 1.41° | Mochizuki et al. (2012) |
| **CNRM-CM5** | 1.41° | 1.41° | Voldoire et al. (2013) |
| **ACCESS1.0** | 1.88° | 1.24° | Franklin et al. (2013) |
| **ACCESS1.3** | 1.88° | 1.24° | Franklin et al. (2013) |
| **IPSL-CM5A-MR** | 2.50° | 1.26° | Dufresne et al. (2013) |
| **INMCM4** | 2.00° | 1.50° | Volodin et al. (2010) |
| **MPI-ESM-LR** | 1.88° | 1.88° | Jungclaus et al. (2010) |
| **MPI-ESM-MR** | 1.88° | 1.88° | Jungclaus et al. (2010) |
| **CSIRO-Mk3.6.0** | 1.88° | 1.88° | Gordon et al. (2010) |
| **CMCC-CMS** | 1.88° | 1.88° | Scoccimarro et al. (2011) |
| **NorESM1-M** | 2.50° | 1.88° | Tjiputra et al. (2013) |
| **NorESM1-ME** | 2.50° | 1.88° | Tjiputra et al. (2013) |

**Table 2: Meta information on the satellite and reanalysis products. All products were resampled into 1 Lat/Lon degree using bilinear interpolation or spatial averaging in the paper. All data were accessed on 15 December 2018.**

| Variable | Version | Time Span | Spatial Resolution | Data Availability | Usage |
|---|---|---|---|---|---|
| **DSR** | CERES EBAF-surface Ed4.0 | 2001.01–2015.12 | 1°×1° | https://ceres.larc.nasa.gov/order_data.php | calibration |
| **DLR** | CERES EBAF-surface Ed4.0 | 2001.01–2015.12 | 1°×1° | https://ceres.larc.nasa.gov/order_data.php | calibration |
| **TOA albedo** | CERES TOA-surface Ed4.0 | 2001.01–2015.12 | 1°×1° | https://ceres.larc.nasa.gov/order_data.php | attribution & depressing effect |
| **AOD** | MOD/MYD08 C6.1 | 2001.01–2015.12 | 1°×1° | https://earthengine.google.com/ | attribution |
| **cloud fraction** | MOD/MYD08 C6.1 | 2001.01–2015.12 | 1°×1° | https://earthengine.google.com/ | attribution |
| **atmospheric water vapor** | MOD/MYD08 C6.1 | 2001.01–2015.12 | 1°×1° | https://earthengine.google.com/ | attribution |
| **AOD** | SeaWIFS 1.0_L3M | 1998.01–2010.12 | 1°×1° | https://disc.gsfc.nasa.gov/datasets?page=1 | attribution |
| **aerosol index** | TOMS & OMI Aerosol Index L3 | 1980.01–1993.12, 1997.01–2015.12 | 1°×1.25° | https://disc.gsfc.nasa.gov/datasets?page=1 | attribution |
| **PM 2.5** | Global Annual PM2.5 Grids from MODIS, MISR and SeaWiFS AOD, v1 | 2000.01–2015.12 | 0.01°×0.01° | http://fizz.phys.dal.ca/~atmos/martin/?page_id=140 | attribution |
| **dust** | MERRA2 | 2000.01–2015.12 | 0.5°×0.625° | https://disc.gsfc.nasa.gov/datasets?page=1 | attribution |
| ~~**cloud fraction**~~ | ~~MOD/MYD08 C6.1~~ | ~~2001.01–2015.12~~ | ~~1°×1°~~ | ~~https://earthengine.google.com/~~ | ~~attribution~~ |
| **cloud fraction** | Corrected ISCCP and PATMOS-X monthly cloud fraction | 1984.01–2007.12 | 1°×1° | https://rda.ucar.edu/datasets/ds741.5/ | attribution |

| | | | | | |
|---|---|---|---|---|---|
| **cloud fraction** | ERA5 | 1979.01–2015.12 | 0.25°×0.25° | https://cds.climate.copernicus.eu | attribution |
| **total column water vapor** | ERA5 | 1979.01–2015.12 | 0.25°×0.25° | https://cds.climate.copernicus.eu | attribution |
| **TOA ASR** | DEEP-C TOA _ASR v02 | 1985.01–2015.12 | 1°×1° | http://www.met.reading.ac.uk/~sgs02rpa/research/DEEP-C/ | attribution |
| **albedo** | GLASS albedo V05 | 2001.01–~~2015~~2011.12 | 0.05°×0.05° | http://glass-product.bnu.edu.cn | depressing effect |
| **albedo** | CERES EBAF-surface Ed4.0 | 2001.01–2011.12 | 1°×1° | https://ceres.larc.nasa.gov/order_data.php | depressing effect |
| **albedo** | CLARA-SAL | 2001.01–2011.12 | 0.25°×0.25° | https://wui.cmsaf.eu/safira | depressing effect |
| **albedo** | GlobAlbedo | 2001.01–2011.12 | 0.5°×0.5° | http://www.GlobAlbedo.org | depressing effect |
| **surface emissivity** | ASTER_GED v4.1 | 2001.01–2015.12 | 0.05°×0.05° | https://lpdaac.usgs.gov/dataset_discovery/community/community_products_table/ag5kmmoh_v041 | depressing effect |

**Variables: DSR, downward shortwave radiation; DLR, downward longwave radiation; TOA albedo, top of atmosphere albedo; AOD, aerosol optical depth; PM2.5, Particulate matter 2.5; ASR, absorbed solar radiation. Products' name are illustrated in the Section 2.**

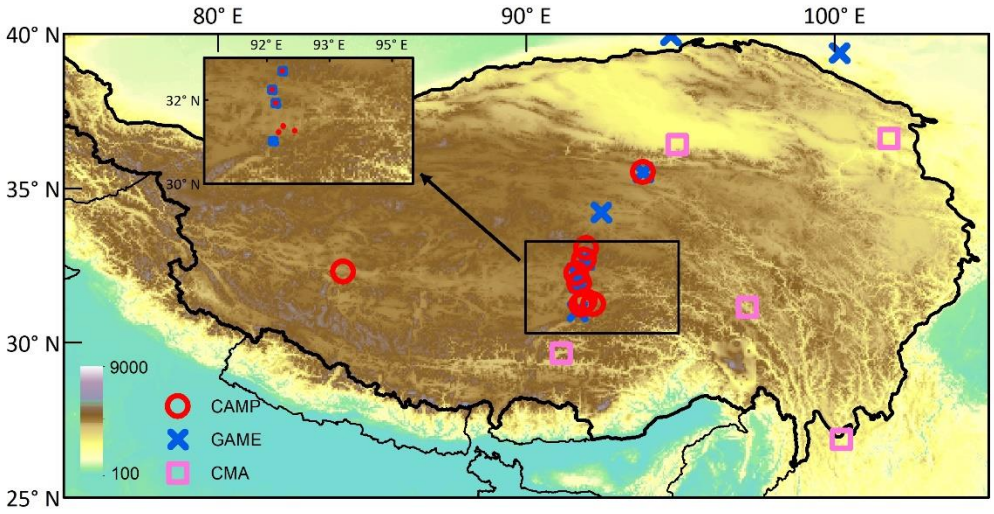


**Figure 1: Site distribution. Observations from three ground networks (Global Energy and Water Exchanges [GEWEX] Asian Monsoon Experiment [GAME], Coordinated Energy and Water Cycle Observation Project [CEOP] Asia-Australia Monsoon Project [CAMP], and China Meteorological Administration (~~Global Energy Balance Archive [GEBA]~~CMA) are from 1960–2005. Vector layer data is free for academic use licensed by Database of Global Administrative Areas (GADM). Elevation data is provided by National Oceanic and Atmospheric Administration (NOAA) (GLOBE).**

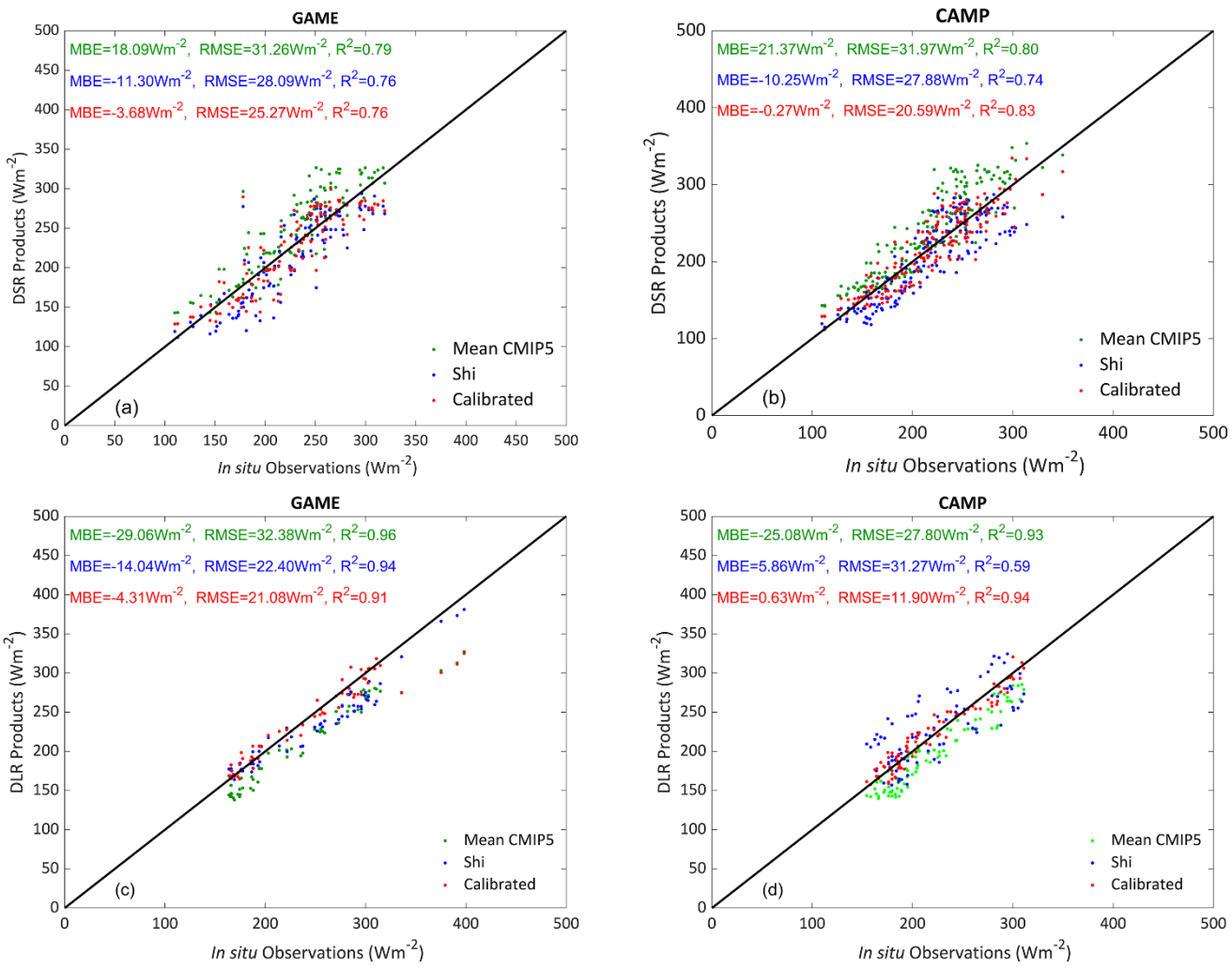


795

**Figure 2: Scatterplot of site validation results from two ground networks: (a, b) downward shortwave radiation (DSR), (c, d) downward longwave radiation (DLR).**

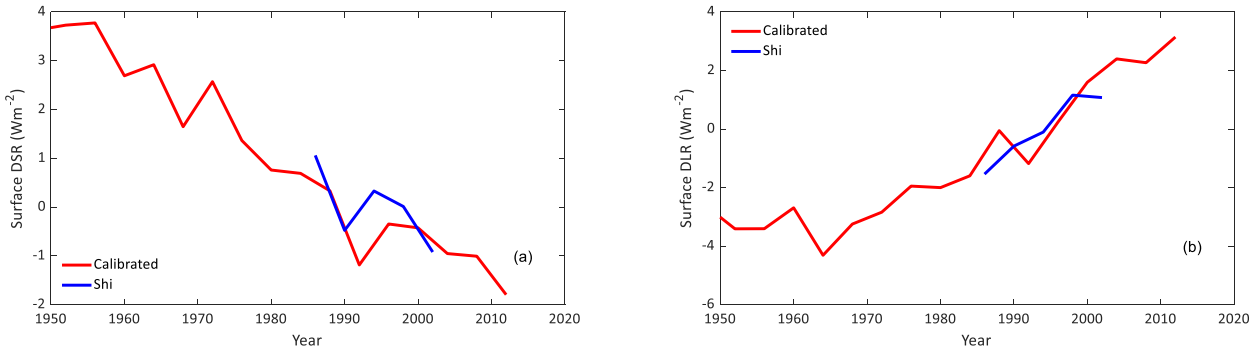


**Figure 3: Trend comparison between calibrated downward radiation datasets and Shi and Liang (2013). Temporal variations over the Tibetan Plateau (TP) in (a) and (b) were averaged by the 5-year moving window in order to remove the impact of annual variability.**

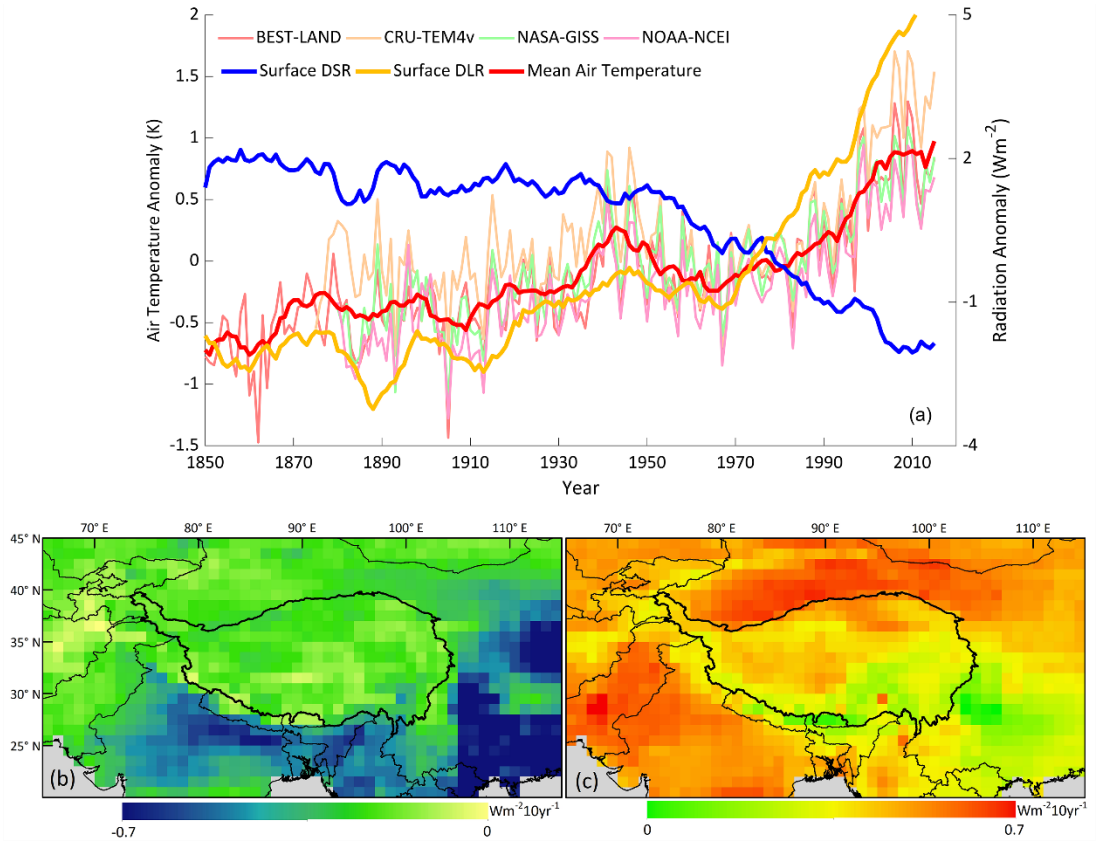


**Figure 4: Spatiotemporal variations in surface downward shortwave radiation (DSR) and downward longwave radiation (DLR) over the Tibetan Plateau (TP) and its neighboring regions from 1850 to 2015 based on calibrated radiation results. Mean air temperature is calculated by the four air temperature datasets. Temporal variations in (a) were averaged by the 10-year moving window in order to remove the impact of annual variability. The trends of DSR (b) and DLR (c) are significant, with p-values < 0.01. Vector layer data is free for academic use licensed by GADM.**

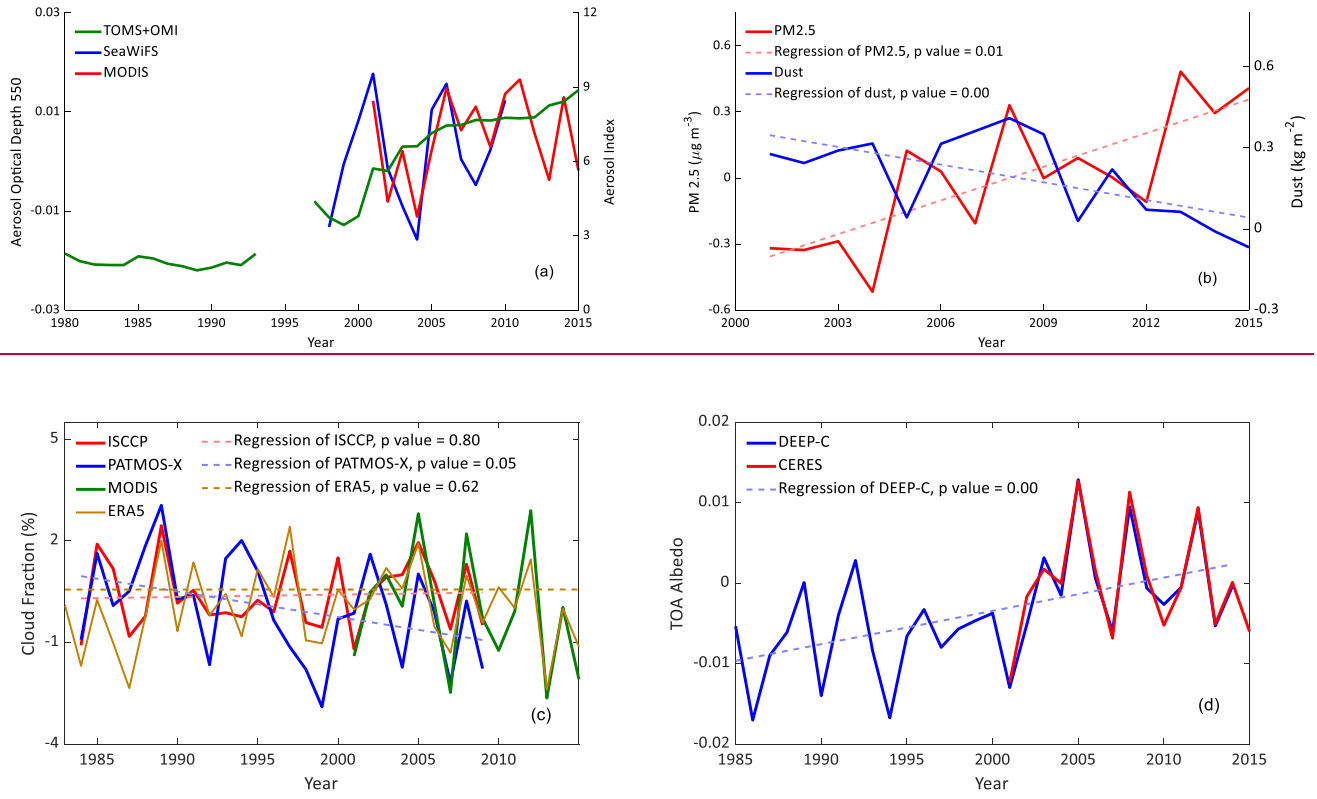


**Figure 5: Temporal variation in detected factors from remote sensing products over the Tibetan Plateau (TP): (a) aerosol optical depth (AOD) and aerosol index, (b) Particulate matter (PM)2.5 and dust, (c) cloud fraction, and (d) top-of-atmosphere (TOA) albedo.**

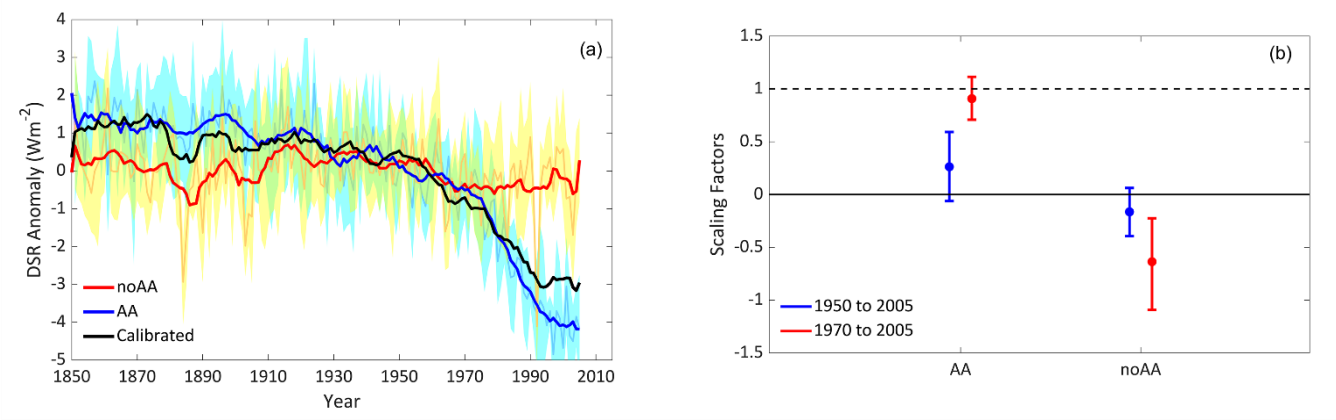


**Figure 6: (a) Temporal variations of the calibrated, anthropogenic aerosol–driven (AA-driven) and noAA-driven DSR. Temporal variations were averaged by a 10-year moving window to remove the impact of annual variability. The shaded area is the standard deviation of model average. (b) Scaling factors of the AA and noAA forcing simulation on downward shortwave radiation (DSR) based on optimal fingerprinting method. The p value of the impact factor in 1950 – 2005 (1970 - 2005) is 0.22 (0.04).**

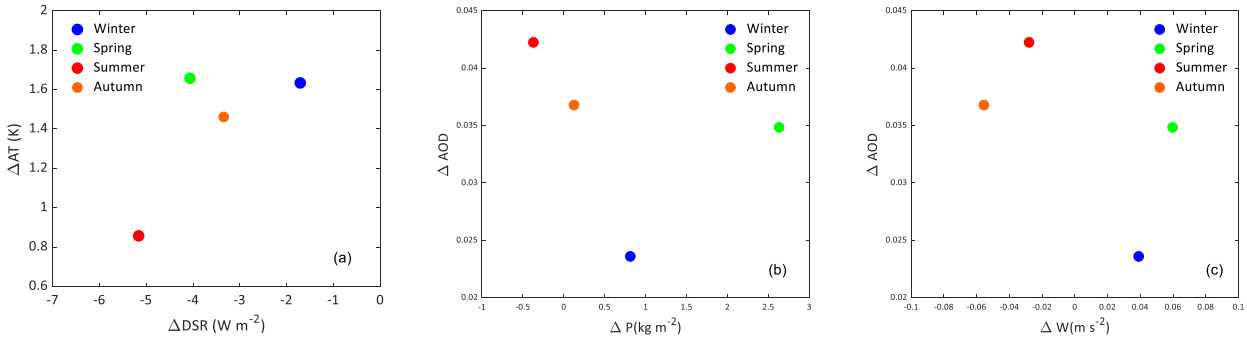


**Figure 7: Relationships between variable ~~change~~changed magnitudes~~s~~ at the seasonal scale from 1850 to 2015: (a) the decrease in downward shortwave radiation (DSR) and increase in air temperature, (b) precipitation change and aerosol optical depth (AOD) increase, (c) wind speed change and AOD increase. Data are from CMIP5 model average.**

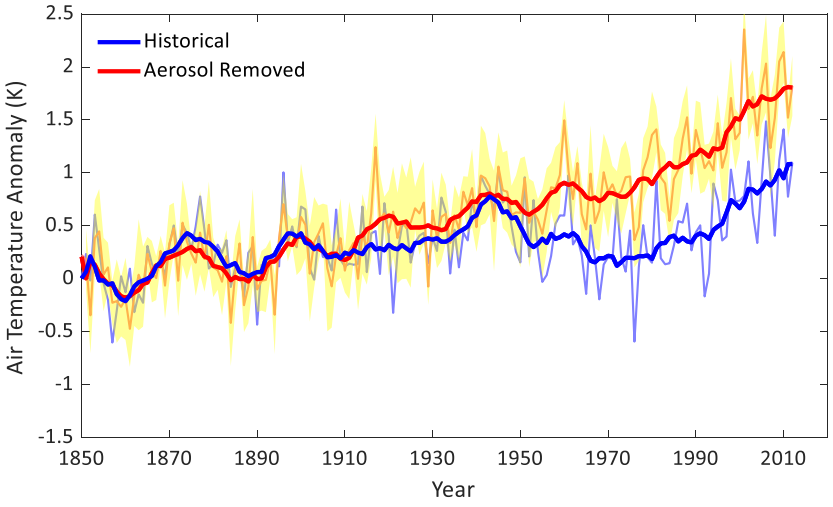


**Figure 8: Temporal annual variation in air temperature, and air temperature with the depressing effect of aerosols removed in the summer season. The shaded area is the standard deviation of model average.**

# Supplement of "Air pollution slows down surface warming over the Tibetan Plateau"

Aolin Jia[1], Shunlin Liang[1], Dongdong Wang[1], Bo Jiang[2], Xiaotong Zhang[2]

[1] Department of Geographical Sciences, University of Maryland, College Park, MD, 20742, USA

[2] State Key Laboratory of Remote Sensing Science, Faculty of Geographical Science, Beijing Normal University, Beijing, China

## S1. Data

### S1.1 Surface air temperature datasets

**Table S1 (Rao *et al.*, 2018). Meta information on the four surface air temperature datasets. All datasets were resampled into 1 Lat/Lon degree, and the climatology periods were transferred to 1961–1990 in the paper. All data were accessed on 20 July 2018.**

| Data | Spatial Resolution | Climatology Period | No. of Sites | Homogenization method | Interpolation method | Data Availability | Notes |
|---|---|---|---|---|---|---|---|
| BEST-LAND | 1°×1° | 1951–1980 | 36866 | scalpel: Split time series using detected break points and automatically adjust weight for each time series | Gaussian process regression/ Kriging | http://berkeleyearth.org/data/ | Muller et al. (2013a) and Rohde et al. (2013b) |
| CRU-TEM4v | 5°×5° | 1961–1990 | 5583 | Comparing with neighbor stations | No interpolation implemented | http://www.cru.uea.ac.uk/data | Jones et al. (2012) |
| NASA-GISS | 2°×2° | 1951–1980 | 7290 | Comparing with neighbor stations; urbanization adjustment | Distance-dependent weighted average of station observations within a 1200-km radius | https://data.giss.nasa.gov/gistemp/ | Hansen et al. (2010) |
| NOAA-NCEI | 5°×5° | 1961–1990 | 7280 | Comparing with neighbor stations | Two-step (low and high frequency) reconstruction using Empirical Orthogonal Teleconnection | https://governmentshutdown.noaa.gov/ | Smith et al. (2008) and Vose et al. (2012) |

## S2. Supplementary Results

### S2.1 CERES EBAF Surface Downward Shortwave Radiation Assessment

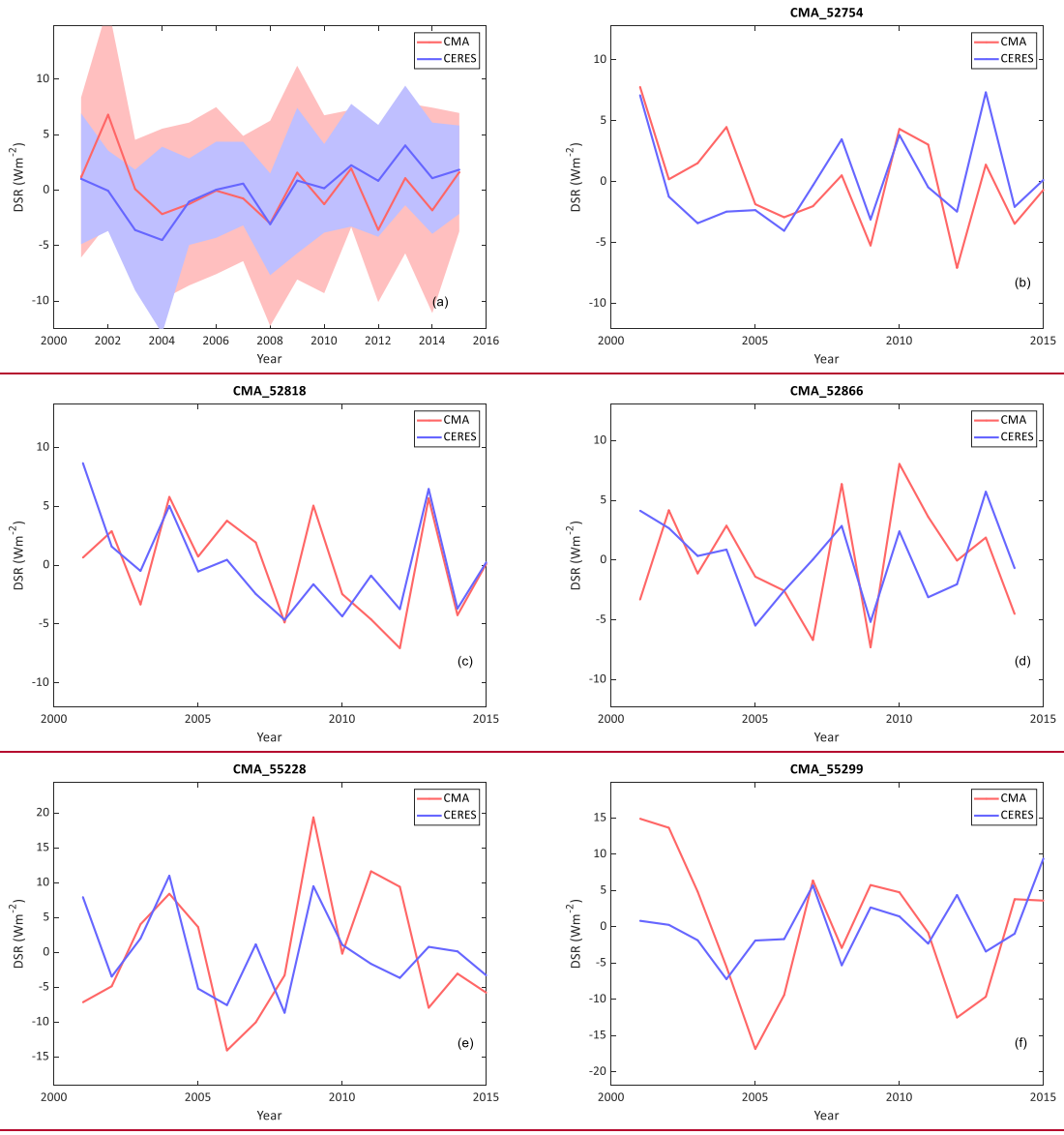

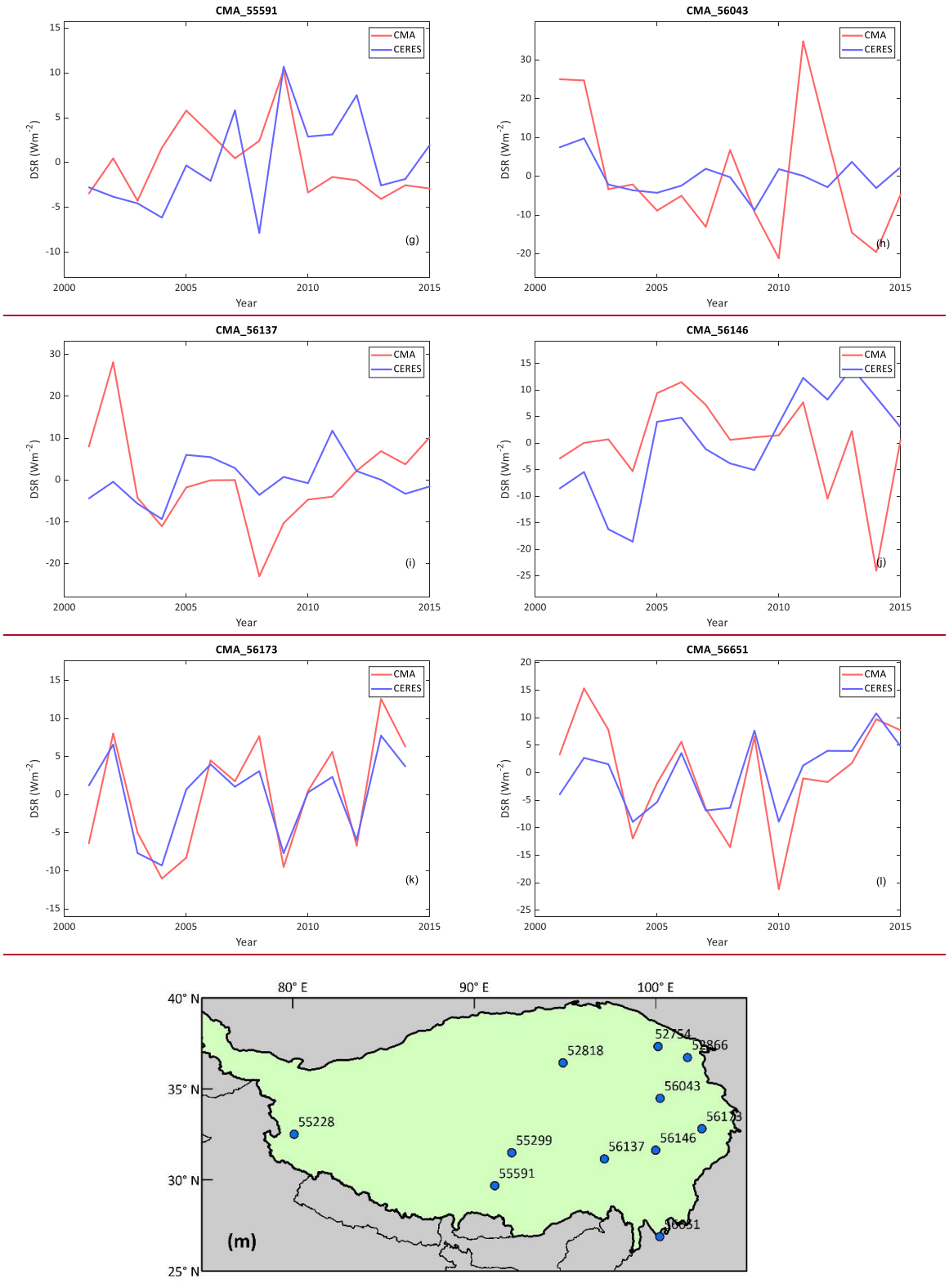


**Fig. S1: Surface DSR temporal variation of CERES and all CMA radiation sites at TP (a) 11 CMA sites mean, (b-l) individual sites, and (m) 11 sites distribution.**

## S2.~~1~~ 2 Analysis of Long-Term Surface Downward Solar Radiation Measurements since 195~~860~~

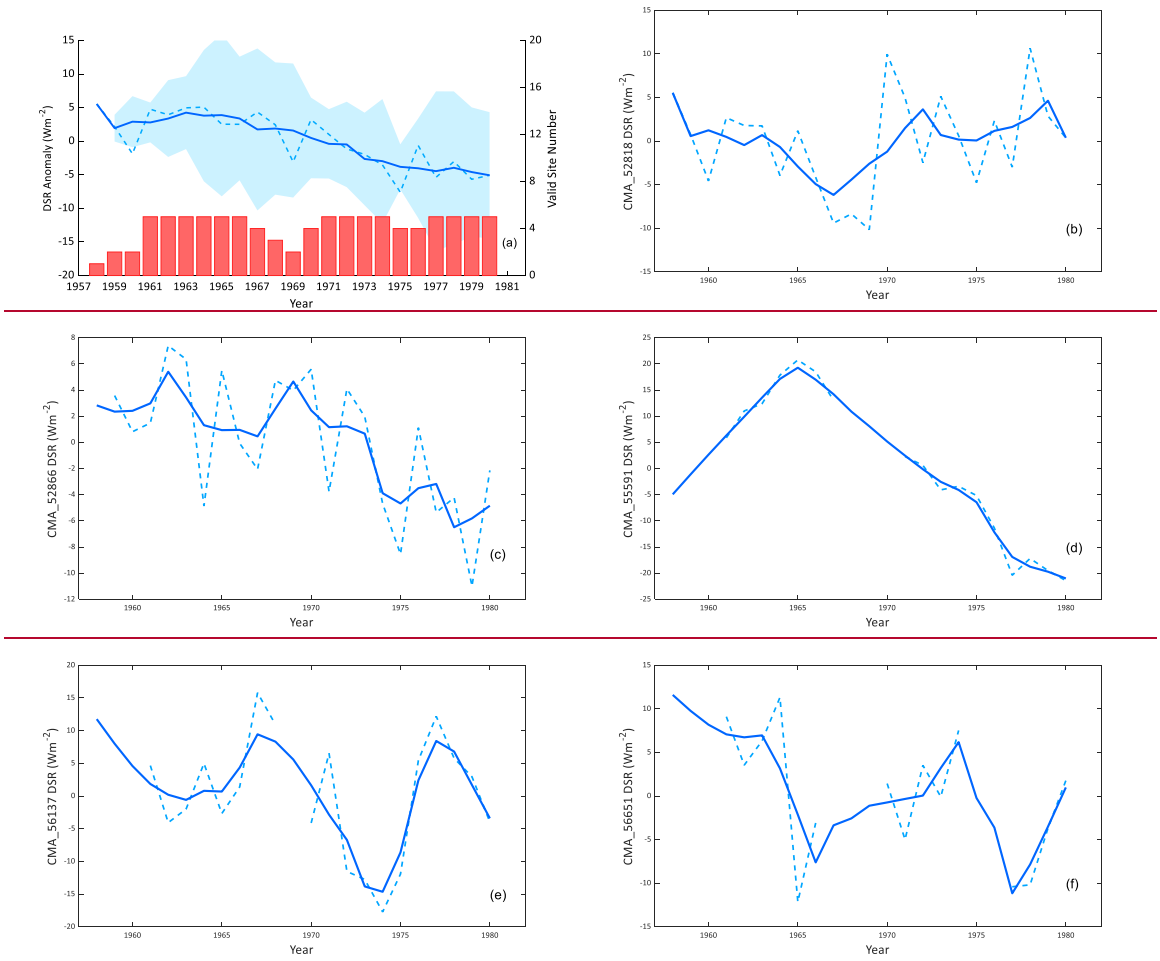


**Fig. ~~S1~~S2: Surface DSR temporal variation of (a) 5 ~~GEBA~~ CMA sites mean, (b-f) individual sites. Temporal variations were averaged by the ~~10~~5-year moving window in order to remove the impact of annual variability. ~~Influences of large volcano eruptions in 1980s and early 1990s were ignored while calculating the average variation~~Observations after 1980 were abandoned due to the data discontinuity.**

## S2.~~2~~ 3 Analysis of Deep Convective Clouds and Atmospheric Water Vapor

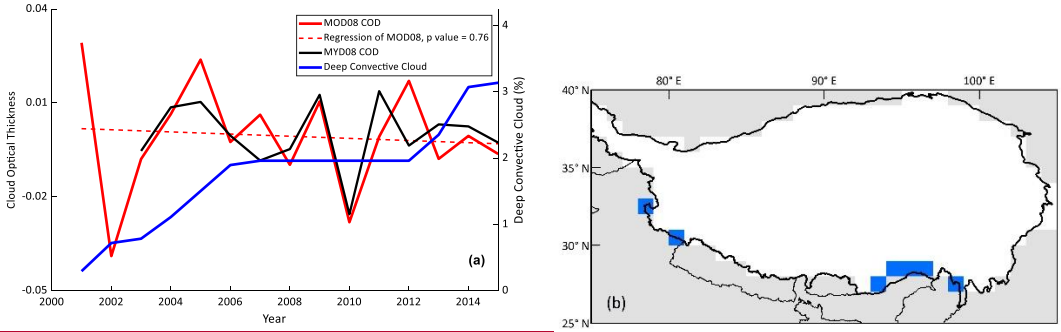


**Fig. ~~S2~~S3: (a) Temporal variation of the cloud optical depth and deep convective clouds from the MODIS 08 products; (b) Deep convective cloud distribution over the TP. The blue pixels are the location of the deep convective cloud once it appeared.**

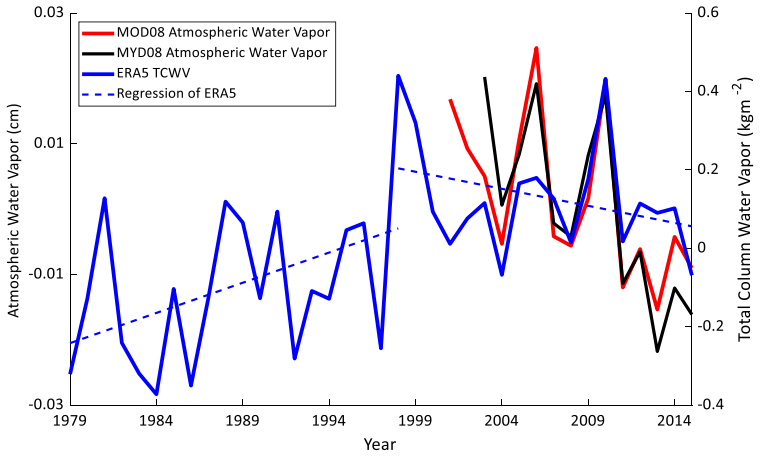


**Fig. ~~S3~~S4: Temporal annual variation of the atmospheric water vapor from MODIS atmospheric products and ERA5. ERA5 shows a considerable turning point in 1998 and the decreasing trend matches with satellite products very well. The *p* value of the regression in 1979-1998 (1999 - 2015) is 0.04 and 0.10.**

## S2.~~3~~ 4 Aerosol data analysis

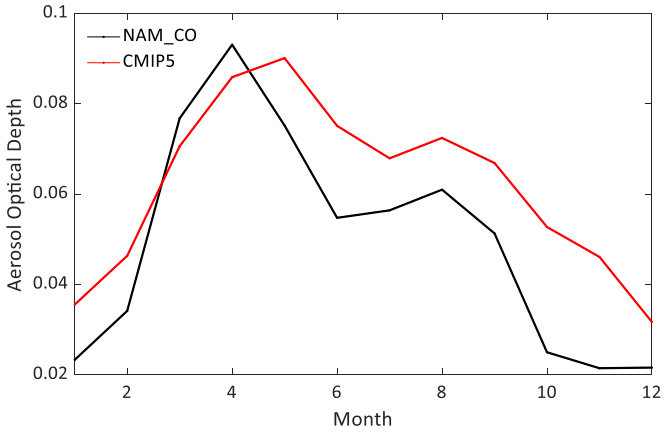


**Figure ~~S4~~S5: Monthly climatology of aerosol optical depth from the CMIP5 estimation and AERONET(AErosol RObotic NETwork) NAM_CO site observation.**

## S2.~~4~~ 5 Radiative Forcing of Anthropogenic Aerosols

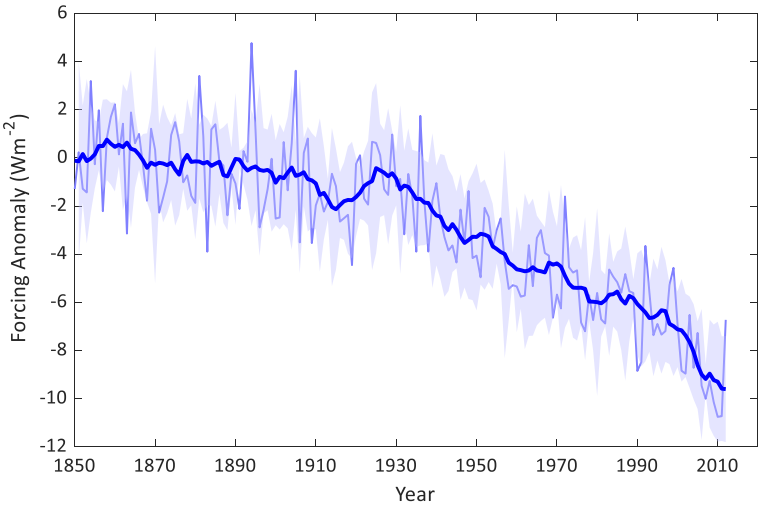


**Fig. ~~S5~~S6: Temporal variation in the aerosol radiative forcing anomalies. The shaded area is the standard deviation of model average.**

## S2.~~5~~ 6 Depressing Effect Calculated by Two Methods

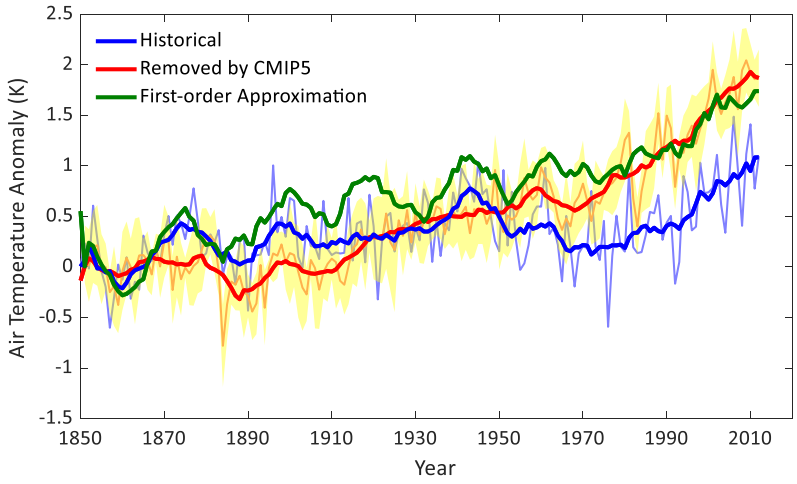


**Fig. ~~S6~~S7: The temporal annual variation in air temperature, and air temperature with the depressing effect of aerosols removed in the summer season, using two methods. The shaded area is the standard deviation of model average.**

## S2.7 Surface and TOA Variable Analysis

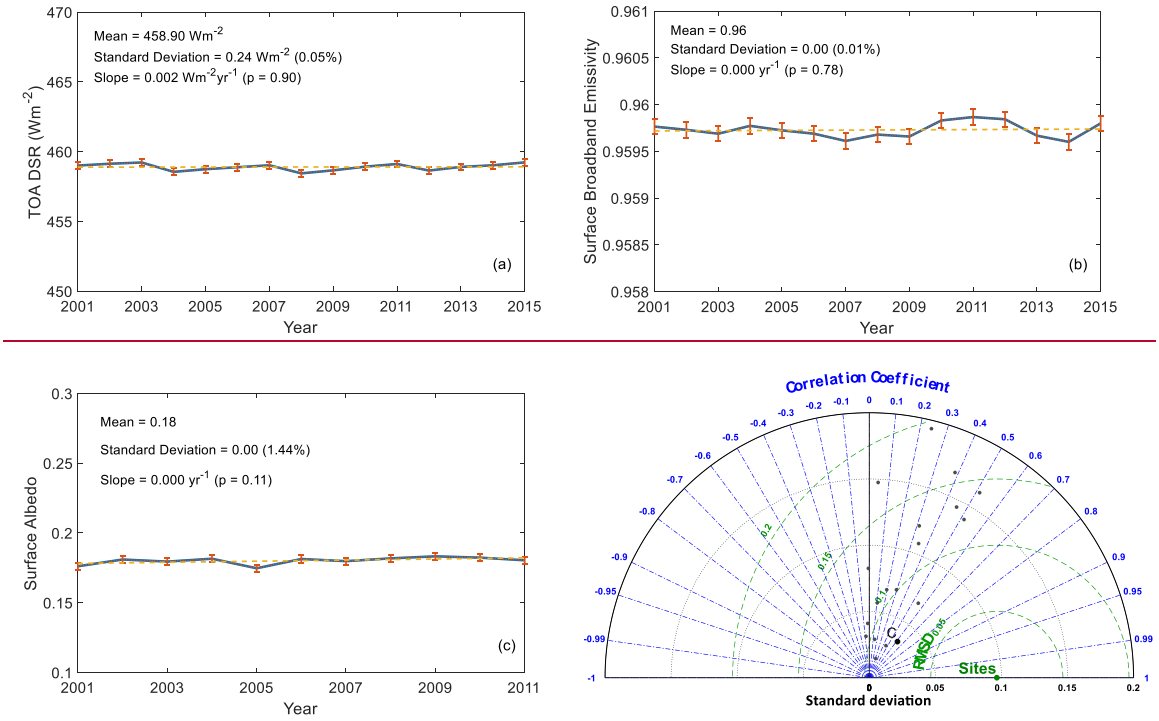


**Fig. S8: (a - c) The temporal annual variation in TOA DSR, surface broadband emissivity, and surface albedo over the TP in the summer season. The Figures show stable variation of the three variable. (d) Taylor diagram of solar validation of CERES EBAF (black dot C) and 18 CMIP5 models (grey dots) based on CAMP network. The result shows combined albedo satellite product has higher accuracy than individual model simulations.**

**References**

Hansen, J., R. Ruedy, M. Sato, and K. Lo (2010), Global surface temperature change, Reviews of Geophysics, 48(4).

Jones, P., D. Lister, T. Osborn, C. Harpham, M. Salmon, and C. Morice (2012), Hemispheric and large‐scale land‐surface air temperature variations: An extensive revision and an update to 2010, Journal of Geophysical Research: Atmospheres, 117(D5).

Rao, Y., S. Liang, and Y. Yu (2018), Land Surface Air Temperature Data Are Considerably Different Among BEST-LAND, CRU-TEM4v, NASA-GISS, and NOAA-NCEI, Journal of Geophysical Research: Atmospheres, 123(11), 5881-5900, doi: 10.1029/2018jd028355.

Rohde, R., R. Muller, R. Jacobsen, E. Muller, S. Perlmutter, A. Rosenfeld, J. Wurtele, D. Groom, and C. Wickham (2013a), A new estimate of the average Earth surface land temperature spanning 1753 to 2011. Geoinfor Geostat Overview 1: 1, of, 7, 2.

Rohde, R., R. Muller, R. Jacobsen, S. Perlmutter, A. Rosenfeld, J. Wurtele, J. Curry, C. Wickhams, and S. Mosher (2013b), Berkeley Earth Temperature Averaging Process. Geoinfor Geostat: An Overview 1: 2, of, 13, 20-100.

Smith, T. M., R. W. Reynolds, T. C. Peterson, and J. Lawrimore (2008), Improvements to NOAA's historical merged land–ocean surface temperature analysis (1880–2006), Journal of Climate, 21(10), 2283-2296.

Vose, R. S., D. Arndt, V. F. Banzon, D. R. Easterling, B. Gleason, B. Huang, E. Kearns, J. H. Lawrimore, M. J. Menne, and T. C. Peterson (2012), NOAA's merged land–ocean surface temperature analysis, Bulletin of the American Meteorological Society, 93(11), 1677-1685.